Subduction of oceanic lithosphere in the Alps: Selective and archetypal from (slow-spreading) oceans

Philippe Agard

Subduction of oceanic lithosphere in the Alps: selective and archetypal from (slow-spreading) oceans

P. Agard

[1]Sorbonne Université, CNRS-INSU, Institut des Sciences de la Terre Paris, ISTeP UMR 7193, F-75005 Paris

Abstract

The Alps are amongst the best subduction archives in the world, with abundant blueschists and eclogites preserving fragments of mantle, gabbros, thinned continental margin and pelagic sediments partly within their pre-collisional architecture. But to what extent is the Alpine record representative of the subduction of oceanic lithosphere worldwide? What is its significance, merits and limits for understanding subduction (and exhumation) dynamics? This contribution shows that this record is neither exceptional nor atypical but rather exemplifies the fate of relatively short-lived and small, slow-spreading and slowly closing North Atlantic-type oceans (in this case a ~400-700 km-wide domain closed over 60 Ma, at ~1 cm/a), whose subducting slabs do not reach below the Mantle Transition Zone. Subducted fragments experienced conditions typical of mature subduction worlwide and show no sign of significant tectonic overpressure. Contrasts in rock recovery with time and space outline distinct subduction dynamics. During the first half of the subduction lifetime (~30 Ma), no subducted oceanic fragments were recovered. A marked difference is observed between metasediment- and mafic/ultramafic-dominated units (S and MUM units). Underplating of S units took place intermittently and preferentially at ~30-40 km depth. The MUM units of the Western Alps deeply subducted to ~80 km were only recovered late, i.e. within a few Ma at most before continental subduction and initially lied close to the margin. At the scale of the orogen, the recovery of subducted fragments allows to recognize four distinct sectors and demonstrates a strong influence of initial margin architecture and/or continental subduction. Whilst typical of subduction zone thermal regimes, the subduction archive appears to selectively preserve slow-spreading oceans and/or hyperextended margins.

1. Introduction: what sort of 'oceanic' subduction in the Alps?

Subduction of oceanic lithosphere into the mantle is a key driver of plate tectonics (Forsyth and Uyeda, 1975; Ricard et al., 1993; Conrad and Lithgow-Bertelloni, 2002; Coltice et al., 2019) and a major seismic and volcanic hazard. Understanding processes acting along the subduction plate boundary, such as mechanical coupling or fluid migration, is a prerequisite for elucidating subduction dynamics, element and fluid transfer to subarc depths or risk assessment (e.g., Stern, 2002 and references therein).

The subduction of oceanic lithosphere (coined as 'oceanic subduction' in the following) mostly happens at depths beyond reach for sampling and observation. Basic geometries are only accessible down to a few km by seismic imaging (e.g., Calahoranno et al., 2008; Shillington et al., 2015); monitoring of displacements and earthquakes provides limited time series (typically 1-100 yrs; Chlieh et al., 2011; Bedford et al., 2013); interpretation of geophysical measurements is commonly equivocal when assessing material behavior and constraining rheology (e.g., Vp/Vs ratios and lithology: Audet and Burgmann, 2014; magnetotelluric data and fluids: Wannamaker et al., 2014). A complementary approach is to use samples exhumed from fossil subduction zones (e.g., Jolivet et al., 2003; Chopin, 2003; Bebout, 2007), which mostly originate from the downgoing plate (or 'slab'; Agard et al., 2018).

The Alps is one of the best such locations worldwide: subducted remnants (blueschists and eclogites) are comparatively abundant and well-preserved (Goffé et al., 2004); metamorphic reworking of these remnants by later collision has been only moderate, except in some parts of the Central Alps; active topography makes up for many good exposures (Sternai et al., 2019). Two centuries of detailed structural investigations have shown, in addition, that major units and paleogeographic domains have not been tremendously offset with respect to former convergence directions (e.g., Schmid et al., 2017). The Alpine belt is moreover small enough that its whole structure can be envisioned in 3D and lateral variations be investigated in tight connection to geophysical imaging (e.g., Schmid and Kissling, 2000; Hétenyi et al., 2018; Kästle et al., 2019). Alpine subducted fragments thus seem ideal probes to study deep subduction processes, or to reconstruct the initial subduction geometry.

The Alps are in fact intimately associated with the birth of subduction ideas (Ampferer and Hammer, 1911), and one Alpine study even coined the term (Amstutz,

1951; White et al., 1970). Effective recognition of past oceanic subduction in the Alps came from petrological investigations ~50 years ago, shortly after the advent of plate tectonics. Building on studies conducted in the Western United States, early authors associated the presence of relict metamorphic minerals making up blueschists and eclogites (e.g., glaucophane, lawsonite, sodic pyroxene) to former subduction (Ernst, 1971, 1975; Dal Piaz et al., 1972; Michard, 1977; Dal Piaz and Ernst, 1978).

The search for deeply buried rocks, yet maintained relatively cold, i.e. equilibrated under high pressure low temperature conditions (HP-LT), intensified in the 80s (e.g., Goffé and Chopin, 1986; Pognante and Kienast, 1987) and culminated with the discovery of coesite in continent-derived fragments, which revealed the existence of deep continental subduction (Chopin, 1984). A tectono-metamorphic overview of the Alps was published in 2004 (Handy and Oberhänsli, 2004; Oberhänsli and Goffé, 2004) and parly updated a few years later (Bousquet et al., 2008; Berger and Bousquet, 2008; Agard et al., 2009. Beltrando et al., 2010; Bousquet et al. 2012).

Lithostratigraphic and petrological studies have shown, in parallel, that these subducted remnants once belonged to a slow-spreading ocean (Lemoine et al., 1970, 1984, 1987; Lagabrielle and Cannat, 1990) whose margins are relatively well-preserved (Manatschal and Müntener, 2009; Mohn et al., 2011, 2012; Lagabrielle et al., 2015). Paleogeographic reconstructions (Dercourt et al., 1986; Stampfli and Marchant, 1997; Vissers et al., 2013; van Hinsbergen et al., 2020) and tomographic studies investigating the presence, number and polarity of slabs, or potential tear faults and slab breakoff events (Lippitsch et al., 2003; Handy et al., 2010; Kästle et al., 2019), place important constraints on the subduction history (Handy et al., 2010).

But to what extent is the Alpine example representative of subduction dynamics worldwide? Subduction of the Alpine ocean is special in a number of ways: a relatively small ~500 km wide domain characterized by Atlantic type, slow-spreading oceanic lithosphere disappeared between Europe and Adria, leaving no volcanic arc behind and trench sediments quite different from Peri-Pacific subduction zones today.

How much and what sort of 'oceanic subduction' prevailed in the Alps? Has the picture changed since the 2004 overview (Handy and Oberhänsli, 2004; Berger and Bousquet, 2008)? While many studies have improved our understanding of subduction processes, some issues still need clarification and/or new areas of

contention have emerged (i.e., the possibility of tectonic overpressures, the issue of representativity, processes of mélange formation or the role of tectonic inheritance; Balestro et al., 2015; Yamato and Brun, 2017; Luisier et al., 2019; Moulas et al., 2019; McCarthy et al., 2018).

The aim of the present study is to evaluate what is left of the Alpine oceanic lithosphere, what the Alpine record tells us about subduction and/or exhumation dynamics, to assess major differences along the belt and the role of tectonic inheritance and examine the new insights gained over the last decade on processes acting along the plate interface (e.g., report of fossil earthquakes, fingerprinting of fluid-rock interactions). The ensuing, short-lived continental subduction is only mentioned here to the extent it affected the fate of subducted oceanic fragments.

2. Petrological and geodynamic context

Oceanic fragments bearing diagnostic subducted-related HP-LT mineral assemblages are found within the core of the entire Alpine orogen, from the Ligurian Alps to the Rechnitz window, from Genova to Vienna (Fig. 1). They are found in the Liguro-Piemont and Valais domains (Upper and Lower Penninic, respectively), two former oceanic domains merging to the east but separated in the Western and Central Alps by a continental fragment (Briançonnais, or 'Middle-Penninic'; see Fig. 1 for the definition of Western, Central and Eastern Alps used here). The schematic cross-section illustrates the structural organization of the major paleogeographic domains recognized in the belt, from the Austro-Alpine units on top to the European units below (Fig. 1b). A detailed account of the architecture of the Alps or of the evolution of ideas on the Alpine orogeny is beyond the scope of the present study (e.g., for a selective 'tour': Argand, 1924; Debelmas and Lemoine, 1970; Tricart, 1984; Froitzheim et al., 1996; Stampfli et al., 1998; Rosenbaum & Lister, 2005; Schmid et al., 2004, 2017; Nagel, 2008; Manzotti et al., 2014).

2.1. Evidence for subduction of oceanic lithosphere

Owing to its importance for characterizing the subduction of oceanic lithosphere, a brief outline of HP-LT metamorphic rocks is given here (see chapter 3 for details) before recalling available first-order paleographic and geodynamic constraints.

As noted by Dal Piaz and Ernst (1978), Alpine subducted oceanic fragments are dominated by 'Mesozoic calc-schists, greenstones and serpentinized peridotites'. Subduction of such rocks, deeply buried under cool conditions, produces a distinctive metamorphic mineralogy, e.g., lawsonite, sodic clinopyroxene ('omphacite'), blue amphibole (glaucophane and 'crossite'), garnet, in metamafic rocks; ferro-magnesio-carpholite, lawsonite, chloritoid, garnet, talc, coesite in metasedimentary rocks; antigorite, titano-clinohumite, titano-chondrodite in metaperidotites. Noteworthily, the names antigorite and eclogite, now commonly associated with HP-LT environments, were born in the Alps (Hauÿ, 1822; Godard, 2001).

Following early reports of HP-LT metamorphism in the Alps (e.g., Kienast and Velde, 1970; Dal Piaz et al., 1972; Goffé et al., 1973), a first overview of their mineralogy and distribution was provided forty years ago (26th Int. Geol. Congress; Saliot et al., 1980). It was soon realized that, in the case of the Western Alps, the intensity of HP-LT metamorphism increases towards the southeast. This distribution of metamorphosed oceanic units in the Western Alps, from blueschist to transitional blueschist-eclogite to eclogite facies (Fig. 2b), advocates for southeast-directed subduction of oceanic lithosphere below the Adriatic plate. The same fossil subduction zone is exposed in the Central and Eastern Alps, indicating subduction below the Austroalpine and South Alpine domains; Fig. 1c). It is therefore relatively easy to bridge the gap, geometrically, between the present-day architecture and the subduction history (compare Figs. 1b and 1c).

A distinct record of late Cretaceous intracontinental subduction, unrelated to the closing of the Alpine ocean, is documented in the Eastern Alps through volumetrically small HP-LT remnants in the Saualpe, Koralpe and Porhoje (Fig. 1a). These reached peak burial between 105-90 Ma (Froitzheim et al., 1996; Miller and Thöni, 1997; Thöni, 1999; Faryad and Hoinkes, 2003; Stüwe and Schuster 2010). In the broader Alpine region, Jurassic high pressure metamorphism is also found in the Western Carpathians and the Dinarides, where it is generally thought to result from the closure of the westward closing westernmost sector of the Neotethys, the Vardar/Meliata/Sava ocean (Stampfli and Borel, 2002; van Hinsbergen et al., 2020; Schmid et al. 2020, see § 2.3).

172
173
174 *2.2. Oceanic material: types and peculiarities*
175
176 Sedimentary and magmatic features show that the Liguro-Piemont and Valais
177 domains were small ocean basins (Auzende et al., 1983; Lemoine et al., 1986)
178 characterized by extensive ocean-continent transition domains (OCT; e.g., in the
179 Central Alps: Err-Plata; Manatschal and Nievergelt, 1997; Mohn et al., 2011), with a
180 series of larger continental fragments in between (e.g., from the largest to the
181 smallest: Briançonnais, Sesia Zone, Emilius, Pilonnet; Dal Piaz et al., 2001; Manzotti
182 et al., 2014). Information from lithostratigraphy, paleogeography, magmatic petrology
183 and kinematics (§ 2.3) is provided in figure 3. Figure 3a combines these data into a
184 schematic view of the initial status of the Alpine domain prior to subduction (key
185 locations as in Figs. 1a and 2).
186
187
188 *2.2.1. Sedimentary cover: lithostratigraphic constraints*
189 Systematic lithostratigraphic studies, mostly in the 1970s and 1980s, recognized
190 pre-rift (Triassic), syn-rift (early to mid-Jurassic) and post-rift series in the Liguro-
191 Piemont and Valais oceanic domains and their adjacent continental margins
192 (Lemoine et al., 1986). The two former types, overall carbonate-dominated, are found
193 on the stretched portions of the European and Adria margins, in the OCT domain and
194 in extensional allochtons (Fig. 3a). Post-rift sediments are found almost across the
195 entire domain, mainly as calcschists and flysch deposits, whereby it is often uncertain
196 which of these post-rift sediments were deposited on a truly oceanic substratum and
197 which on the adjacent continental margin. Unmetamorphosed, or little
198 metamorphosed equivalents are found in the Prealps (Fig. 1a; Gets and Simme
199 nappes; Ricou and Siddans, 1986; Stampfli et al., 1998) and in the Flysch nappes
200 (e.g., Winkler et al., 1985; Merle, 1982).
201 Sediments truly deposited on ophiolitic seafloor, which make up the Schistes
202 Lustrés and Bündnerschiefer complexes (Elter, 1971), comprise radiolarian cherts,
203 shales, pelagic limestones and calcschists (Figs. 4a-f). These pelagic metasediments
204 range from the Callovo-Oxfordian (e.g., De Wever and Caby, 1981) to the early
205 Paleocene but are volumetrically mostly Cretaceous in age (Fig. 3b; Caron, 1977;

Lemoine et al., 1984; Lemoine and Polino, 1984). Their average thickness prior to subduction ranges between 200 and ~400 m (Lemoine et al., 1984; Lemoine and Polino, 1984; Lemoine and Tricart, 1986; Michard et al., 1996).

They commonly exhibit syntectonic cm- to km-scale detrital intercalations (Figs. 4d,e; Tricart et al., 1982; Dumont et al., 1984; Lagabrielle et al., 1985), particularly in Late Jurassic and Early Cretaceous beds (Elter, 1971; Tricart and Lemoine, 1991). Ophiolitic pebbles or hm-scale fragments (Polino and Lemoine, 1984; Le Mer et al 1986) are common in oceanic metasediments (Balestro et al., 2014; Corno et al., 2019), though not evenly distributed (see § 3). Large hm-/km-sized carbonate (commonly Triassic in age; Tricart et al., 1982; Fig. 4g) or continental fragments found within the Schistes Lustrés and Bündnerschiefer, in both the Liguro-Piemont and Valais domains, mark the transition between the continent and the ocean (e.g., 'Prepiemont' domain; Elter, 1971; Tricart et al., 1982; Tricart and Lemoine, 1986). Large bodies are commonly interpreted as extensional allochtons from the stretched continental margin (Beltrando et al., 2014 and references therein).

Flysch-type deposits represent the other main type of oceanic sediments (e.g., Helminthoid or Prättigau flyschs; Merle, 1982; Merle and Brun, 1984; Mueller et al., 2020) and range from the late Cretaceous to the Paleocene (Trümpy, 1960, 2006). They are interpreted as trench sediments and mark the existence of an accretionary margin associated with oceanic subduction (see Fig. 6 of Handy et al., 2010 for a recent compilation).

Alpine sediments are dominated by carbonates, calcschists and pelites, commonly organic-rich (Fig. 4a). This feature appears largely specific to Tethyan rocks, as opposed to the more 'mafic' metagraywackes from the circum-Pacific (Maruyama et al., 1996). Present-day analogues of Alpine-type sediments are being deposited in the Sunda region for example (see discussion in Epstein et al., 2019).

2.2.2. Oceanic crust/lithosphere: mafic and ultramafic material

'Ophiolitic' fragments of oceanic crust/lithosphere are relatively abundant in the Liguro-Piemont domain (Fig. 2c) and sparser in the Valais domain. The Alpine lithosphere was early on recognized as made of extensive amounts of exhumed mantle and discontinuous patches of crust (Lagabrielle, 1987; Lemoine et al., 1987) directly overlain by ophicarbonates and sediments (Fig. 4h; Tricart et al., 1982), with

noticeable differences between sections (Fig. 3b; e.g., Queyras and Monviso; Tricart and Lemoine, 1991). These characteristics are at odds with the Penrose type lithosphere (1972) examplified by the Semail ophiolite (Nicolas, 1989).

The importance of mantle exhumation, asymetric rifting, slow spreading Atlantic-type lithosphere was acknowledged by Lemoine et al. (1986; for a historical perspective see Lagabrielle, 2009) and later authors (Lagabrielle and Cannat, 1990; Lagabrielle and Lemoine, 1997; Cannat et al., 1997, 2009; Manatschal and Müntener, 2009). Concepts of mantle exhumation and formation of oceanic core-complexes in fact partly derive from Alpine examples (e.g., mega-mullions: Tricart and Lemoine, 1986; mantle exhumation: Trommsdorff et al., 1993).

Peridotites are for the most part variably serpentinized, partly refertilized abyssal type lherzolites (Barnes et al., 2014), compositionally intermediate between oceanic/asthenospheric and sub-continental mantle (e.g., Malenco, Central Alps; Lanzo, Western Alps; McCarthy and Müntener, 2015; Picazo et al., 2016). Basalts and gabbros show a typical MORB-type affinity (e.g., Chalot-Prat et al., 2003), although ridge-type magmatism was probably limited in the Alpine ocean. Alpine gabbros essentially cluster between ~165 and 150 Ma (Bortolotti and Principi, 2005; Manatschal and Müntener, 2009).

Some (almost) unmetamorphosed fragments from the eastern Central Alps allow to map out the OCT domain (e.g., Err-Plata; Froitzheim et al., 1996; Manatschal and Nievergelt, 1997), identify oceanic core-complexes or the transition from initial extension to necking and rifting/spreading stages (e.g., Mohn et al., 2011), assess the paleogeographic position of some Alpine massifs (e.g., Tasna as stretched margin to OCT on the Briançonnais side, and Err-Platta near Adria; Mohn et al., 2012; Fig. 3) and assign them to specific portions of the seafloor (e.g., Chenaillet as near mid-oceanic; Manatschal et al., 2011; Lagabrielle et al., 2015). The comparison between unmetamorphosed protoliths and those having experienced blueschist and/or eclogite facies conditions may be used to study oceanic processes (petrogenesis, interactions between magmatism and tectonics, hydrothermal alteration) or disentangle the effects of subduction-related transformations, (e.g., Chalot-Prat et al., 2003; Bucher and Grapes, 2009; Tartarotti et al., 2011; Lafay et al., 2013; see § 5).

2.3. Geodynamic setting: boundary conditions for oceanic subduction

Plate kinematics reconstructions (Dercourt et al., 1986; Dewey et al., 1989; Stampfli et al., 1998; Rosenbaum et al., 2002; Handy et al., 2010; Vissers et al., 2013; van Hinsbergen et al., 2020), though different in detail, place bounds on the Alpine ocean in terms of size and duration:

— The Alpine oceanic was ~400-700 km wide (Stampfli et al., 1998; Vissers et al., 2013; Fig. 3c) and comprised, in its southern part, the Valais domain to the west and the Liguro-Piemont domain to the east, separated by the ~100-150 km wide Briançonnais continental fragment (including its stretched Prepiemont or sub-Briançonnais margins; Lemoine et al., 1986). The Liguro-Piemont domain was ~300-400 km wide (Stampfli et al., 1998; e.g., their Fig. 14) and partly floored by refertilized sub-continental mantle (Manatschal and Müntener, 2009; Picazo et al., 2016). The SW branch of the Valais (hereafter termed Valaisan, for clarity) was 50-200 km wide only, and represented a strongly stretched margin and/or OCT first affected by Jurassic rifting. It lacked ophiolitic material except in portions (e.g., Internal Valais Versoyen units) extended further during the early Cretaceous (> 130 Ma; Loprieno et al., 2011). The NE portions of the Valais and Liguro-Piemont oceans were respectively larger and smaller than their SW portions.

— Slow opening of the ocean occurred between 170 and ~120 Ma (< 2cm/a; Vissers et al., 2013; Fig. 3d). The age cluster of the Liguro-Piemont gabbros (~165-150 Ma) suggests that either subsequent magmatism was insignificant and/or that all oceanic lithosphere formed between 150 and 120 Ma, be it 'normal' or slow-spreading, was subducted. The Alpine seafloor did not resemble the thick, Pacific-type crust with stratified 'ocean plate stratigraphy' (Kusky et al., 2014) but rather, in terms of size and constitution, parts of the North Atlantic such as between Greenland and Norway.

— The onset of subduction is poorly constrained and its locus even less so (see Fig. 3a). It is usually dated by the deposition of the first flysch-type sediments. It is considered to lie within 110-80 Ma, and may have started somewhat earlier in the east (Trumpy, 1960; Lemoine et al., 1986; Wagreich, 2001; Handy et al., 2010). We herein consider it to be ~100-95 Ma based on the presence of well-dated Cenomanian-Turonian flysch (Stampfli et al., 1998). No subduction-related magmatic

arc formed in the Alps (Stampfli et al., 1998; McCarthy et al., 2018). Collision started at 34-32 Ma in the Western Alps (Simon-Labric et al., 2009; Beltrando et al., 2009).

— Metamorphic ages associated with the subduction of oceanic lithosphere range from Cretaceous to Eocene (Handy and Oberhänsli, 2004; Berger and Bousquet, 2008). Most of them lie between 60 and 35 Ma. Some older (Cretaceous) ages are presently disregarded as biased (by excess argon for example), while some correspond to the paleogeographically distinct Eoalpine domain (Froitzheim et al., 1996). Episodes of continental subduction are documented for the Sesia Zone (75-65 Ma), the Briançonnais and the Internal Basement Complexes (i.e., Monte Rosa, Grand Paradiso and Dora Maira; ~42-35 Ma). Further details and their significance are addressed below.

— Since 400-700 km of lithosphere (including the Briançonnais fragment; Vissers et al., 2013) was subducted within ~60 Ma (from 100-95 to 40-35 Ma), the subduction rate was ~1 cm/a (see also Schmid et al., 1997). Independent, rough petrological constraints yield 0.5-1 cm/a (Lapen et al., 2003). A minimum of ~200-300 km of this subduction was truly oceanic in the Liguro-Piemont domain (for a similar estimate: Manzotti et al., 2014), although this amount varied along strike due to the obliquity of Alpine subduction (Handy et al. 2010). It is plausible that the Alpine slab never reached the 660 km mantle discontinuity and that slab dynamics, and any slab retreat, was confined to small-scale convection (e.g., Royden and Faccenna, 2018).

3. Oceanic fragments in the Western Alps: contrasting modes of subduction and recovery

Due to the absence of a strong collision-related metamorphic overprint, contrary to parts of the Central Alps (Engi et al., 2004; Berger et al., 2005; Keller et al. 2005; Fig. 2b), subducted HP-LT oceanic fragments are best preserved in the Western Alps (Goffé et al., 2004). This metamorphic record is examined first and then compared to that of the Central and Eastern Alps (§ 4). The Ligurian Alps and Corsica, which share many similarities, are not addressed here except in passing.

Two main types of tectono-metamorphic units can be recognized (Figs. 5-9), dominated either by metamorphosed pelagic sediments (i.e., calcschists of the Schistes Lustrés and Bündnerschiefer), hereafter called S units, or by mafic and

ultramafic bodies with only minor calcschists (Lagabrielle and Cannat, 1990), hereafter called MUM units. Their respective, partly separate spatial distribution over the Western Alps (Figs. 2c, 7a-b) reveals that these initial lithological contrasts (§ 2.2) were amplified by later tectonics. A similar divide is observed in Corsica (Vitale-Brovarone et al., 2013 and references therein).

In the Cottian Alps (Fig. 7a-d), dominantly metasedimentary blueschist-facies units are located to the west, whereas large, mainly eclogitic mafic and ultramafic bodies crop out to the east, next to the continental Dora Maira massif (e.g., Rocciavre, Monviso; Fig. 2c). Despite large spatial variations, available cross-sections (e.g., Deville et al., 1992; Fudral, 1996; Lardeaux et al., 2006), map compilations and personal observations provide rough indications on the relative proportions of sediment to mafic/ultramafic rocks, around ~20:1 in S units and ~1:5 in MUM units.

3.1. Metasedimentary dominated (S) units from the Liguro-Piemont ocean, Western Alps

From south to north, the main exposures are found in the Queyras, Cottian, Maurienne (Deville et al., 1992) and in somewhat lesser volumes in the Combin (or 'Tsaté'; Marthaler and Stampfli, 1989; Fig. 2c). They comprise intensely folded calcschists and rare but diagnostic marbles (e.g., Crête de la Taillante: Fig. 4f) with minor fragments of oceanic crust/mantle (Fig. 4i). The latter are mostly ultramafic but in places large mafic bodies also exist (Fig. 5b; e.g., in Queyras: Pelvas d'Abries, Bric Bouchet; Tricart et al., 1982; Lagabrielle et al., 2015; in Platta; Mohn et al., 2012). Tectonic patterns are characterized by a composite, flat lying to gently west-dipping schistosity with stretching mineral lineations trending N090 to N110 on average (Fudral, 1996; Agard et al., 2001). Structural patterns indicate protracted stretching and deformation parallel to subduction movements (e.g., Caby, 1973; Platt et al., 1989; Rosenbaum and Lister, 2005).

3.1.1. Contrasting P-T conditions for metasedimentary-dominated units (SW Alps):

Each region evidences stacking of distinct several km-long, hm- to km-thick tectonic units separated into upper, middle and lower units, based on lithology and

metamorphic grade (e.g., Lagabrielle, 1987; OP1/OP2 units of Pognante, 1991). Three or four units are recognized depending on latitude and authors (Fig. 7c; Fudral, 1996; Polino et al., 2002; Barfety et al, 2006; Plunder et al 2012; Lagabrielle et al., 2015).

- Upper S unit: This lawsonite- and/or Fe-Mg-carpholite-bearing blueschist facies unit (Fig. 5c-e) is well preserved in the Queyras and Cottian Alps, or as discrete klippen in the Maurienne area (Fig. 4c). It is commonly pelitic and rich in organic matter (Fig. 4a). Subtle m-hm scale lithological differences influence the nature and/or proportion of HP-LT mineralogy (e.g., lawsonite abundance; Lefeuvre et al., 2020). Large km-scale carbonate fragments of Prepiemont origin found close to the Briançonnais (Fig. 4g; Tricart et al., 1982) suggest that this unit initially lied close to the OCT domain, unless they represent an uppermost, dismembered unit on top of the nappe stack. The upper S unit contains minor mafic/ultramafic fragments and/or tectonic slivers made of serpentinites, blueschist facies lawsonite-glaucophane-bearing metabasalts and metagabbros (Fig. 5e) and deerite-bearing metacherts (e.g., Lago Nero unit; Martin and Polino, 1984). P-T estimates range between 1.1 GPa - 330°C and 1.4 GPa - 350°C (Figs. 7e,f).

- Middle S unit: This lawsonite- to epidote-blueschist facies unit commonly represents more than 50% of the Schistes Lustrés complex (Fig. 4c,d). It is dominated by calcareous schists and almost pure pelagic metacarbonates (e.g., Grande Sassière, or Charbonnel-Rocciamelone unit in the Maurienne; Fudral et al., 1987). Most of the Combin exposures also belong to this unit. It locally contains detrital material, both oceanic and continental in origin. Sheared metaophiolitic material (mainly serpentinite) can be found as dismembered tectonic horizons, preferentially at the base of the unit. Metapelitic horizons contain chloritoid (Fig. 5g,h) and lawsonite pseudomorphs. Garnet is generally absent and epidote is found in the warmest portions only. P-T estimates are mostly in the range 1.5-2 GPa and 370-450°C (Fig. 7e).

- Lower S unit: This lowermost unit is located immediately above the Gran Paradiso (Le Bayon et al., 2006) or Dora Maira internal basement complex (Chopin, 1981). It is made of metasediments locally rich in volcanic debris and cherts, overlying an ophiolitic 'basement' or interleaved with substantial mafic bodies (Fig. 7d). Metamorphic grade is eclogitic or transitional between blueschist and eclogite facies and characterized by variably retrogressed chloritoid ± garnet ± epidote

assemblages. P-T estimates are in the range 2-2.3 GPa and 470-550°C (Fig. 7e). Whether this unit represents the former cover of mafic/ultramafic dominated units such as the Rocciavre and Monviso units (Fig. 7b) or a separate unit remains unclear (see § 3.2). It is considered as one single unit in Maurienne (Villaron–Gran Uia; Fudral, 1996) and two distinct ones in Queyras (Lagabrielle et al., 2015).

Estimates of peak pressure and temperature experienced by these units align along a consistent P-T gradient of ~ 8°C/km in a P-T diagram, assuming lithostatic pressure (Agard et al., 2001; Figs. 7e, 9a). In the Cottian Alps, these three units are, from bottom to top, the Pietre Verde, Albergian/Cerogne-Ciantiplagna and Lago Nero units (Fig. 5a; Caron, 1977; Polino et al., 2002; Burroni et al., 2003; Corno et al., 2019). The spatially restricted, unmetamorphosed ~150 Ma mafic and ultramafic dominated Chenaillet unit (Fig. 7d; Mével et al., 1978; Costa and Caby, 2001; Manatschal et al., 2011) overlies the Lago Nero unit. All ocean-derived units were originally thrust on top of the Briançonnais and Prepiemont cover or basement units and remained there in places (e.g., Combin or Maurienne, north and south of Ambin; Fig. 7c,d). Backfolding of the Briançonnais, associated with the Mischabel and/or Vanzone early collisional stages (Argand, 1924; Ballèvre et Merle, 1993; Bucher et al., 2003), which varies considerably in dip and intensity along strike, also emplaced continent-derived sediments from the Briançonnais margin above oceanic units (e.g., Cottian Alp; Figs. 7a,c; e.g., Michard et al. 2004).

3.1.2. Nappe stacking of the S units

The Schistes Lustrés metasediments were scraped off their underlying oceanic crust/mantle during subduction (Deville et al., 1992; Agard, 1999; Schwartz, 2000) and represent a deep accretionary complex (Marthaler and Stampfli, 1989), as for the Franciscan complex (Platt, 1986; Dumitru et al., 2010). The stacking of these metasedimentary units partly coincides with lithostratigraphic contrasts: the metapelitic-rich upper S unit is mostly made of early Cretaceous metasediments, whereas the middle S unit is mostly made of late Cretaceous calcschists (Fig. 3a; Lemoine & Tricart, 1986; Deville et al., 1992).

While most fossil accretionary complexes show preferential accretion/underplating at 30-40 km depth, thus close to the upper plate Moho (Agard et al., 2018; e.g.: Willner, 2005; Angiboust et al., 2014), this occurs across a larger depth range in the southern Western Alps. A rather continuous evolution of P-T

conditions is indeed observed in the Queyras, Cottian and Maurienne regions, from 1.2-1.3 GPa-350°C to ~2.0 GPa-500°C, as exemplified by the progressive eastward increase of the phengitic substitution in carpholite- or chloritoid-bearing assemblages (Agard et al., 2001a,b; Figs. 7d,e), and the consistent P-T estimates from dm-sized mafic bodies scattered in the Schistes Lustrés complex (Schwartz, 2000) or in the vicinity of former extensional allochtons (Corno et al., 2019).

Despite the stacking of distinct tectonic units, maximum temperatures (Fig. 7c) increase fairly regularly across the Queyras, Cottian (Agard et al., 2001a; Beyssac et al., 2002; Schwartz et al., 2013) and Maurienne units (Gabalda et al., 2009; Plunder et al., 2012): they are commonly lower than 400 °C for the upper unit, between 400 and 500 °C for the middle unit, and greater than 500 °C for the lower unit (Fig. 7f). A more restricted range of temperatures is observed for the Schistes Lustrés complex west of Grivola (Bousquet, 2008) or in the Combin area (mostly 420-550°C; Negro et al., 2013; Angiboust et al., 2014a). This absence of major P-T gaps across the distinct units argues for early stacking, before their main exhumation stage, since a more irregular temperature pattern would be expected otherwise (Plunder et al., 2012).

The age of peak burial of the Schistes Lustrés complex clusters between 55 and 62 Ma, at least for the middle and upper S units, although prograde deformation accompanying burial was largely erased (Agard et al., 2002). Early exhumation was accompanied by east-vergent relative movements while subduction was still active (D2 stage, 45-40 Ma; Agard et al., 2001a, 2002; see also Ghignone et al., 2020). This was followed, at ~40-37 Ma, by west-vergent exhumation, associated with exhumation of the Monviso and Dora Maira units (D3 stage; Agard et al., 2001a; Plunder et al., 2012; Angiboust et al., 2014a). Some early tectonic contacts, notably between the lower and middle S units, were reactivated through locally extensional exhumation shear zones in the Queyras or Combin (Fig. 5a,b; Pognante, 1991; Ballèvre et al., 1990; Ballèvre and Merle, 1993; Schwartz et al., 2009; Lagabrielle et al., 2015).

Conceivably, structurally upper units may have been underplated earlier (Bachmann et al., 2009a,b; Dumitru et al., 2010; Plunder et al., 2012; Menant et al., 2020). More in-situ ages and P-T constraints are nevertheless needed to reconstruct the Alpine accretionary wedge and correlate (stacks of) units from the southern Queyras to the northernmost Combin. To the west of Grivola, peak burial conditions

were estimated between 48 and 44 Ma (Bucher et al., 2003; Villa et al., 2014). Age constraints in the Combin/Tsaté area cluster around 42 to 37 Ma, and show a complex spatial distribution (Dal Piaz et al., 2001; Reddy et al., 2003). Diachronous juxtaposition and underplating of material detached from 25-35 km depth along the Alpine subduction interface was documented there (Angiboust et al., 2014a).

3.2 Mafic and Ultramafic dominated (MUM) units, Western Alps

Large, km- to 10 km-long portions of mafic/ultramafic MUM material representing portions of the top of the Liguro-Piemont 'slab' (Fig. 1c) are exposed in Monviso (Fig. 6a), around Gran Paradiso, north and south of the Aosta valley (Fig. 2c), as well as in the Ligurian Alps (Fig. 1a; e.g., Beiga and Erro-Tobio units; Scambelluri et al., 1995) or Corsica (Vitale-Brovarone et al., 2013). Such large-scale fragments are seldom recovered from the Valais ocean. As for the Schistes Lustrés, these oceanic fragments are composite, usually very deformed and crosscut by a number of shear zones (Fig. 6a). Metasediments are subordinate and, although large variations exist within tectonic slices or from massif to massif, the relative proportion of mafic and ultramafic material is in first approximation roughly equivalent (Angiboust et al., 2009). The description below illustrates the diversity of the MUM units (Figs. 6b-d; further magmatic-related details in: Manatschal and Müntener, 2009; Beltrando et al., 2014; Lagabrielle et al., 2015) and outlines some of their most important features, from north to south.

— Zermatt-Saas (N. Aosta valley):

This MUM unit is well-exposed in Val Tournanche and Val d'Ayas (Italy), or near Täsch, Pfülwe and Saas (Switzerland). These occurrences are characterized by a number of hm- to km-scale tectonic duplications (Angiboust and Agard, 2010). The Zermatt-Saas unit is generally underlying the Schistes Lustrés Combin units (Ballèvre et Merle, 1993; Groppo et al., 2009), but the two units are tectonically interleaved in places due to large-scale post-nappe emplacement refolding and/or backthrusting (e.g., Ellero and Loprieno, 2017). Metamorphosed mafic rocks comprise variably retrogressed eclogitic minerals, most commonly garnet, clinopyroxene ± lawsonite pseudomorphs, glaucophane, talc, chloritoid depending on

511 the exact protolith chemistry and prior hydothermal alteration on the seafloor (Fig.
512 6b,e; Angiboust and Agard, 2010). In particular, abundant, several cm-long lawsonite
513 pseudomorphs around former pillows, preserving evidence of seafloor hydration, are
514 found around Zermatt (e.g., near Britannia Hütte or Pfülwe pass; Figs. 6b,e).
515 Pressure and temperature estimates (by Raman spectroscopy of organic matter,
516 thermobarometry and thermodynamic modelling), were shown to be relatively
517 constant from Saas to south of the Aosta valley at ~2.5 GPa and 550°C (Angiboust et
518 al., 2009; Angiboust and Agard, 2010; Fig. 6b), consistent with earlier estimates for
519 the Zermatt area (Bucher et al., 2005; 2.8 GPa, 570°C). Similar conditions with
520 slightly higher temperature were inferred for the Allalin metagabbro (2.5 GPa, 600°C;
521 Bucher and Grapes, 2009) or some Valtournanche localities (2.55 GPa, 600°C;
522 Zanoni et al., 2016). In contrast, a small, hm-thick, 2 km^2 tectonic slice with coesite-
523 bearing metasediments indicative of higher, UHP conditions at ~2.8-3..2 GPa and
524 600°C (Reinecke, 1998; Groppo et al 2009; Frezzoti et al., 2011) was found in Lago
525 di Cignana (Reinecke, 1991, 1998; van der Klauw, 1997; Compagnoni and Rolfo,
526 2003). Nearby serpentinites hosting Ti-chondrodite indicate consistent with UHP
527 conditions (Luoni et al., 2018).
528 Based on Lu-Hf in garnet (Amato et al., 1999; Lapen et al., 2003; Skora et al.,
529 2015), Ar/Ar on phengite in garnet (Gouzu et al., 2006) and U/Pb on zircon (Rubatto
530 et al., 1998), most age constraints for peak burial cluster at 43 ± 4 Ma (see age
531 compilations in Berger and Bousquet, 2008; Rebay et al., 2018; Dragovic et al.,
532 2020), with indications for prograde growth around 49-48 Ma (Lapen et al., 2003;
533 Skora et al., 2015). One contrasting age at 65 Ma was obtained by Rebay et al.
534 (2018).
535
536 *— Avic (S. Aosta valley):*
537 Similar tectonic slices comprising horizons of mafic and ultramafic rocks are
538 found south of the Aosta valley (e.g., Val Clavalité, St Marcel; Angiboust and Agard,
539 2010). A remarkable, several km-long metaperidotite body with minor gabbros is
540 found in Monte Avic (Fig. 6c-d), where former oceanic structures are partly preserved
541 despite eclogite facies metamorphism (Tartarotti et al., 2011). Fewer P-T estimates
542 exist for the area (2.3 GPa, 545°C; Angiboust et al., 2009).
543 Below the Zermatt□Saas (MUM) unit and immediately overlying the Gran
544 Paradiso massif, the Grivola□Urtier unit (Dal Piaz et al., 2001; Tartarotti et al., 2019)

is made of metaflysch and calcschists envelopping blocks and slices of both mafic and gneissic, continental derived material. This unit can be regarded as a former OCT domain. In the Entrelor-Grivola unit, P-T conditions for MUM type slivers are 2.3 GPa, 550°C (Bousquet, 2008).

— *Rocciavre:*

The Rocciavre massif is a ~8 km long dominantly metagabbroic (gabbro-noritic) massif surrounded by serpentinized peridotite, with Fe-Ti metagabbros showing garnet-omphacite eclogitic parageneses similar to those found in Monviso (see below). Pressure-temperature conditions, estimated prior to the advent of multi-equilibrium techniques and thermodynamic modelling (Pognante 1991; Bouffette and Caron, 1991), should however be reappraised. Given the similar mineralogy and mineral compositions to other massifs, P-T conditions can be predicted to lie in the range 2-2.5 GPa and 550°C ± 50°C.

— *Lanzo*

The Lanzo massif is a large, ~30 km long fragment of irregularly eclogitized mantle. Whether this massif represents former sub-continental or oceanic mantle is disputed. It was cut across by ~160 Ma dykes now eclogitized (Piccardo et al., 2010). The massif was exposed on the seafloor as shown by the presence of thin sediment horizons, ophicarbonates, and seafloor serpentinization (Lagabrielle et al., 1990; Debret et al., 2013). It was subducted during Alpine subduction at around 55–46 Ma (Rubatto et al., 2008). Metagabbros in metaperidotites, metasedimentary horizons hosting kyanite-talc-chloritoid ± garnet assemblages and incipient antigorite de-serpentinization indicate P-T conditions around 2–2.5 GPa and 550–620 °C (Kienast and Pognante, 1988; Pelletier and Müntener, 2006; Debret et al., 2013). A similar peridotite massif is found in the Ligurian Alps (Erro-Tobbio; e.g., Scambelluri et al., 1995).

— *Monviso*

Since the seminal mapping of Lombardo (1978), the Monviso massif has been extensively studied (Philippot, 1990; Cliff et al., 1998; Schwartz, 2000; Castelli et al., 2002), particularly over the last decade (Groppo and Castelli, 2010; Angiboust et al.,

578 2011, 2012a,b; Locatelli et al., 2019a,b). A new map was recently published by
579 Locatelli et al. (2019a).
580 The Monviso ophiolitic massif contains two major units (Fig. 6a), the overturned
581 blueschist to eclogite facies Monviso unit on top with nicely preserved metapillows
582 (Fig. 6h), and the eclogitic Lago Superiore unit below. Both are dominantly made of
583 metaperidotites, metagabbros (mostly Mg-rich) and metabasalts (Lombardo, 1978).
584 In the 15 km long, 1.5-2 km-thick eclogitic Lago Superiore unit, one finds, from
585 bottom to top, a ~500m thick serpentinized basal peridotite unit (Gilio et al., 2020),
586 Mg-rich metagabbros, sills, dykes and a discontinuous layer of Fe-Ti metagabbros
587 hosting garnet, omphacite, abundant rutile (Fig. 6i), lawsonite pseudomorphs and
588 eclogite breccias (Fig. 8a,b). These are finally capped by metabasalts and a few
589 meters of metamorphosed calcschists at the very top.
590 The Lago Superiore unit is probably the most intact and best documented
591 eclogitized slab fragment reported so far in the world. Large-scale shear zones
592 formed prior to its detachment from the downgoing slab (e.g., Lower Shear Zone; Fig.
593 8c; Philippot and Kienast, 1989; Angiboust et al., 2011) host metagabbros brecciated
594 under eclogitic facies conditions, now mostly embedded in serpentinites, that
595 preserve evidence for brittle, possible seismic fracturing (Fig. 8d-f; Angiboust et al.,
596 2012a; Locatelli et al., 2019b). Progressive brecciation and fluid ingression (Locatelli
597 et al., 2019b), together with abundant omphacite veins (Spandler et al., 2011), allow
598 studying fluid migration pathways in the Lago Superiore unit (see chapter 5). P-T
599 estimates for this unit, around 2.6-2.7 GPa, 550-580°C (Locatelli et al., 2018 and
600 references therein), were reached ~46 Ma ago (46 ± 3 Ma; Monié and Philippot,
601 1989; Cliff et al., 1998; Rubatto and Hermann, 2003; Rubatto and Angiboust, 2015),
602 with indications for prograde growth around 49 Ma (Duchëne et al., 1997). A gap of
603 ~4-5 GPa and 70°C exists between the Lago Superiore and the overlying Monviso
604 unit (Angiboust et al., 2012a,b; Angiboust and Glodny, 2020). P-T conditions for the
605 latter unit (2.1 GPa, 480°C) resemble those of the lower and middle S units (Fig. 7e).
606
607 — Several general characteristics of the MUM units can be outlined:
608 (i) They show significant lateral variations in internal structure or in the amount
609 and type of crustal components, e.g. more metabasalts near Zermatt-Saas and more
610 Mg-rich metagabbros in Rocciavre and Monviso. However, nearly all MUM fragments
611 experienced strikingly similar P-T conditions, at 2.6 ±0.2 GPa and 560°C ± 20°C (Fig.

612 9b), except for the thin slice of the Cignana UHP unit. Another exception is the
613 Monviso sub-unit, which is transitional between blueschist and eclogite facies. These
614 P-T conditions align along the same P/T gradient as the Schistes Lustrés complex,
615 and that for mature subduction zones (Fig. 10; Agard et al., 2018).
616 (ii) Detailed tectonic mapping shows evidence for hm- to km-thick tectonic slices
617 with lithological continuities along several km (e.g., Zermatt-Saas Antrona, Avic;
618 Tartarotti et al., 2011) and km-thick bodies (in Monviso, Rocciavre, Lanzo). Some of
619 the pristine architecture of the top of the slab is still preserved, together with oceanic
620 structures (see also Beltrando et al., 2014; Fig. 8gd). This rules out the possibility
621 that the MUM units correspond to a large-scale mélange of rocks mixed up in a
622 subduction channel (as in early numerical models; Cloos, 1982; Gerya et al., 2002).
623 Local mélanges, at the m- to hm-scale, are inherited from sedimentary and/or
624 magmatic processes and reworked during subduction and exhumation (Fig. 8g;
625 Balestro et al., 2015; Tartarotti et al., 2017; Locatelli et al., 2018).
626 Observations nevertheless advocate for intense deformation, with duplications,
627 tectonic intercalations and shearing along the plate interface. This is shown by the
628 juxtaposition of km-long sub-units such as the Lago Superiore and Monviso units
629 (slab fragments with reverse polarity and contrasting P-T; Fig. 6a; Locatelli et al.,
630 2018) or the Bardonney and Broillot units (Ellero and Loprieno, 2017),
631 notwithstanding later complications during final exhumation and later Alpine
632 tectonics.
633 (iii) The age of HP (and UHP for Cignana) metamorphism of the MUM fragments
634 appears to be very restricted, with most ages falling in the range ~45±3 Ma (see the
635 compilation in Rebay et al., 2018; Fig. 9b). A more conservative value around 45± 5
636 Ma probably accounts for methodological uncertainties (e.g., Lu/Hf garnet ages of 40
637 or 46-52 Ma for the same type of samples near Zermatt-Saas; Amato et al., 1999;
638 Lapen et al., 2003; Skora et al., 2015). Lanzo might have reached peak burial slightly
639 before but ages overlap (52-46 Ma). Ages around 41-38 Ma are only found for
640 fragments located in the immediate vicinity of the Internal Basement complexes.
641 The Ligurian Alps evidence a similar tectonic organization (Messiga et al., 1995;
642 Federico et al., 2004; Vignaroli et al., 2009, 2010), with lithologies, tectonic units and
643 P-T conditions either resembling those of the Schistes Lustrés (e.g., Voltri group) or
644 Zermatt-Saas and Monviso units (Beiga and Erro-Tobio units). Mafic/ultramafic

bodies are smaller on average than for the Zermatt-Saas and Monviso units, and large mafic fragments tens of km long and more than km thick are not found.

3.3. Exhumation and juxtaposition of S and MUM units from the Liguro-Piemont ocean and relationship to continental HP-LT units (Western Alps)

Radiochronological constraints indicate that both S and MUM units were largely exhumed by 35 Ma (Fig. 9a; Agard et al., 2002; Meffan-Main et al., 2004). This is consistent with zircon fission-track thermochronological data indicating cooling below ~200°C at 32±2 Ma (Malusà et al., 2005; for apatite see Perrone et al., 2011) and with the presence of blueschist/eclogite facies minerals in Oligocene sediments (de Graciansky, 1972; Schwartz et al., 2012; Mark et al., 2016), at a time when the altitude of the internal Alps was already high (Fauquette et al., 2015). Significant differences in stacking history and exhumation patterns exist between the S and MUM units of the Western Alps (Fig. 9b):

— Successive underplating is evidenced in the S units from ~ 60 to ~ 50-45 Ma at least in the Cottian Alps and over 40-36 Ma in the Combin. It takes place at different depths, from ~30 to 55-60 km. Exhumation velocities are on the order of 1-2 mm/yr (Fig. 9b; Agard et al., 2002).

— The detachment of MUM units from the downgoing slab occurs at almost constant depths (corresponding to ~2.6 GPa ± 0.2, hence ~ 80 km) and is followed by internal deformation and slicing along the plate interface (Figs. 8c,g). Their limited imbrication with the S units (e.g., Entrelor, Grivola-Urtier; Ellero and Loprieno, 2017) shows that the exhumation of S and MUM units occurred largely independently. More generally, the absence of large-scale mixing of units, either in the S or in the MUM units, suggests that subducted fragments were mostly returned as coherent tectonic slices and nappes along the subduction interface (i.e., not as 'subduction mélange' in the sense of Festa et al., 2019).

— The MUM units correspond to fragments metamorphosed and exhumed late during the oceanic subduction history (Fig. 9b). The many age constraints for the blueschist to greenschist facies exhumation of the MUM units (particularly in the Zermatt-Saas area) reveal syn-convergence exhumation between ~40 and 36 Ma, prior to collision, through large-scale shear zones: 45-36 Ma (Reddy et al., 2003),

679 and 42-36 Ma (Angiboust et al., 2014a) near the Aosta valley and Dent Blanche; 40-
680 36 Ma (Amato et al., 1999) and 41-37 Ma (Gouzu et al., 2016) for Val Tournanche;
681 38-36 Ma (Angiboust and Glodny, 2020) for Monviso. Considering an average age
682 for peak burial at ~45 Ma for the MUM units (at 2.6 GPa or ~80 km) and shear zone
683 activity at ~350-400°C (i.e., at ~0.5 GPa, ~15 km depth), exhumation velocities are
684 on the order of 1 cm/yr (Fig. 9b).

685 — Contrary to the S units, MUM units are always tectonically underlain by the
686 Internal Basement Complexes (IBC: Monte Rosa, Grand Paradiso and Dora Maira).
687 They spatially (cartographically) coincide with the presence of these IBC and share
688 similar NS to NNW-SSE lineations (Philippot, 1990; Schmid et al., 2017). Several
689 authors have therefore suggested that the exhumation of MUM units could be
690 assisted by the buoyancy of continent material (Agard et al 2002, 2009; Lapen et al.,
691 2007; Angiboust and Agard, 2010; Skora et al., 2015), although this was recently
692 questioned (Angiboust and Glodny, 2020). Peak burial for the IBC are 42-43 Ma for
693 the Gran Paradiso (Meffan-Main et al., 2004; Manzotti et al., 2018) and 42.6 for
694 Monte Rosa (Lapen et al., 2007). Ages seem somewhat younger for Dora Maira (40-
695 35 Ma: Tilton et al, 1991; Gebauer et al., 1997; Vaggelli et al., 2006; Rubatto and
696 Hermann, 2001). Very young ages (e.g., 32.7 Ma; Duchêne et al., 1997; Rubatto and
697 Hermann, 2001) are probably geologically meaningless since collision had started by
698 ~34-32 Ma (Rosenbaum and Lister, 2005; Simon-Labric et al., 2009). For the above
699 reasons, exhumation of the MUM and/or their detachment from the slab seems at
700 least in part related to the subduction of the continental margin (see also Vitale-
701 Brovarone et al., 2014a and further discussion below).

702 Some other continental fragments were subducted earlier, as mentioned in
703 chapter 2, in particular the large Sesia body (± Ivrea ; Manzotti et al., 2014; Giuntoli
704 et al., 2018), whose peak burial clusters at ~70-65 Ma (Duchêne et al., 1997; Rubatto
705 et al., 1999, 2011; see Berger and Bousquet, 2008). Recently, a Lu/Hf garnet of 57
706 Ma was obtained for a small hm-thick continental fragment from the Zermatt-Saas
707 region, subducted at 1.7 GPa and 520 °C and interpreted as a former extensional
708 allochthon (Theodul Glacier; Bucher et al., 2020).

709

710

711 *3.4. The specific record of the Valais domain (Valaisan)*

712

Small subducted oceanic fragments associated with the closure of the Valais domain are found further west, in the Petit Saint Bernard and Versoyen units (Antoine, 1972; Cannic et al., 1996; Fügenschuh et al., 1999; Bousquet et al., 2002; Loprieno et al., 2011). A similar tectonic differentiation between metasedimentary dominated (Petit Saint Bernard) and more mafic tectonic units (Versoyen) can be observed, but they show no gap in P-T conditions. Both units are characterized by peak burial under blueschist facies conditions, as shown by the presence of lawsonite, Fe-Mg carpholite and chloritoid, at 1.5–1.7 GPa and 350–400 °C (Bousquet et al., 2002). Low pressure 'eclogites' formed through heating on exhumation (~1.5 GPa, 500°C). Closure of the Valais domain is less well-constrained than for Liguro-Piemont, but exhumation-related ages suggest a timing between 40 and 35 Ma in the Petit Saint-Bernard area (Markley et al., 1998; Villa et al., 2014).

4. Subduction dynamics through space and time in the Alps

Before examining the subduction record for the entire Alps, the tectonic insights gained from the Western Alps are set back in the general tectonic evolution from the subduction of oceanic lithosphere to subduction of the continental margin and then final collision (Fig. 9c, after Agard et al., 2002; see also: Polino et al., 1990; Dal Piaz et al., 2001; Jolivet et al., 2003; Bucher et al., 2003; Lapen et al., 2007; Berger and Bousquet, 2008; Manzotti et al., 2014). This schematic reconstruction is used here as a template to evaluate along-strike changes in the Alpine belt (§ 4.2). It outlines the progressive shortening and accretion during the subduction of oceanic lithosphere (step 1, bottom sketch in Fig. 9c), continental subduction (steps 2-3) and collision with the External Massifs along the Pennine Frontal thrust (step 4).

4.1. Geodynamics of the Western Alps as a template

P-T-t-lithostratigraphic data for the Western Alps reveal a marked structural and metamorphic contrast between the S and MUM units (Fig. 9). Underplating and partial exhumation of the Schistes Lustrés complex along the plate interface occurred during convergence after 65 Ma (Fig. 9b), when sediments from the slab were scraped off from the underlying mafic and ultramafic MUM units.

MUM units show higher P-T values, larger coherent tracts of mafic units, lithostratigraphic features ascribable to OCT in several locations and were buried (and exhumed) during the final stages of the subduction process (Figs. 9b,c; see Agard et al., 2009), i.e. a few Ma at most before the Internal Basement Complexes went into subduction.

Several important observations can be underlined:

— (1): The S- and MUM units share the same P/T regime, consistent with rocks formed in the same subduction zone (Fig. 10). This P/T consistency also rules out significant overpressure, which would not allow for such consistency in P and T and would scatter P/T estimates. The same cut-off in maximum pressure is observed at ~2.8-3 GPa as for other localities worldwide (Fig. 10; Agard et al., 2018). Beyond this cut-off, corresponding to a depth of some 90 km, mafic rocks (± serpentinites) become negatively buoyant (Agard et al., 2009. Angiboust and Agard, 2010) and recoupled to mantle counterflow (van Keken et al., 2011; Agard et al., 2020). Noticeably, no deep fragment of the overlying plate/mantle is recovered in the Western Alps, as is the case for many subduction-driven orogenies worldwide (Agard et al., 2018).

—(2): P-T conditions for the Western Alps align along the typical gradient for mature subduction (8-10°C/km; Agard et al., 2018; Fig. 7e). No remnants of early subduction are found in the Western Alps: none of them testifies to warmer P/T gradients accompanying subduction initiation (Fig. 10); all subducted fragments from the Liguro-Piemont (and Valais) oceans were metamorphosed after ~60-65 Ma (Fig. 9b), i.e. postdate the subduction of the Sesia Zone. No slices were recovered from depth between the start of subduction at 100-95 (chapter 2.3) and 65 Ma. The contrasting rock recovery between S and MUM units through space and time also testifies to different mechanical coupling states between the subducting slab and the thinner HP/LT slices rising towards the surface. Strain localization steps down deeper into the subducting slab, to reach the slab mantle and scrape off the MUM units (see § 5), only near the end of oceanic subduction.

—(3): A more detailed restoration of the subduction configuration for the Western Alps is proposed at ~60 Ma (Fig. 11a), after subduction and partial exhumation of the Sesia micro-continental sliver. This idealized section is composite since the Sesia Zone is projected here onto the southern Western Alps traverse. Assuming convergence velocities around 1-2cm/a, burial of the MUM eclogitic units to 80 km

depth required ≥4 Ma. If the average estimate for their peak burial is 45 Ma (Fig. 6b), then these units started to subduct near 50 Ma. The Lanzo massif, regarded by many as closer to Sesia, may have reached its peak slightly before if an older age is confirmed (52-46 Ma; Rubatto et al., 2008).

Assuming the same 1-2cm/a convergence velocity, the ~5 Ma difference between the MUM and Internal Basement Complexes (these reached their peak depth on average by 38-42 Ma: Fig. 9b) suggests that they were located ≤~50-100 km apart and places the MUM not far outboard of the continent (Figs. 3a,11a). With this velocity, the entrance of the (thinned) continental margin must have taken place ~5 Ma before, hence precisely when the MUM were at peak pressure conditions (45 Ma). This supports a causal link between the detachment of MUM units from the sinking slab and the entrance of the continental margin. The faster exhumation velocities, tighter P-T loops (Fig. 9a) and spatial association of the MUM units with the HP-UHP continental IBC is therefore not fortuitous**.** Data suggest that (i) the entrance of the continental margin at ~45 Ma (Fig. 9c) triggered the detachment of MUM units from the slab, possibly facilitated by their discontinuous and/or OCT nature, and that (ii) the detachment and exhumation of HP-UHP continental rocks from the sinking plate dragged back the MUM units along the plate interface during part (or all) of their return path (Fig. 11steps 2-3, Fig. 9c).

— (4): Final exhumation of the deep-seated MUM units took place through major extensional shear zones such as those separating the blueschist from eclogitic units in the Queyras and Cottian Alps (Figs. 5a-b,7b; e.g., Kienast, 1983; Ballèvre et al., 1990; Ballèvre and Merle, 1993; Reddy et al., 1999). Most of the exhumation took place prior to the onset of collision of the Briançonnais and Liguro-Piemont oceanic units with the External Massifs (c. 34-32 Ma; Fig. 6b). In a broader orogenic perspective, the Alpine belt can be seen as the result of the imbrication of three successive, different scale accretionary/decoupling systems (A-B-C, Fig. 9c): oceanic (between the S and MUM units), crustal (between continental sediments of the Briançonnais and the deeper subducted crust making the Internal Basement Complexes), and finally lithospheric (with the Ivrea indenter during collision).

4.2. Lateral variations of subducted oceanic fragments along the Alps

The Alpine subduction record of the Central and Eastern Alps (Figs. 1,12) appears far less abundant and lacks the many spectacular eclogites of the W Alps. But those oceanic remnants are similar in that:

(i) No subducted fragment is recovered from the first part of the subduction history (Fig. 9b; i.e., ~100-95 to 70 Ma in the Western Alps, ~100-65 Ma in the Central Alps).

(ii) They align along the same subduction P-T gradient as for the Western Alps (Fig. 10). Maximum pressures differ significantly: no deeply buried rocks are recovered east of the Simplon/Lepontine Central Alps (Berger and Bousquet, 2008; Fig. 10). Before proceeding further with the comparison between the different Alpine transects, a brief overview of the key information on the Central and Eastern Alps is provided here (Fig. 12; see references for details).

4.2.1. Complementary information from the Central and Eastern Alps

— Lepontine dome:

Along the western Central Alps, near the Lepontine dome (Fig. 1), both the Liguro-Piemont and Valais subducted oceanic fragments have been largely overprinted by later collisional metamorphism (Bousquet et al., 2004; Engi et al., 2004; Wiederkehr et al. 2008, 2009, 2011). This is for example the case in the Centovalli area (Northern Steep Belt; Colombi and Pfeifer, 1986; Engi et al., 2004). Some metasediments from the Valais domain located close to the Simplon line nevertheless preserved P-T conditions around 1.3 GPa and 400°C (Visp, Fig. 12a; Bousquet et al., 2008).

— Central Alps (eastern part):

- The Valais domain is largely exposed in the Grisons, with a ~10 km thick pile of strongly deformed, blueschist facies metasediments (i.e., the Valais Bündnerschiefer; Frey and Ferreiro, 1999). Two large scale units are recognized, the Grava and Töimul nappes (Weh and Froitzheim, 2001 and references therein). Metasediments host Fe-Mg-carpholite and chloritoid, and P-T conditions were estimated at 1.2-1.4, GPa, 350-400 °C (Bousquet et al., 1998, 2002; Wiederkehr et al., 2008, 2011). Peak burial occurred at 42-40 Ma (Wiederkehr et al., 2009). The

collisional overprint significantly increases from east to west and towards the Misox root zone (Figs. 12a,b; Wiederkehr et al., 2011).

- The Liguro-Piemont domain is represented by a composite stack of different units (Fig. 12b; e.g., Froitzheim et al., 1994, 1996). From bottom to top, it comprises (i) the metasedimentary Avers Bündnerschiefer unit (locally with blue amphibole or garnet-chloritoid; Oberhänsli, 1978; Ring, 1992); (ii) the Malenco and Platta units, mostly made of mafic and ultramafic bodies, which are found at the bottom and top, respectively, of the Margna-Sella micro-continental block subducted to blueschist facies conditions (and considered an equivalent of Sesia); (iii) a ~ km-thick Arosa zone characterized by mixed lithologies, with both oceanic and continental fragments (Ring et al., 1990). The Arosa zone has been interpreted as marking the fossil plate interface of the Alpine subduction zone (Ring et al., 1990; Bachmann et al., 2009b), with P-T conditions increasing north to south from Davos (almost non-metamorphic) to St Moritz (~0.6 300°C).

The Avers Bündnerschiefer were subducted to 1.1-1.3 GPa, 350-400°C (Fig. 12c; Ring, 1992). The Malenco ultramafic massif is a piece of exhumed sub-continental mantle (Fig. 12d; Trommsdorff et al., 1993; Münterner and Hermann, 1996) later subducted to depths approximately comparable to those reached by the Margna-Sella former extensional allochton (Manatschal and Froitzheim, 1997), i.e., ~0.9 GPa 360°C (Fig. 12c; Ioannidi et al., 2020). Below the Malenco ultramafic massif, the km^2 Lanzada tectonic window exposes a fragment of eclogitized metagabbro (~2 GPa, 525°C). Its paleaogeographic origin is uncertain, but thought to represent the southernmost extension of the Avers unit (Droop and Chavrit, 2014). Subduction of the Malenco massif is bracketed between 63 and 55 Ma (Picazo et al., 2019). The Platta OCT (Fig. 12d; Manatschal and Müntener, 2009; Mohn et al., 2011) experienced only HP greenschist-facies metamorphism (Handy et al., 1996).

These observations can set back in a schematic restoration of the subduction configuration for the Central Alps at ~60-55 Ma (Fig. 12e) Above the Arosa zone, a long-lived record of syn-subduction deformation is documented in the upper plate (e.g., Bernina AustroAlpine units; Figs. 12a,b; Bachmann et al., 2009a, their figure 3), mostly between ~80 and 60 Ma. In contrast, (de)formation of the Arosa zone is thought to date back to the very last stages of oceanic subduction, between 58 and 47 Ma (Bachmann et al., 2009a), immediately prior to continental subduction of the Briançonnais domain (around 50 Ma).

These observations are interpreted as marking a switch to short-lived subduction accretion, following ~20 Ma of subduction erosion reflected by the reworking of the base of the AustroAlpine upper plate, the relatively small amounts of flysch-type sediments or the mode of deposition of the Coniacian-early Eocene Gosau basins (Wagreich, 1995; Wagreich and Decker, 2001). Age constraints are lacking, however, to assess when the underplating of the Avers Bündnerschiefer took place. Closure of the Liguro-Piemont domain could be slightly diachronous, from ~50-45 Ma in the Grisons (Bachmann et al., 2009a) to ~40 Ma in the Western Alps (see § 3.3 and 4.1).

— *Engadine window*

This tectonic window exposes the Valais and Liguro-Piemont domains separated by the easternmost units of Briançonnais affinity (Fig. 12a). Both units comprise mostly metasediments, with subordinate ophiolitic material restricted to metabasalts. Diagnostic mineralogy includes Fe-Mg-carpholite and rare lawsonite or glaucophane (Bousquet et al., 1998). P-T estimates for the Valais domain are close to those for the Grisons (and Avers), i.e. 1.1-1.3 GPa, 350-375°C (Fig., 12c; Bousquet et al., 1998) and show a similar age (42-40 Ma; Wiederkehr et al., 2009).

— *Eastern Alps, Tauern window*

Some blueschist facies ocean-derived metasediments crop out in the Tauern window and were attributed to the Valais (Glockner nappe) and Liguro-Piemont units (Reckner ophiolitic Complex and Matreier zone, respectively in the northwest and south-central part of the window; Fig. 1a; Zimmermann et al., 1994; Berger and Bousquet, 2008; Rosenberg et al., 2018). In the absence of a Briançonnais domain, the distinction between the Valais and Liguro-Piemont units is difficult (Schmid et al., 2013). These oceanic fragments, particularly the Glockner nappe, experienced significant heating on exhumation and are commonly strongly retrogressed, with lawsonite pseudomorphs at most (Hoinkes et al., 1999). P-T estimates for peak burial lie around 0.9 and 370°C for the oceanic Matreier Zone (Koller and Pestal, 2003). The Bündnerschiefer and mafic/ultramafic units from the Upper Schieferhülle (Glockner nappe) are generally considered to have reached pressures ≤1 GPa (Berger and Bousquet, 2008), showing a large pressure gap with the continent-derived Eclogite zone below. However, some eclogitic units with P-T conditions

around ~1.7 GPa at 570 °C have been attributed by some authors an oceanic origin, thus raising some doubts on the exact maximum pressure (Dachs and Proyer, 2001; Gross et al., 2020). These deeper buried slices of oceanic metasediments (~2 GPa, 500°C; lower Glockner unit; Groß et al., 2020) represent fragments entrained and deformed during continental subduction and exhumation of the distal European margin. As for the eastern Central Alps, some lower Austro-Alpine units, together with the Reckner ophiolitic Complex (Schmid et al., 2013), were entrained in subduction between 0.8 and 1-1.1 GPa at 350-400°C around 50 Ma (Dingeldey, et al., 1997), well before the 35-30 Ma continental subduction (Christensen et al., 1994).

— *Rechnitz window*

The Rechnitz window provides the easternmost outcrops of Liguro-Piemont subducted fragments, with modest P-T conditions of 0.9-1.0 GPa 370°C (Koller, 2003). These were reached at 57 ± 3 Ma (Ratschbacher et al., 2004).

4.2.2. Along strike changes

Marked contrasts regarding S and MUM type units exist along the strike of the orogen:

— Underplating of metasedimentary-dominated units, in the Bündnerschiefer (mostly Valais) and the Schistes Lustrés (Liguro-Piemont) units is observed all along the belt. Most units experienced P-T conditions around 1-1.3 GPa and ~ 350-380°C (Fig. 9b; from east to west: Tauern, Engadine, Grisons, Valaisan, Combin, and the upper S units of the Maurienne/Cottian/Queyras) corresponding to the worldwide peak of recovery at ~30-40 km for sedimentary piles (i.e., depths with changes in mechanical coupling; Agard et al., 2018). More unique is the underplating of several units at different depths in the Western Alps, south of Gran Paradiso (§ 3.1).

All these units were accreted between ~60 and 35 Ma (Fig. 9b), with evidence for underplating near 60 Ma in the eastern (~57 Ma; Rechnitz window; Ratsbacher et al., 2004) or the south-western Alps (60-55 Ma; Cottian Alps; Agard et al., 2002). The amount of underplated material varies along strike: from up to 10 km in the NE Valais (e.g. in the Grisons; Frey and Ferreiro, 1999; Weh and Froitzheim, 2001) to a few hm in the SW (Valaisan units; Bousquet et al., 2002), and from the km-scale in the

949 Liguro-Piemont Central Alps (Avers) and north-western Alps (Combin) to several km
950 in the south-western Alps (Maurienne to Queyras).
951 — Mafic/ultramafic-dominated units are found all along the belt, but differ
952 significantly between the Western Alps and further east. While extensive eclogite
953 facies bodies are exposed in the Western Alps, MUMs are volumetrically
954 insignificant, blueschist facies and reaching ~1 GPa at most in the Central and
955 Eastern Alps (save possibly for the small Lanzada window, Figs. 12a,c). MUMs of the
956 Western Alps tend to cluster around similar eclogitic conditions and are only
957 recovered late in the oceanic subduction history (peak burial ~45 Ma; Fig. 9b),
958 immediately prior to continental subduction. In contrast, P-T conditions vary in the
959 eastern Central Alps (Platta, Malenco) and subduction ages are somewhat older (60-
960 50 Ma). The unmetamorphosed, isolated and small Chenaillet massif (Fig. 7b;
961 Manatschal et al., 2011) is somewhat of an outlier, similar only to the northern extent
962 of Platta, accreted in the subduction forearc or obducted. Metamorphic soles typifying
963 obduction (Spray, 1984; Wakabayashi and Dilek, 2003) are nowhere found in the
964 Alps, but this may not be diagnostic since they are not expected to form in slow-
965 spreading oceans (Agard et al, 2016). In all zones MUM correspond to portions of
966 discontinuous oceanic lithosphere, OCT and/or exhumed subcontinental mantle.
967 These characteristics favor later recovery, as reflected by the subducted rock record
968 (see Agard et al., 2018).
969 These observations, when superimposed with maps of metamorphic facies for
970 the subducted oceanic fragments (Fig. 13a-c), reveal zones with contrasting
971 histories:
972 — areas where MUM are preferentially recovered, and the only ones where
973 eclogitic MUMs are found, coincide with the spatial extent of the subducted micro-
974 continental Briançonnais and Sesia domains (see also § 4.2.3). Subduction of Sesia
975 (~75-65 Ma) furthermore represents a major divide in the ~ 100-40 Ma period of
976 oceanic subduction, with no recovery of subducted oceanic rocks before (Fig. 9b).
977 These observations suggest a strong influence of both margin segmentation and
978 continental subduction.
979 — The relationship between the amount of oceanic MUM and continental
980 subduction can be scrutinized further: more MUM units are recovered in the vicinity
981 of the Gran Paradiso-Monte Rosa Internal Basement Complexes (and the Sesia
982 Zone) than around Dora Maira. Dora Maira is the only Internal Basement Complex

for which (i) one unit shows UHP conditions (the Brossasco-Isasca unit), with peak pressure larger than that of adjacent MUMs and (ii) five to six distinct hm- to km-thick slices were recognized (Henry et al., 1993; Compagnoni and Rolfo, 2003). The thinner Dora Maira slices, hinting to a more extended portion of the Eureopean basement (forming the Briançonnais), may have been more readily and deeply subducted (hence in part UHP) yet not buoyant enough to help return dense MUM units.

— On the other hand, continental subduction in the Western Alps was not greater than in the Central Alps: the Briançonnais-derived nappes (Tambo, Suretta) and even the more external European margin-derived units (Adula) reached the greatest depths in the Alps (~4-5 GPa in Alpe Arami or Gagnone; Frey et al., 1999; Figs. 12a,b), and not much later (peak burial of the Adula nappe by ~38-35 Ma; Herwartz et al., 2011; Sandmann et al., 2014). While the Central Alps oceanic fragments are strongly overprinted by collisional (Lepontine, barrovian) metamorphism into variegated facies (Engi et al., 2004), there is no indication that these rare MUM slivers were buried to pressures as high as in the Western Alps. The initial lithological nature of the oceanic rocks (e.g., OCT with variable proportions of mafic crust) and/or the geometrical configuration of the margin (e.g., presence of Sesia) therefore probably play a primary role in promoting chances of rock recovery.

4.3. Four distinct sectors: paleogeographic contrasts in subduction dynamics

Based on first-order contrasts in subducted-related history, and with some reservations due to inevitable P-T-t-d-cartographic-paleogeographic uncertainties, it is possible to identify several distinct sector along the Alpine belt (Fig. 13):

— *Sector A*, *south of Gran Paradiso* (along CIFALPS and south of the ECORS geophysical proflles; Fig. 1a), encompasses the Queyras, Cottian, Maurienne, Rocciavre, Monviso and Dora Maira sectors of the internal Alps. This sector is characterized by S units subducted across a range of depths and recovered across a relatively long period (~60-40 Ma), by the presence of pluri-km large gabbroic bodies (Rocciavre, Monviso) and, compared to the other sectors, a lesser influence of collision. It shows, at least from present exposures, the longest (mid-Penninic) Briançonnais margin subducted between high-grade blueschists and eclogites, with

Ambin, Acceglio and Dora Maira (see the detailed reconstruction by Michard et al., 2004). The Dora Maira IBC is the only Briançonnais-derived continental UHP massif and the most composite one, with five or six slices including one UHP slice. There is almost no Valais domain along this sector (Fig. 8a-c).

— *Transect B, Gran Paradiso and NE Monte Rosa* (and possibly into the western Central Alps; along the NFP20-W profile), encompasses the most voluminous MUM massifs (Zermatt-Saas, Antrona, Avic, Lanzo), which also show the largest individual mantle-dominated bodies (Lanzo, Avic). The S units are less abundant than in sector A and maximum pressures far less variable. No ages older than ~45 Ma were found for these metasedimentary units. The Gran Paradiso and Monte Rosa Internal Basement Complexes record P-T conditions similar to or slightly lower than the MUM units. Neither of them is UHP nor shows a complex stack of units (two only in Gran Paradiso; Manzotti et al., 2015). This sector is characterized by the presence of the subducted continental Sesia Zone (± Ivrea-Canavese), which is located in a more internal position (hinterland) than ocean-derived units. This sector is also where very low-grade nappes stacked in the Préalpes preserve a record of accretionary wedge formation; and where the Ivrea body, interpreted as a shallow piece of upper plate mantle, is also found (Fig. 13c).

— *Transect C, (eastern) Central Alps and Engadine window* (along the NFP20-E profile), is overall metasedimentary-dominated and oceanic fragments reached maximum pressures around 1.2-1.3 GPa. The S units can be several km thick but are not subdivided as much (yet?) as in sectors A or B. The MUM remnants are made of recognizable and well-characterized OCT and subcontinental mantle which were not deeply subducted. Subducted oceanic remnants are younger than 65 Ma (although subduction initiated ~100 Ma; Bachmann et al., 2009a). A continental sliver, Margna-Sella, smaller than the Sesia Zone, is present in the same structural position. Contrary to sectors A and B the Briançonnais massifs are fairly restricted (Tambo, Suretta; absence of Internal Basement Complex). On the other hand, the very distal European margin experienced locally UHP conditions (e.g., 4-5 GPa in Alpe Arami).

— *Transect D, east of the Engadine window* (i.e., along the TRANSALP profile), only preserves volumetrically small subducted fragments of the Alpine ocean (e.g., Matrei, Rechnitz) with maximum pressures around 1.2-1.3 GPa. There is no Briançonnais domain. The European margin was subducted as along sector C but far less deep

(e.g., 1.8 GPa in the Eclogite zone). This sector also coincides with the area affected by the former Eoalpine (Cretaceous) metamorphism in the Austro-Alpine nappes

For sectors A and B, the eclogitic facies MUM units are closely related to the Internal Basement Complexes. UHP conditions in Penninic domains (oceanic: Cignana; continental: Dora Maira) are only found in these two sectors. There is evidence for subduction erosion of the upper plate basement in sectors B-C-D, marked by prolonged deformation and recovery of subducted micro-continental slivers at 55-50 Ma at the base of the Austro-Alpine domain (B: Dent Blanche, Angiboust et al., 2014a; C: Bernina, Bachmann et al., 2009a; D: Tauern, Dingeldey, 1997; see also Polino et al., 1990).

These lateral contrasts in subduction dynamics along the Alpine belt are depicted in a snapshot of the Alpine oceanic subduction at ~40 Ma, towards the end of oceanic subduction (Fig. 14, to be compared with Fig. 3a). Further work could help determine whether this segmentation of the former Alpine subduction zone chiefly results from (i) margin segmentation inherited from the Variscan orogeny (Pfeifer et al., 1989; von Raumer et al., 1999, 2002; Manzotti et al., 2016; Ballevre et al., 2018), (ii) rifting processes and/ or magmatic production (Mohn et al., 2011), (iii) differential response during material subduction, i.e. mechanical (rheology) or chemical (via fluid liberation), (iv) differential kinematics and/or (v) sedimentary inputs.

5. Alpine insights into subduction interface processes

The good preservation of subducted fragments and of at least some of the Alpine subduction architecture allows tracking processes occurring along the plate boundary during active subduction, e.g. strain localization and fluid transfer (Fig. 15a). The section below provides a provisional overview of such investigations on S and MUM units, and sets them back into the tectonic frame described above (Fig. 15b) and against other fossil subduction zones (e.g., Bebout and Penniston-Dorland, 2016; Scambelluri et al., 2019).

5.1 Insights onto plate interface dynamics

Changes in mechanical coupling between the sinking slab and the overlying mantle wedge have a strong impact on strain partitioning across the plate interface (Agard et al., 2018): when the interface is perfectly decoupled strain is localized on the subduction fault; when it gets locked, strain becomes distributed across some distance and develops either (1) downward into the slab, promoting off-scrapping, underplating and potential rock recovery via subsequent exhumation or (2) into the upper plate base, removing material entrained at depth by subduction 'erosion' (or basal erosion; Fig. 15a).

The Alpine example provides evidence for both:

- Stacking of the S units demonstrates significant underplating at depths >20-40 km in the Alps (Fig. 11a; Bousquet et al., 1998, 2002; Agard et al., 2001a; Seno et al., 2003, 2005; Plunder et al., 2012; Angiboust et al., 2014a). This implies tectonic decoupling between sediments and mafic/ultramafic protoliths, as in other fossil subduction complexes (e.g., Sanbagawa-Shimanto, Japan; Franciscan complex, California; Kimura and Ludden, 1995). Similar decoupling between the rising MUM units and the downgoing slab mantle took place near 80 km depth (Figs. 8c, 15b). Both suggest activation of deep décollement horizons, analogous to their shallow counterparts in present-day or fossil shallow accretionary wedges (e.g.; Nankai, Japan; Makran, Iran; Helminthoid flysch, Western Alps).

- On the contrary, long-lived reworking of the base of the AustroAlpine nappes argues for subduction erosion for some period of time (e.g., Bachmann et al., 2009a) for three of the Alpine sectors (B-D; Fig. 14). This is consistent with the relative lack of rock recovery in the eastern Central Alps before ~60-55 Ma.

Whether strain (re)localization operates through seismic activity or rather via distributed shear, and what role fluids play in the process is not well known yet (see Agard et al., 2018; Menant et al., 2019). Pseudotachylites produced by past earthquakes during oceanic subduction were documented in the Alps both at shallow depth in the upper plate (Austro-Alpine: Bachmann et al., 2009a; for cataclstic deformation: Angiboust et al., 2015) and in dry protoliths from the downgoing slab at eclogite facies conditions in Lanzo (~80 km depth; Scambelluri et al., 2017). In Monviso, eclogite breccia formed at ~80 km depth during subduction testify to the existence of discrete brittle and possibly seismic events along newly formed shear zones near the top of the slab (Angiboust et al., 2012a). This brecciation operates though several discrete steps/events and preludes to the detachment of the large

tectonic slice of the Lago Superiore from the slab (Figs. 8,15b; Locatelli et al., 2019b). Diffusion modelling suggests that the whole brecciation process lasted ≤ ~ 2Ma and that healing of the fractures may be on the order of 100 ka at most (Broadwell et al., 2019).

5.2 Insights onto element budgets in subduction zones

Alpine sedimentary, mafic and ultramafic protoliths were used to assess systematic element changes across depths, estimate element budgets or fingerprint exchanges between lithologies through trace element concentrations of large lithophile and fluid-mobile elements (LILE and FMEs) or isotopic signatures (H, Li, B, C, N, O, Cl, S, Fe and Zn). The assessment of element/fluid budgets across the plate interface is however limited by the absence of mantle wedge fragments in the Alps (as for most subducted complexes worldwide).

The relatively continuous suite of P-T conditions of the Cottian metasedimentary units (Fig. 7e) has been used to monitor chemical changes with depth. They evidence significant element retention, with strong preservation of LILE (K, Rb, Ba and Cs), N, Li and Sr (but loss of As and Sb; Busigny et al., 2003; Bebout et al., 2013; Barnes et al., 2019), at odds with trends observed for the Franciscan subduction complex marked by intense devolatilization (Bebout et al., 1999; Bebout, 2007). This high element retention (Bebout et al., 2013) may reflect the contrast between the cold and steady Alpine subduction gradient (~8°C/km; Figs. 7e,10) and the warmer and transient gradient of the Franciscan. Efficient carbon sequestration was also documented, both in blueschist facies metasediments (>80-90%; Cook-Kollars et al., 2014; Lefeuvre et al., 2020) and in basalts and ophicarbonates across grade (Collins et al., 2015), suggesting that any significant decarbonation (e.g., Kelemen and Manning, 2015) must take place deeper, at sub-arc depths.

Evolution of fluid chemistry with depth documented by fluid inclusions suggests the existence of moderately saline fluids in metasedimentary blueschists and hypersaline fluids in mafic eclogites (Scambelluri et al., 1997; Philippot et al., 1998; Agard et al., 2000; Scambelluri and Philippot, 2001). Fluid inclusions also provide evidence for carbon dissolution at UHP conditions (Frezzotti et al., 2011). The release of hypersaline and/or sulfate-rich fluids during prograde metamorphism of

serpentinites (Monviso-Queyras traverse; Schwartz et al., 2013) may in addition oxydyze the mantle wedge (Debret et al., 2016).

5.3 Insights onto scales of fluid mobility

The wealth of HP-LT metamorphic veins at seismogenic zone depths, i.e. ~ 30-35 km in the S units (e.g., Lefeuvre et al., 2020) or intermediate depth near ~80 km in the MUM units (omphacite veins; e.g., Monviso; Philippot and Kienast, 1989; Spandler et al., 2011), attests to considerable fluid mobility within oceanic subducted fragments. In the S units, the lack of significant isotopic shift in volatiles (C, O, H) nevertheless suggests limited external fluid infiltration (for the Cottian, Maurienne and/or Combin: Henry et al., 1996; Cook-Kollars et al., 2014; Epstein et al. 2019), except along major tectonic contacts (Jaeckel et al., 2018). Similarly, mafic rocks from Monviso or Zermatt-Saas MUM units show local, mm-cm-scale fluid derivation, and even strong preservation of primary hydrothermal alteration signatures (Nadeau et al., 1993; Selverstone and Sharp, 2013). Most fluids percolating through these oceanic fragments appear internally-derived and/or derived from similar lithologies, in support of closed-system behavior at the meter scale and possibly up to the 100 m-scale (Fig. 15b), at least for components other than H_2O.

Many observations nevertheless point to a more complex interaction between sedimentary, mafic and ultramafic lithologies (Fig. 15b). In serpentinized peridotites from the Queyras, a trap-and-release mechanism was proposed to account for the enrichment of serpentinites in B, Li, Cs, As, Sb (at T<~360-390°C) by fluids derived from nearby metasediments, and their progressive loss at higher temperature with crystallization of antigorite (Lafay et al., 2013). Specific enrichments in Ba, Rb, U, Cs, and Pb in serpentinites from the Combin and Lanzo areas were also interpreted as reflecting the influx of sedimentary-derived fluids (Barnes et al., 2014). Differential release of fluids from metasediments or serpentinites with temperature could moreover exert a complex control on decarbonation (Queyras: Debret et al., 2018).

Contrasting ultramafic/sedimentary contributions are documented when comparing Monviso, Lanzo and Zermatt-Saas (Gilio et al., 2020). In Monviso, km-scale shear zones cross-cutting metagabbros evidence a major influx of serpentinite-derived fluids (Spandler et al 2011; Angiboust et al., 2011) with additional

contribution from metasediments (Rubatto and Angiboust, 2015). The influx of external-derived fluid appears transient and episodic in both metagabbros and eclogite breccia, and partly achieved via brittle fractures: incremental brecciation forms successive matrices recording internally- and then externally-derived fluids (Locatelli et al., 2018, 2019b), whose formation may short-lived (i.e., a few 100 ka; Broadwell et al., 2019). Ingression of externally-derived fluids occurs once sufficient brecciation has enabled full-scale connectivity across the shear zones (i.e., permeability, fluid ingression and strain localization; after formation of the M2 matrix in Fig. 8b; Locatelli et al., 2019b).

6. What did we learn?

6.1. A faithful and useful subduction record

6.1.1. A reliable proxy for the subduction of oceanic lithosphere

The present study confirms that HP-LT oceanic fragments from the Alps provide a reliable P-T record diagnostic of cold subduction zones worldwide, one of the most extensive fossil examples so far. Several reasons allow to rule out significant tectonic overpressure in subducted Alpine fragments (see also Froitzheim, 2020):

(i) Subducted remnants consistently align along the same P/T gradient (Fig. 10). Any significant overpressure would engender variable P/T ratios in the oceanic rock record (and in the Internal Basement Complexes, which align along the same P/T gradient). This P/T gradient is also typical of mature subduction worldwide (Agard et al., 2018).

(ii) Maximum recorded pressures for mafic eclogites (~2.8-3 GPa) correspond to the threshold beyond which slab crust becomes negatively buoyant with respect to the surrounding mantle (Agard et al., 2009; Angiboust and Agard, 2010) and fully coupled to the upper plate (Wada et al., 2008; Agard et al., 2020). The match between the depth inferred from thermodynamic pressure and the depth of viscous coupling, at 80-90 km, strengthens the conclusion that overpressure is limited.

(iii) Mineral parageneses found either in rheologically weak (sediments) or strong material (mafics and ultramafics) yield the same pressure estimates. The

spatial distribution of pressures is also non random, as shown by the clear W-E gradient in the Western Alps or within a given unit (e.g., upper S unit: Figs. 2b, 7c-e).

All this, however, does not preclude local but minor overpressure. The hm-thick Cignana UHP sub-unit could reflect overpressure of at most ~10% (3.2 vs. 2.8 GPa; Fig. 9a; or represent a deeper thin strip of slab).

6.1.2. A direct access to subduction interface processes

Structural relationships and P-T-time-lithostratigraphic-petrological data preserve a good access to the subduction history: the collision-related metamorphic overprint is moderate or insignificant in many places (e.g., Berger and Bousquet, 2008); the distribution of tectonic units and deformation shows that subduction structures are not completely messed up. The organization of Alpine fragments does not result from some large-scale 'mélange' process in a subduction channel (unlike Cuba or Sistan: Garcia-Casco et al., 2002; Bonnet et al., 2018) but corresponds to tectonic slices/imbrications formed along the plate interface which were later variably disrupted by deformation (Angiboust and Agard, 2010; Tartarotti et al 2017, 2019; Agard et al., 2018; Locatelli et al., 2018; see models by Ruh et al., 2015). These features allow studying:

(i) the former geometry of the plate interface, in some places at the hm-km scale, such as the down dip geometries of metasedimentary-dominated units south of Gran Paradiso, the geometry of OCT domains and/or specific horizons, or the shallow accretion of the Préalpes and Helminthoid flyschs.

(ii) dynamic processes such as underplating, strain localization or subduction rheology. Dominant underplating at ~30-40 km (1 GPa), for example, could either be coupling-dependent (i.e., driven by some upper plate Moho barrier and/or fluid-related process) and/or buoyancy-controlled (e.g., assisted by joint subduction with lower density extensional allochthons). Rheological contrasts between specific sedimentary horizons may explain preferential localization of décollements in metapelite- or carbonate-dominated sequences (e.g., Vannucchi et al., 2017), hence the successive accretion of the upper (more pelitic) and middle (more carbonate-rich) S units. Alternatively, strain localization could be chiefly controlled by fluids (Kimura and Ludden, 1995. Menant et al., 2019) or mineral reactions, as suspected from fluid redistribution associated with the growth of lawsonite veins, lawsonite breakdown or

garnet formation (Dragovic et al., 2012; Vitale-Brovarone and Agard, 2013; Vitale-Brovarone et al., 2014b; Lefeuvre et al., 2020).

6.1.3. A window onto fluid-rock interactions along subduction zones

The Alpine archive can contribute to refining the picture of element/fluid transfer along the slab in cold subduction environments (Fig. 15b; Spandler and Pirard, 2013; Bebout and Penniston-Dorland, 2016; Scambelluri et al., 2017, 2019):

(i) The frequent preservation of chemical and isotopic signatures advocates for relatively closed system behaviour except along some shear zones in both S units (Henry et al., 1996; Lafay et al., 2013; Barnes et al., 2019) and MUM units (Spandler et al., 2011; Locatelli et al., 2019b). Rock hybridization appears limited except at primary sedimentary/mafic/ultramafic lithological contacts and heterogeneities, as shown by syn-subduction Ca□metasomatism of metagabbros in former sedimentary mélanges (Avic: Tartarotti et al., 2019; Corsica: Vitale-Brovarone et al., 2014b; Piccoli et al., 2018) or in metasomatic rinds formed along shear zones (Angiboust et al., 2014b). Mass-balance calculations are probably fraught with large uncertainties, however, given the variations in bulk composition of slow-spreading oceans (e.g., serpentinite to sediment ratio).

(ii) Fluid flow appears to be episodic (Spandler et al., 2011; Angiboust et al., 2012a; Locatelli et al., 2018). External fluid ingression accompanies progressive strain localization across shear zones (Locatelli et al., 2019b). Fluid (re)distribution amongst the various protoliths is probably complex, however, since hydration of relatively dry protoliths (e.g., Allalin gabbro, Zermatt-Saas unit; Bucher and Grapes, 2009) may coincide with dehydration from nearby rocks (e.g., metapillows; Angiboust and Agard, 2010).

6.1.4. An access to along-strike segmentation

The along-strike contrasts in subduction dynamics of sectors A-D can help refine the initial setting/paleogeography of the Alpine subduction (Fig. 13; see § 4.3): the Briançonnais continental margin was likely more stretched along sector A during rifting (i.e., Dora Maira); the presence of the Sesia Zone resulted in specific subduction dynamics along sector B; its subduction triggered a change in boundary conditions which initiated the recovery of oceanic rocks (~60-40 Ma). Figure 13c shows, in addition, that these lateral contrasts largely persisted during continental

subduction and collision (as shown, for example, by the Préalpes and Ivrea body located along sector B).

From ~65-60 to ~50 Ma, subduction appears to have been erosive along sectors B-D (particularly in the eastern Central Alps) but accretionary along sector A. During the first period (pre-Sesia subduction), the Alpine subduction was either (entirely?) in erosive mode, sediment starved and/or efficiently lubricated so that underplating was impeded at depth.

These lateral contrasts could be ascribed to inherited structures (Variscan- or rifting-related), differences in incoming material impacting subduction (nature, proportions; e.g., sediment input, magmatic production) or differential kinematics. The present-day Chilean example shows such lateral contrasts in accretionary/erosive mode and sediment input along one single subduction zone (Maksymovicz, 2015). The four A-D sectors recognized here may be further tied to geophysical slab imaging to read through tomographic images and assess some of the later, Oligocene to Present evolution of the Alpine slab (Handy et al., 2010; Hétenyi et al., 2018).

Worthy of note, the Alpine example shows that slab retreat, which may assist exhumation (Brun and Faccenna, 2008), did not trigger the offscraping from the slab (see also Agard et al., 2018): the detachment of the MUM units, shortly followed by exhumation, occurs only when subduction dies out. And there was no S unit returned during the first 30 Ma, a long enough period for the slab to retreat (nor is there any exhumation of HP-LT rocks in retreating subduction zones from south-east Asia).

6.2. Why such a profuse subducted record? How (a)typical is the Alpine example?

6.2.1. Why are so many HP-LT oceanic fragments returned and is this abnormal?

It should first be stressed that subducted fragments are abundant only in the Western Alps (Fig. 13a) and that no oceanic rocks were recovered between the onset of subduction (~100 Ma) and ~60 Ma. It only started after suduction of the Sesia Zone (Fig. 9b). Subduction may have been more 'classical' before 70-65 Ma, i.e. not returning anything, as many large-scale subduction zones today (e.g., Chile or Japan). The 165-150 Ma cluster of Liguro-Piemont magmatic ages (Fig. 3d) shows that the oceanic lithosphere formed between ~150 and 120 Ma (even possibly with

thicker crust) was entirely subducted, over roughly the same amount of time (~30 Ma, from ~100 to 70 Ma).

The local abundance of subducted oceanic fragments most likely results from the slow-spreading character of the ocean and the presence of OCT domains. This configuration provides many primary discontinuities/weaknesses facilitating later strain localization and offscraping along the subduction interface (Ruh et al, 2015), together with relatively buoyant material. The separation between sediments and crustal fragments, on the one hand, and between mafic/strongly serpentinized ultramafic and a drier mantle, on the other hand, appears most effective. The Alpine record is indeed characterized by (i) a marked contrast between units that are metasedimentary-dominated (S units) and others representing km-thick portions of slab lithosphere (MUM units); (ii) a contrast in their relative timing of burial and exhumation; (iii) the role of continental margin subduction on initiating detachment from the slab (and partly exhumation; Fig. 11); (iv) the preferential recovery of OCT domains (as for Corsica; Vitale-Brovarone et al., 2013, 2014a).

The Alpine situation stands in contrast with large-scale subduction zones from fast-spreading oceans characterized by a more regular ocean-plate stratigraphy (Kusky et al., 2014; Wakabayashi, 2015, 2017). For these, underplating (and/or shallow accretion) is commonly restricted to slivers of metagraywackes with interleaved horizons of metabasalts (Kimura and Ludden, 1995) and to depths of ~30-40 km. This is the case in subduction complexes from the Sanbagawa-Shimanto belt (Japan; Yamaguchi et al., 2012), Kodiak-Alaska (Sample and Fisher, 1986; Fisher and Byrne, 1987) or New Zealand (Fagereng, 2011). The Alpine example supports the view that there is a recovery/exhumation filter in the rock record, which preferentially returns eclogitic fragments from slow-spreading oceans or thinned margins (Agard et al., 2018).

6.2.2. Are Alpine subducted fragments informative about subduction processes or rather inherited from earlier stages?

The question, then, is the extent to which the intermittent rock recovery accompanying the subduction of oceanic lithosphere is controlled by plate interface rheology and kinematics or rather by structures inherited from the former (passive) margin, seafloor structure and/or sediment type. The answer probably lies

somewhere in between. While the Alpine record shows that discontinuous oceanic structure, margin segmentation and heterogeneous stretching exert an important control, not every tectonic feature is inherited. New structures (i.e. further damage) form during subduction lifetime as shown, for example, by intermediate depth earthquakes, strain localization along freshly nucleated shear zones, overturned km-scale folds or eclogite breccias genuinely formed along the plate interface (§ 5; Fig. 5; Scambelluri et al., 2017; Locatelli et al., 2018).

The extent to which recovery (i.e., detachment and exhumation) relates to the impingement of the continental margin could be quantified. While increased coupling via continental micro-slivers induces downstepping of the subduction interface (Angiboust et al., 2014a), this process is most likely size dependent: e.g., the 100m-thick and 2 km-long Theodul Glacier sliver (Bucher et al., 2020) did not trigger the recovery of the large-scale Zermatt-Saas units. Determining the size threshold would inform on effective rheological properties. The step down of the décollement deeper into the slab at the end of oceanic subduction shows, in any case, that the plate interface widens and advocates for greater interplate coupling (Fig. 15a).

6.2.3. Some remaining unknowns

The lack of a magmatic arc atop the subduction zone is a long-standing enigma. It was recently associated to the slow-spreading nature of the ocean (McCarthy et al., 2018, 2020). These authors suggested that serpentinization of the upper portion of the sinking lithospheric mantle and efficient decoupling from the dry mantle below had caused its shallow accretion, thereby preventing enough water transfer at depth. Evidence for significant underplating of serpentinized mantle or shallow serpentinite diapirs (such as in the Izu-Bonin subduction zone; Tamblyn et al., 2019) is lacking in the Alpine record. Two alternative explanations may be put forward: (i) 200-300 km of oceanic subduction may not be sufficient to hydrate the mantle wedge at sub-arc depths, depending on the fertility of the sub-continental mantle, and/or (ii) the Alpine slab may have been too short (Fig. 14) to trigger sufficient counter-flow and mantle upwelling, thereby hindering the formation of a magmatic arc (in the Izu-Bonin, the time-lag between subduction initiation and mature arc magmatism corresponds to the time needed for the slab to reach the 660 mantle discontinuity; Ishizuka et al., 2020; see also Agard et al., 2020).

The initiation process of Alpine subduction is unknown, as for (nearly) all subduction zones. Subduction initiation was likely intra-oceanic since initiation next to a continent has not been documented yet (e.g., Leng and Gurnis, 2015). The Alpine subduction archive and paelogeographic record suggest that subduction initiated next to the Adria margin (which also explains subduction of exhumed mantle pieces from Adria; i.e. Lanzo, Malenco). Although intra-oceanic subduction initiation appears most likely, there was either no obduction in the Alpine domain or a different one from that of large-scale ophiolites (as noted by Auzende et al., 1983). Conceivably, it would also be difficult to detect: no diagnostic metamorphic sole is expected to form along a relatively cold subcontinental mantle (Agard et al., 2016) and low rigidity of slow-spreading ophiolite would probably favor short-lived overthrusting.

7. Conclusions

Two hundred years of thorough studies have made the Alps a uniquely detailed and informative orogen. The relatively modest collisional-related thermal imprint across most of the Alps, its simple organization and the 3D nature of the Alpine belt enable restoring a significant part of the history and dynamics of oceanic subduction. Realizing the importance of seafloor (and margin) inheritance has enabled to access even further details of subduction processes. The Alpine record of subducted oceanic lithosphere appears overall quite good and representative:

(1) The Alpine P-T record is representative of subduction processes.

The consistent P/T gradient of oceanic fragments, similar to mature subduction, their recovery below a maximum pressure threshold (2.8-3 GPa), their consistent distribution along spatial gradients and within units, all indicate that the oceanic subduction record can be trusted and used as a reliable proxy of the pressure and temperature regime of subduction (one of the best we have at least), and that tectonic overpressure is limited (<~10%). For example, the Alpine record can inform on how underplating, fluid transfer or subduction earthquakes took place during ~60 Ma of slow-spreading ocean subduction.

(2) Spatiotemporal variations allow reconstructing subduction dynamics.

Significant contrasts exist between (i) underplating of metasediments, locally long-lived and across variable depths (e.g., south-west of Gran Paradiso; Liguro-Piemont ocean) or volumetrically large (e.g., Grisons; Valais ocean), (ii) spikes of rock recovery, as for the large mafic/ultramafic (MUM) eclogitic bodies or (iii) the greater recovery next to micro-continental slivers (Briançonnais, Sesia Zone), which demonstrates a strong influence of margin segmentation and continental subduction. Along-strike contrasts allow recognizing four main sectors, respectively south of Gran Paradiso (A), between Gran Paradiso and NE Monte Rosa (B), between the (eastern) Central Alps and the Engadine window (C), and east of the Engadine window (D).

During the first half of the subduction period, between the onset of subduction (~100-95 Ma) and ~70-65 Ma, no subducted oceanic fragment was recovered; this only started after suduction of the Sesia Zone. Subduction to ~80 km depth of the MUM units of the Western Alps (which represent fragments of oceanic crust formed early at ~165-150 Ma), a few Ma before continental subduction, shows that only oceanic domains next to the continental margin and/or OCT domains are recovered. All other fragments formed between ~150 and 120 Ma have disappeared over a similar amount of time, during the first 30 Ma of subduction. Between ~65 and 50 Ma, subduction erosion is documented along sectors B-D (particularly in the eastern Central Alps) whereas subduction accretion prevailed along sector A. Before that time, the Alpine subduction was therefore either erosive, sediment starved and/or efficiently lubricated (thereby impeding rock recovery).

(3) Preservation of the Alpine subduction record is remarkable but not atypical.

The Alpine subduction record is only exceptional in that it exposes many subducted fragments, particularly in the Western Alps, and documents the closure of a short-lived (60 Ma), slow-spreading, slowly closing ocean. Past seafloor essentially comprised variably refertilized exhumed mantle, irregularly distributed magmatic rocks and pelagic sediments, together with OCT domains and extensional allochtons. Nothing such as the incoming ocean plate stratigraphy observed off Chile or Japan today. In addition to plate kinematics, syn-subduction sedimentation and plate interface rheology, the Alpine record shows that inherited features (i.e., former Variscan- or rifting-related structures, distribution of magmatic bodies/provinces

and/or sediments) largely impacted the subduction dynamics of the oceanic lithosphere.

What the Alpine record examplifies is the preferential recovery of eclogitic fragments from slow-spreading oceans. This conclusion is strengthened by the spectacular subduction-related rock record of the Cyclades/Pindos 'ocean', recently reappraised as a former stretched continental margin (Schmid et al., 2020). In contrast with the Cyclades, however, at least ~200-300 km of real Atlantic-type seafloor disappeared in the Alps. With such a short slab the Alpine subduction likely never reached the 660 km discontinuity, another significant difference with large-scale subduction zones associated with wholesale mantle convection.

ACKNOWLEDGMENTS

This contribution is dedicated to Marcel Lemoine, a man of energy, vision and wisdom. Twenty years after a short field excursion together, the systematic combination of lithostratigraphy and detailed metamorphic petrology still appears very promising. Very warm thanks are due to B. Goffé and L. Jolivet for their initial enthusiasm, and to C. Rosenberg for pushing me to do this. S. Schmid and L. Jolivet are greatly thanked for their many suggestions. This contribution would not have been possible without the students with whom I have shared so many good moments in the Alpine trails, i.e. S. Angiboust, M. Locatelli, B. Lefeuvre, C. Herviou. As well as with P. Yamato and H. Raimbourg, and with R. Bousquet and M. Patriat in the good old days. Special thanks go to P. Monié, G. Bebout and A. Verlaguet. Many colleagues, too many to name here, are thanked for inspiration. Special thoughts go to my ZIP and EFIRE colleagues and friends. Finally, please bear with the author: I have tried to acknowledge the merits of as many studies as possible and be representative. I sincerely apologize to those either not cited or insufficiently acknowledged here.

References

Agard, P., 1999. Evolution métamorphique et structurale des métapélites océaniques dans l'orogène Alpin: l'exemple des Schistes Lustrés des Alpes occidentales (Alpes Cottiennes). PhD dissertation, 324 p.

Agard, P., Goffé, B., Touret, J.L., Vidal, O., 2000. Retrograde mineral and fluid evolution in high-pressure metapelites (Schistes lustrés unit, Western Alps). Contributions to Mineralogy and Petrology 140, 296–315.

Agard, P., Jolivet, L., Goffe, B., 2001a. Tectonometamorphic evolution of the Schistes Lustre's complex: implications for the exhumation of HP and UHP rocks in the western Alps. Bull. Soc. Geol. Fr. 172, 617–636. https://doi.org/10.2113/172.5.617

Agard P., Vidal O., Goffé B., 2001b. Interlayer and Si content of phengite in HP-LT carpholite-bearing metapelites. Journal of metamorphic geology, 19, 477-493.

Agard, P., Monie, P., Jolivet, L., Goffe, B., 2002. Exhumation of the Schistes Lustres complex: in situ laser probe Ar-40/Ar-39 constraints and implications for the Western Alps. J. Metamorph. Geol. 20, 599–618. https://doi.org/10.1046/j.1525-1314.2002.00391.x

Agard, P., Yamato, P., Jolivet, L., Burov, E., 2009. Exhumation of oceanic blueschists and eclogites in subduction zones: Timing and mechanisms. Earth-Science Reviews 92, 53–79. https://doi.org/10.1016/j.earscirev.2008.11.002

Agard, P., Yamato, P., Soret, M., Prigent, C., Guillot, S., Plunder, A., Dubacq, B., Chauvet, A., Monie, P., 2016. Plate interface rheological switches during subduction infancy: Control on slab penetration and metamorphic sole formation. Earth Planet. Sci. Lett. 451, 208–220. https://doi.org/10.1016/j.epsl.2016.06.054

Agard, P., Plunder, A., Angiboust, S., Bonnet, G., Ruh, J., 2018. The subduction plate interface: rock record and mechanical coupling (from long to short timescales). Lithos 320–321, 537–566. https://doi.org/10.1016/j.lithos.2018.09.029

Agard, P., Prigent, C., Soret, M., Dubacq, B., Guillot, S., Deldicque D., 2020. Slabitization: mechanisms controlling subduction development and viscous coupling. Earth-Science Reviews 103259

Amato, J.M., Johnson, C.M., Baumgartner, L.P., Beard, B.L., 1999. Rapid exhumation of the Zermatt-Saas ophiolite deduced from high-precision Sm-Nd and Rb-Sr geochronology. Earth and Planetary Science Letters 171, 425–438.

Ampferer, O., Hammer, W., 1911. Geologischer Querschnitt durch die Ostalpen vom Allgäu zum Gardasee. Jahrbuch der Kaiserlich-Königlichen Geologischen Reichsanstalt 61, 532–710.

Amstutz, A., 1951. Sur l'évolution des structures alpines. Arch. Sci 4, 323–329.

Angiboust, S., Agard, P., 2010. Initial water budget The key to detaching large volumes of eclogitized oceanic crust along the subduction channel? Lithos 120, 453–474. https://doi.org/10.1016/j.lithos.2010.09.007

Angiboust, S., Glodny, J., 2020. Exhumation of eclogitic ophiolitic nappes in the W. Alps: New age data and implications for crustal wedge dynamics. Lithos 105374.

Angiboust, S., Agard, P., Jolivet, L., Beyssac, O., 2009. The Zermatt-Saas ophiolite: the largest (60-km wide) and deepest (c. 70-80 km) continuous slice of oceanic lithosphere detached from a subduction zone? Terr. Nova 21, 171–180. https://doi.org/10.1111/j.1365-3121.2009.00870.x

Angiboust, S., Agard, P., Raimbourg, H., Yamato, P., Huet, B., 2011. Subduction interface processes recorded by eclogite-facies shear zones (Monviso, W. Alps). Lithos 127, 222–238. https://doi.org/10.1016/j.lithos.2011.09.004

Angiboust, S., Agard, P., Yamato, P., Raimbourg, H., 2012a. Eclogite breccias in a subducted ophiolite: A record of intermediate-depth earthquakes? Geology 40, 707–710. https://doi.org/10.1130/G32925.1

Angiboust, S., Langdon, R., Agard, P., Waters, D., Chopin, C., 2012b. Eclogitization of the Monviso ophiolite (W. Alps) and implications on subduction dynamics. J. Metamorph. Geol. 30, 37–61. https://doi.org/10.1111/j.1525-1314.2011.00951.x

Angiboust, S., Wolf, S., Burov, E., Agard, P., Yamato, P., 2012c. Effect of fluid circulation on subduction interface tectonic processes: Insights from thermo-mechanical numerical modelling. Earth Planet. Sci. Lett. 357, 238–248. https://doi.org/10.1016/j.epsl.2012.09.012

Angiboust, S., Glodny, J., Oncken, O., Chopin, C., 2014a. In search of transient subduction interfaces in the Dent Blanche-Sesia Tectonic System (W. Alps). Lithos 205, 298–321. https://doi.org/10.1016/j.lithos.2014.07.001

Angiboust, S., Pettke, T., De Hoog, J.C.M., Caron, B., Oncken, O., 2014b. Channelized Fluid Flow and Eclogite-facies Metasomatism along the Subduction Shear Zone. J. Petrol. 55, 883–916. https://doi.org/10.1093/petrology/egu010

Angiboust, S., Kirsch, J., Oncken, O., Glodny, J., Monie, P., Rybacki, E., 2015. Probing the transition between seismically coupled and decoupled segments along an ancient subduction interface. Geochem. Geophys. Geosyst. 16, 1905–1922. https://doi.org/10.1002/2015GC005776

Anonymous, 1972. Penrose field conference on ophiolites. Geotimes 17, 24–25.

Antoine, P., 1972. Le domaine pennique externe entre Bourg-Saint-Maurice (Savoie) et la frontière italo-suisse. Géol. Alpine 48, 5–40.

Argand, E., 1924. Des Alpes et de l'Afrique.

Audet, P., Bürgmann, R., 2014. Possible control of subduction zone slow-earthquake periodicity by silica enrichment. Nature 510, 389.

Auzende, J.-M., Polino, R., Lagabrielle, Y., Olivet, J.-L., 1983. Considérations sur l'origine et la mise en place des ophiolites des Alpes occidentales: apport de la connaissance des structures océaniques. Comptes Rendus de l'Academie des Sciences Serie II 296.

Bachmann, R., Glodny, J., Oncken, O., Seifert, W., 2009a. Abandonment of the South Penninic–Austroalpine palaeosubduction zone, Central Alps, and shift from subduction erosion to accretion: constraints from Rb/Sr geochronology. Journal of the Geological Society 166, 217–231.

Bachmann, R., Oncken, O., Glodny, J., Seifert, W., Georgieva, V., Sudo, M., 2009b. Exposed plate interface in the European Alps reveals fabric styles and gradients related to an ancient

seismogenic coupling zone. Journal of Geophysical Research: Solid Earth 114. https://doi.org/10.1029/2008JB005927

Balestro, G., Festa, A., Dilek, Y., Tartarotti, P., 2015. Pre-Alpine extensional tectonics of a peridotite-localized oceanic core complex in the late Jurassic, high-pressure Monviso ophiolite (Western Alps). Episodes 38, 266–282.

Balestro, G., Lombardo, B., Vaggelli, G., Borghi, A., Festa, A., Gattiglio, M., 2014. Tectonostratigraphy of the northern Monviso meta-ophiolite complex (Western Alps). Italian Journal of Geosciences 133, 409–426.

Ballèvre, M., Merle, O., 1993. The Combin fault: compressional reactivation of a Late Cretaceous-Early Tertiary detachment fault in the Western Alps. Schweizerische Mineralogische und Petrographische Mitteilungen 73, 205–227.

Ballevre, M., Lagabrielle, Y., Merle, O., 1990. Tertiary ductile normal faulting as a consequence of lithospheric stacking in the western Alps. Mémoires de la Société géologique de France (1833) 156, 227–236.

Ballevre, M., Manzotti, P., Dal Piaz, G.V., 2018. Pre□Alpine (Variscan) Inheritance: A Key for the Location of the Future Valaisan Basin (Western Alps). Tectonics 37, 786–817.

Barfety, J.-C., Polino, R., Mercier, D., Caby, R., Fourneaux, J., 2006. Notice de la carte géologique Névache-Bardonecchia-Modane, 799, Bureau des Recherches Géologiques et Minières.

Barnes, J.D., Beltrando, M., Lee, C.-T.A., Cisneros, M., Loewy, S., Chin, E., 2014. Geochemistry of Alpine serpentinites from rifting to subduction: A view across paleogeographic domains and metamorphic grade. Chemical Geology 389, 29–47.

Barnes, J.D., Penniston-Dorland, S.C., Bebout, G.E., Hoover, W., Beaudoin, G.M., Agard, P., 2019. Chlorine and lithium behavior in metasedimentary rocks during prograde metamorphism: A comparative study of exhumed subduction complexes (Catalina Schist and Schistes Lustrés). Lithos 336, 40–53.

Barnicoat, A., Rex, D., Guise, P., Cliff, R., 1995. The timing of and nature of greenschist facies deformation and metamorphism in the upper Pennine Alps. Tectonics 14, 279–293.

Bebout, G.E., 2007. Metamorphic chemical geodynamics of subduction zones. Earth and Planetary Science Letters 260, 373–393. https://doi.org/10.1016/j.epsl.2007.05.050

Bebout, G.E., Penniston-Dorland, S.C., 2016. Fluid and mass transfer at subduction interfaces—The field metamorphic record. Lithos 240–243, 228–258. https://doi.org/10.1016/j.lithos.2015.10.007

Bebout, G.E., Ryan, J.G., Leeman, W.P., Bebout, A.E., 1999. Fractionation of trace elements by subduction-zone metamorphism—effect of convergent-margin thermal evolution. Earth and Planetary Science Letters 171, 63–81.

Bebout, G.E., Agard, P., Kobayashi, K., Moriguti, T., Nakamura, E., 2013. Devolatilization history and trace element mobility in deeply subducted sedimentary rocks: Evidence from Western Alps HP/UHP suites. Chemical Geology 342, 1–20.

Bechennec, F., Le Metour, J., Rabu, D., Beurrier, M., Bourdillon-Jeudy-de-Grissac, C., De Wever, P., Tegyey, M., Villey, M., 1989. Geologie d'une chaine issue de la Tethys; les montagnes d'Oman. Bulletin de la Société géologique de France 167–188.

Bedford, J., Moreno, M., Baez, J.C., Lange, D., Tilmann, F., Rosenau, M., Heidbach, O., Oncken, O., Bartsch, M., Rietbrock, A., 2013. A high-resolution, time-variable afterslip model for the 2010 Maule Mw= 8.8, Chile megathrust earthquake. Earth and Planetary Science Letters 383, 26–36.

Beltrando, M., Compagnoni, R., Lombardo, B., 2010. (Ultra-) High-pressure metamorphism and orogenesis: an Alpine perspective. Gondwana Research 18, 147–166.

Beltrando, M., Lister, G.S., Forster, M., Dunlap, W.J., Fraser, G., Hermann, J., 2009. Dating microstructures by the 40Ar/39Ar step-heating technique: deformation–pressure–temperature–time history of the Penninic Units of the Western Alps. Lithos 113, 801–819.

Beltrando, M., Manatschal, G., Mohn, G., Dal Piaz, G.V., Brovarone, A.V., Masini, E., 2014. Recognizing remnants of magma-poor rifted margins in high-pressure orogenic belts: The Alpine case study. Earth-Science Reviews 131, 88–115.

Berger, A., Bousquet, R., 2008. Subduction-related metamorphism in the Alps: review of isotopic ages based on petrology and their geodynamic consequences. Geological Society, London, Special Publications 298, 117–144.

Berger, A., Mercolli, I., Engi, M., 2005. The central Lepontine Alps: Notes accompanying the tectonic and petrographic map sheet Sopra Ceneri (1: 100'000). Schweizerische Mineralogische und Petrographische Mitteilungen 85, 109–146.

Beyssac, O., Goffé, B., Chopin, C., Rouzaud, J., 2002. Raman spectra of carbonaceous material in metasediments: a new geothermometer. Journal of metamorphic Geology 20, 859–871.

Bonnet, G., Agard, P., Angiboust, S., Monié, P., Jentzer, M., Omrani, J., Whitechurch, H., Fournier, M., 2018. Tectonic slicing and mixing processes along the subduction interface: The Sistan example (Eastern Iran). Lithos 310–311, 269–287. https://doi.org/10.1016/j.lithos.2018.04.016

Bortolotti, V., Principi, G., 2005. Tethyan ophiolites and Pangea break□up. Island Arc 14, 442–470.

Bouffette, J., Caron, J.-M., 1991. Trajets métamorphiques prograde et rétrograde dans des éclogites piémontaises (Ouest du massif du Rocciavrè, Alpes cottiennes). Comptes rendus de l'Académie des sciences. Série 2, Mécanique, Physique, Chimie, Sciences de l'univers, Sciences de la Terre 312, 1459–1465.

Bousquet, R., 2008. Metamorphic heterogeneities within a single HP unit: overprint effect or metamorphic mix? Lithos 103, 46–69.

Bousquet, R., Engi, M., Gosso, G., Berger, A., Spalla, M.I., Zucali, M., Goffè, B., 2004. Explanatory notes to the map: Metamorphic structure of the Alps. Presented at the Central Alps. Mitt. Österr. Miner. Ges, Citeseer.

Bousquet, R., Goffe, B., Vidal, O., Oberhansli, R., Patriat, M., 2002. The tectono-metamorphic history of the Valaisan domain from the Western to the Central Alps: New constraints on the evolution of the Alps. Geol. Soc. Am. Bull. 114, 207–225. https://doi.org/10.1130/0016-7606(2002)114<0207:TTMHOT>2.0.CO;2

1645 Bousquet, R., Oberhansli, R., Goffe, B., Jolivet, L., Vidal, O., 1998. High-pressure-low-temperature
1646 metamorphism and deformation in the Bundnerschiefer of the Engadine window: implications
1647 for the regional evolution of the eastern Central Alps. J. Metamorph. Geol. 16, 657–674.
1648 https://doi.org/10.1111/j.1525-1314.1998.00161.x
1649 Bousquet, R., Oberhänsli, R., Goffé, B., Wiederkehr, M., Koller, F., Schmid, S.M., Schuster, R., Engi,
1650 M., Berger, A., Martinotti, G., 2008. Metamorphism of metasediments at the scale of an
1651 orogen: a key to the Tertiary geodynamic evolution of the Alps. Geological Society, London,
1652 Special Publications 298, 393–411.
1653 Bousquet, R.; Oberhänsli, R.; Schmid, S.M.; Berger, A.; Wiederkehr, M.; Robert, Ch.; Möller, A.;
1654 Rosenberg, C.; Zeilinger, G.; Molli, G.; Koller, F., 2012: Metamorphic Framework of the Alps.
1655 Map 1 : 1 000 000. CCGM/CGMW (Commission for the Geological Map of the World, Paris).
1656 http://www.geodynalps.org
1657 Bowtell, S., Cliff, R., Barnicoat, A., 1994. Sm□Nd isotopic evidence on the age of eclogitization in the
1658 Zermatt□Saas ophiolite. Journal of Metamorphic Geology 12, 187–196.
1659 Broadwell, K.S., Locatelli, M., Verlaguet, A., Agard, P., Caddick, M.J., 2019. Transient and periodic
1660 brittle deformation of eclogites during intermediate-depth subduction. Earth and Planetary
1661 Science Letters 521, 91–102.
1662 Brun, J.-P., Faccenna, C., 2008. Exhumation of high-pressure rocks driven by slab rollback. Earth and
1663 Planetary Science Letters 272, 1–7. https://doi.org/10.1016/j.epsl.2008.02.038
1664 Bucher, K., Fazis, Y., De Capitani, C., Grapes, R., 2005. Blueschists, eclogites, and decompression
1665 assemblages of the Zermatt-Saas ophiolite: High-pressure metamorphism of subducted
1666 Tethys lithosphere. Am. Miner. 90, 821–835. https://doi.org/10.2138/am.2005.1718
1667 Bucher, K., Grapes, R., 2009. The eclogite-facies Allalin Gabbro of the Zermatt–Saas ophiolite,
1668 Western Alps: A record of subduction zone hydration. Journal of Petrology 50, 1405–1442.
1669 Bucher, K., Weisenberger, T.B., Weber, S., Klemm, O., Corfu, F., 2020. The Theodul Glacier Unit, a
1670 slab of pre-Alpine rocks in the Alpine meta-ophiolite of Zermatt-Saas, Western Alps. Swiss
1671 Journal of Geosciences 113, 1–22.
1672 Bucher, S., Schmid, S.M., Bousquet, R., Fügenschuh, B., 2003. Late□stage deformation in a
1673 collisional orogen (Western Alps): nappe refolding, back□thrusting or normal faulting? Terra
1674 Nova 15, 109–117.
1675 Burroni, A., Levi, N., Marroni, M., Pandolfi, L., 2003. Lithostratigraphy and structure of the Lago Nero
1676 unit (Chenaillet massif, western Alps): comparison with internal liguride units of northern
1677 Apennines. Ofioliti 28, 1–11.
1678 Busigny, V., Cartigny, P., Philippot, P., Javoy, M., 2003. Ammonium quantification in muscovite by
1679 infrared spectroscopy. Chemical Geology 198, 21–31.
1680 Caby, R., 1973. Les plis transversaux dans les Alpes occidentales; implications pour la genese de la
1681 chaine alpine. Bulletin de la Société géologique de France 7, 624–634.
1682 Calahorrano, A., Sallarès, V., Collot, J.-Y., Sage, F., Ranero, C.R., 2008. Nonlinear variations of the
1683 physical properties along the southern Ecuador subduction channel: Results from depth-
1684 migrated seismic data. Earth and Planetary Science Letters 267, 453–467.

1685 Cannat, M., Lagabrielle, Y., Bougault, H., Casey, J., de Coutures, N., Dmitriev, L., Fouquet, Y., 1997.
1686 Ultramafic and gabbroic exposures at the Mid-Atlantic Ridge: Geological mapping in the 15 N
1687 region. Tectonophysics 279, 193–213.
1688 Cannat, M., Manatschal, G., Sauter, D., Peron-Pinvidic, G., 2009. Assessing the conditions of
1689 continental breakup at magma-poor rifted margins: what can we learn from slow spreading
1690 mid-ocean ridges? Comptes Rendus Geoscience 341, 406–427.
1691 Cannat, M., Mevel, C., Maia, M., Deplus, C., Durand, C., Gente, P., Agrinier, P., Belarouchi, A.,
1692 Dubuisson, G., Humler, E., 1995. Thin crust, ultramafic exposures, and rugged faulting
1693 patterns at the Mid-Atlantic Ridge (22–24 N). Geology 23, 49–52.
1694 Cannic, S., Lardeaux, J., Mugnier, J., Hernandez, J., 1996. Tectono-metamorphic evolution of the
1695 Roignais-Versoyen Unit (Valaisan domain, France). Eclogae Geologicae Helvetiae 89, 321–
1696 343.
1697 Caron, J.-M., 1977. Lithostratigraphie et tectonique des Schistes lustrés dans les Alpes cottiennes
1698 septentrionales et en Corse orientale. Persée-Portail des revues scientifiques en SHS.
1699 Castelli, D., Rostagno, C., Lombardo, B., 2002. JD-QTZ-bearing metaplagiogranite from the Monviso
1700 meta-ophiolite (Western Alps). Ofioliti 27, 81–90.
1701 Castelli, Daniele, Rostagno, C., Lombardo, B., 2002. Jd-Qtz-bearing metaplagiogranite from the
1702 Monviso meta-ophiolite (Western Alps). Ofioliti 27, 81–90.
1703 Chalot-Prat, F., Ganne, J., Lombard, A., 2003. No significant element transfer from the oceanic plate
1704 to the mantle wedge during subduction and exhumation of the Tethys lithosphere (Western
1705 Alps). Lithos 69, 69–103.
1706 Chlieh, M., Perfettini, H., Tavera, H., Avouac, J., Remy, D., Nocquet, J., Rolandone, F., Bondoux, F.,
1707 Gabalda, G., Bonvalot, S., 2011. Interseismic coupling and seismic potential along the Central
1708 Andes subduction zone. Journal of Geophysical Research: Solid Earth 116.
1709 Chopin, C., 1981. Mise en evidence d'une discontinuite du metamorphisme alpin entre le massif du
1710 Grand Paradis et sa couverture allochtone (Alpes occidentales francaises). Bulletin de la
1711 Societe Geologique de France 7, 297–301.
1712 Chopin, C., 1984. Coesite and pure pyrope in high-grade blueschists of the Western Alps: a first
1713 record and some consequences. Contributions to Mineralogy and Petrology 86, 107–118.
1714 Chopin, C., 2003. Ultrahigh-pressure metamorphism: tracing continental crust into the mantle. Earth
1715 and Planetary Science Letters 212, 1–14.
1716 Chopin, C., Schertl, H.-P., 1999. The UHP unit in the Dora-Maira massif, western Alps. International
1717 geology review 41, 765–780.
1718 Christensen, J.N., Selverstone, J., Rosenfeld, J.L., DePaolo, D.J., 1994. Correlation by Rb-Sr
1719 geochronology of garnet growth histories from different structural levels within the Tauern
1720 Window, Eastern Alps. Contributions to Mineralogy and Petrology 118, 1–12.
1721 Cliff, R., Barnicoat, A., Inger, S., 1998. Early Tertiary eclogite facies metamorphism in the Monviso
1722 Ophiolite. Journal of Metamorphic Geology 16, 447–455.

Cloos, M., 1982. Flow Melanges - Numerical Modeling and Geologic Constraints on Their Origin in the Franciscan Subduction Complex, California. Geol. Soc. Am. Bull. 93, 330–345. https://doi.org/10.1130/0016-7606(1982)93<330:FMNMAG>2.0.CO;2

Collins, N.C., Bebout, G.E., Angiboust, S., Agard, P., Scambelluri, M., Crispini, L., John, T., 2015. Subduction zone metamorphic pathway for deep carbon cycling: II. Evidence from HP/UHP metabasaltic rocks and ophicarbonates. Chemical Geology 412, 132–150.

Colombi, A., Pfeifer, H.-R., 1986. Ferrogabbroic and basaltic meta-eclogites from the Antrona mafic-ultramafic complex and the Centovalli-Locarno region (Italy and Southern Switzerland)-first results. Schweizerische Mineralogische und Petrographische Mitteilungen 66, 99–110.

Coltice, N., Husson, L., Faccenna, C., Arnould, M., 2019. What drives tectonic plates? Science advances 5, eaax4295.

Compagnoni, R., Rolfo, F., 2003. UHPM units in the Western Alps. Ultrahigh pressure metamorphism 5, 13–49.

Conrad, C.P., Lithgow-Bertelloni, C., 2002. How mantle slabs drive plate tectonics. Science 298, 207–209.

Cook-Kollars, J., Bebout, G.E., Collins, N.C., Angiboust, S., Agard, P., 2014b. Subduction zone metamorphic pathway for deep carbon cycling: I. Evidence from HP/UHP metasedimentary rocks, Italian Alps. Chem. Geol. 386, 31–48. https://doi.org/10.1016/j.chemgeo.2014.07.013

Corno, A., Mosca, P., Borghi, A., Gatteggio, M., 2019. Lithostratigraphy and petrography of the Monte Banchetta-Punta Rognosa oceanic succession (Troncea and Chisonetto Valleys, Western Alps). Ofioliti 44, 83–95.

Costa, S., Caby, R., 2001. Evolution of the Ligurian Tethys in the Western Alps: Sm/Nd and U/Pb geochronology and rare-earth element geochemistry of the Montgenèvre ophiolite (France). Chemical Geology 175, 449–466.

Dachs, E., Proyer, A., 2001. Relics of high-pressure metamorphism from the Grossglockner region, Hohe Tauern, Austria: Paragenetic evolution and PT-paths of retrogressed eclogites. European Journal of Mineralogy 13, 67–86.

Dal Piaz, G.V., 2001. History of tectonic interpretations of the Alps. Journal of geodynamics 32, 99–114.

Dal Piaz, G., Ernst, W., 1978. Areal geology and petrology of eclogites and associated metabasites of the Piemonte ophiolite nappe, breuil—st. Jacques area, Italian Western Alps. Tectonophysics 51, 99–126.

Dal Piaz G.V., Hunziker J.C., Martinotti G., 1972. La zona Sesia-Lanzo e l'evoluzione tettonico-metamorfica delle Alpi nord-occidentali interne. Memorie della Società Geologica Italiana, 11, 433-466.

Dal Piaz, G., Cortiana, G., Del Moro, A., Martin, S., Pennacchioni, G., Tartarotti, P., 2001. Tertiary age and paleostructural inferences of the eclogitic imprint in the Austroalpine outliers and Zermatt–Saas ophiolite, western Alps. International Journal of Earth Sciences 90, 668–684.

de Graciansky, P., 1972. Le bassin tertiaire de Barrême (Alpes de Haute-Provence): Relations entre déformation et sédimentation; chronologie des plissements. Comptes Rendus de l'Academie des Sciences, Paris 275, 2825–2828.

De Wever, P., Caby, R., 1981. Datation de la base des schistes lustrés postophiolitiques par des radiolaires (Oxfordien-Kimmeridgien moyen) dans les Alpes Cottiennes (Saint Véran, France). Compte rendu de l'académie des Sciences de Paris 292, 467–472.

Debelmas, J., Lemoine, M., 1970. The western Alps: palaeogeography and structure. Earth-Science Reviews 6, 221–256.

Debret, B., Bouilhol, P., Pons, M.L., Williams, H., 2018. Carbonate transfer during the onset of slab devolatilization: new insights from Fe and Zn stable isotopes. Journal of Petrology 59, 1145–1166.

Debret, B., Millet, M.-A., Pons, M.-L., Bouilhol, P., Inglis, E., Williams, H., 2016. Isotopic evidence for iron mobility during subduction. Geology 44, 215–218.

Debret, B., Nicollet, C., Andreani, M., Schwartz, S., Godard, M., 2013. Three steps of serpentinization in an eclogitized oceanic serpentinization front (Lanzo Massif–Western Alps). Journal of Metamorphic Geology 31, 165–186.

Dercourt, J., Zonenshain, L., Ricou, L.-E., Kazmin, V., Le Pichon, X., Knipper, A., Grandjacquet, C., Sbortshikov, I., Geyssant, J., Lepvrier, C., 1986. Geological evolution of the Tethys belt from the Atlantic to the Pamirs since the Lias. Tectonophysics 123, 241–315.

Deschamps, F., Godard, M., Guillot, S., Hattori, K., 2013. Geochemistry of subduction zone serpentinites: A review. Lithos 178, 96–127.

Deville, E., Fudral, S., Lagabrielle, Y., Marthaler, M., Sartori, M., 1992. From oceanic closure to continental collision: A synthesis of the" Schistes lustrés" metamorphic complex of the Western Alps. Geological Society of America Bulletin 104, 127–139.

Dewey, J., Helman, M., Knott, S., Turco, E., Hutton, D., 1989. Kinematics of the western Mediterranean. Geological Society, London, Special Publications 45, 265–283.

Dingeldey, C., Dallmeyer, R.D., Koller, F., Massonne, H.-J., 1997. P-T-t history of the Lower Austroalpine Nappe Complex in the "Tarntaler Berge" NW of the Tauern Window: implications for the geotectonic evolution of the central Eastern Alps. Contributions to Mineralogy and Petrology 129, 1–19.

Dragovic, B., Samanta, L.M., Baxter, E.F., Selverstone, J., 2012. Using garnet to constrain the duration and rate of water-releasing metamorphic reactions during subduction: An example from Sifnos, Greece. Chem. Geol. 314, 9–22. https://doi.org/10.1016/j.chemgeo.2012.04.016

Dragovic, B., Angiboust, S., Tappa, M.J., 2020. Petrochronological close-up on the thermal structure of a paleo-subduction zone (W. Alps). Earth and Planetary Science Letters 547, 116446.

Droop, G.T., Chavrit, D., 2014. Eclogitic metagabbro from the Lanzada Window, eastern Central Alps: confirmation of subduction beneath the Malenco Unit. Swiss Journal of Geosciences 107, 113–128.

1799 Duchêne, S., Blichert-Toft, J., Luais, B., Télouk, P., Lardeaux, J.-M., Albarede, F., 1997. The Lu–Hf
1800 dating of garnets and the ages of the Alpine high-pressure metamorphism. Nature 387, 586–
1801 589.
1802 Dumitru, T.A., Wakabayashi, J., Wright, J.E., Wooden, J.L., 2010. Early Cretaceous transition from
1803 nonaccretionary behavior to strongly accretionary behavior within the Franciscan subduction
1804 complex. Tectonics 29, TC5001. https://doi.org/10.1029/2009TC002542
1805 Dumont, T., Lemoine, M., Tricart, P., 1984. Tectonique synsédimentaire triasico-jurassique et rifting
1806 téthysien dans l'unité prépiémontaise de Rochebrune au Sud-Est de Briançon. Bulletin de la
1807 Société géologique de France 7, 921–933.
1808 Ellero, A., Loprieno, A., 2017. Nappe stack of P iemonte–L igurian units south of A osta V alley: New
1809 evidence from Urtier V alley (W estern A lps). Geological Journal 53, 1665–1684.
1810 Elter, G., 1971. Schistes lustrés et ophiolites de la zone piémontaise entre Orco et Doire Baltée (Alpes
1811 Graies). Hypothèses sur l'origine des ophiolites. Géologie Alpine 47, 147–169.
1812 Engi, M., Bousquet, R., Berger, A., 2004. Explanatory notes to the map: metamorphic structure of the
1813 Alps. Presented at the Central Alps. Mitt. Österr. Miner. Ges, Citeseer.
1814 Epstein, G.S., Bebout, G.E., Angiboust, S., Agard, P., 2020. Scales of fluid-rock interaction and
1815 carbon mobility in the deeply underplated and HP-Metamorphosed Schistes Lustrés, Western
1816 Alps. Lithos 354, 105229.
1817 Ernst, W., 1975. Systematics of large-scale tectonics and age progressions in Alpine and Circum-
1818 Pacific blueschist belts. Tectonophysics 26, 229–246.
1819 Ernst, W., 1971. Metamorphic zonations on presumably subducted lithospheric plates from Japan,
1820 California and the Alps. Contributions to Mineralogy and Petrology 34, 43–59.
1821 Ernst, W.G., 2001. Subduction, ultrahigh-pressure metamorphism, and regurgitation of buoyant crustal
1822 slices—implications for arcs and continental growth. Physics of the Earth and Planetary
1823 Interiors 127, 253–275.
1824 Faccenda, M., 2014. Water in the slab: A trilogy. Tectonophysics 614, 1–30.
1825 https://doi.org/10.1016/j.tecto.2013.12.020
1826 Fagereng, A., 2011. Geology of the seismogenic subduction thrust interface, in: Fagereng, A., Toy,
1827 V.G., Rowland, J.V. (Eds.), Geology of the Earthquake Source: A Volume in Honour of Rick
1828 Sibson. Geological Soc Publishing House, Bath, pp. 55–76.
1829 Faryad, S., Hoinkes, G., 2003. P–T gradient of Eo-Alpine metamorphism within the Austroalpine
1830 basement units east of the Tauern Window (Austria). Mineralogy and Petrology 77, 129–159.
1831 Fauquette, S., Bernet, M., Suc, J.-P., Grosjean, A.-S., Guillot, S., Van Der Beek, P., Jourdan, S.,
1832 Popescu, S.-M., Jiménez-Moreno, G., Bertini, A., 2015. Quantifying the Eocene to Pleistocene
1833 topographic evolution of the southwestern Alps, France and Italy. Earth and Planetary Science
1834 Letters 412, 220–234.
1835 Festa, A., Pini, G.A., Ogata, K., Dilek, Y., 2019. Diagnostic features and field-criteria in recognition of
1836 tectonic, sedimentary and diapiric mélanges in orogenic belts and exhumed subduction-
1837 accretion complexes. Gondwana Research.

Fisher, D., Byrne, T., 1987. Structural evolution of underthrusted sediments, Kodiak Islands, Alaska. Tectonics 6, 775–793.

Forsyth D., Uyeda S., 1975. On the relative importance of the driving forces of plate motion. Geophys. J. R. astr. Soc., 43, 163-200.

Frey, M., Desmons, J., Neubauer, F., 1999. The new metamorphic maps of the Alps: Introduction. Schweizerische Mineralogische und Petrographische Mitteilungen 1–4.

Frey, M., Ferreiro Mählmann, R., 1999. Alpine metamorphism of the Central Alps. Schweizerische Mineralogische und Petrographische Mitteilungen 79, 135–154.

Frezzotti, M.L., Selverstone, J., Sharp, Z.D., Compagnoni, R., 2011. Carbonate dissolution during subduction revealed by diamond-bearing rocks from the Alps. Nat. Geosci. 4, 703–706. https://doi.org/10.1038/NGEO1246

Froitzheim, N., Schmid, S.M. and Conti, P., 1994. Repeated change from crustal shortening to orogen-parallel extension in the Austroalpine units of Graubünden. Eclogae geol. Helv., 87, 559-612.

Froitzheim, N., Manatschal, G., 1996. Kinematics of Jurassic rifting, mantle exhumation, and passive-margin formation in the Austroalpine and Penninic nappes (eastern Switzerland). Geological society of America bulletin 108, 1120–1133.

Froitzheim, N., Schmid, S.M., Frey, M., 1996. Mesozoic paleogeography and the timing of eclogite-facies metamorphism in the Alps: a working hypothesis. Eclogae Geologicae Helvetiae 89, 81.

Froitzheim, N. 2020. Deep subduction and exhumation of continental crust in the Alps, EGU General Assembly 2020, Online, 4–8 May 2020, EGU2020-8378, https://doi.org/10.5194/egusphere-egu2020-8378.

Fudral, S., 1996. Etude géologique de la suture tethysienne dans les Alpes franco-italiennes Nord-Occidentales de la Doire Ripaire (Italie) à la région de Bourg Saint-Maurice.(France).

Fudral, S., Deville, E., Marthaler, M., 1987. Distinction de trois ensembles d'unités dans les «Schistes lustrés» compris entre la Vanoise et le Val de Suse (Alpes franco-italiennes septentrionales): aspects lithostratigraphiques, paléogéographiques et géodynamiques. Comptes rendus de l'Académie des sciences. Série 2, Mécanique, Physique, Chimie, Sciences de l'univers, Sciences de la Terre 305, 467–472.

Fügenschuh, B., Loprieno, A., Ceriani, S., Schmid, S., 1999. Structural analysis of the Subbriançonnais and Valais units in the area of Moûtiers (Savoy, Western Alps): paleogeographic and tectonic consequences. International Journal of Earth Sciences 88, 201–218.

Gabalda, S., Beyssac, O., Jolivet, L., Agard, P., Chopin, C., 2009. Thermal structure of a fossil subduction wedge in the Western Alps. Terra Nova 21, 28–34.

Garcia-Casco, A., Torres-Roldan, R.L., Millan, G., Monie, P., Schneider, J., 2002. Oscillatory zoning in eclogitic garnet and amphibole, Northern Serpentinite Melange, Cuba: a record of tectonic instability during subduction? J. Metamorph. Geol. 20, 581–598. https://doi.org/10.1046/j.1525-1314.2002.00390.x

Gebauer, D., Schertl, H.-P., Brix, M., Schreyer, W., 1997. 35 Ma old ultrahigh-pressure metamorphism and evidence for very rapid exhumation in the Dora Maira Massif, Western Alps. Lithos 41, 5–24.

Gerya, T.V., Stöckhert, B., Perchuk, A.L., 2002. Exhumation of high-pressure metamorphic rocks in a subduction channel: A numerical simulation. Tectonics 21, 6-1-6–19. https://doi.org/10.1029/2002TC001406

Ghignone, Stefano, Balestro, G., Gattiglio, M., Borghi, A., 2020. Structural evolution along the Susa Shear Zone: the role of a first-order shear zone in the exhumation of meta-ophiolite units (Western Alps). Swiss Journal of Geosciences 113, 1–16.

Gilio, M., Scambelluri, M., Agostini, S., Godard, M., Pettke, T., Agard, P., Locatelli, M., Angiboust, S., 2020. Fingerprinting and relocating tectonic slices along the plate interface: Evidence from the Lago Superiore unit at Monviso (Western Alps). Lithos 352, 105308.

Giuntoli, F., Lanari, P., Engi, M., 2018. Deeply subducted continental fragments–Part 1: Fracturing, dissolution–precipitation, and diffusion processes recorded by garnet textures of the central Sesia Zone (western Italian Alps). Solid Earth 9, 167.

Godard, G., 2001. Eclogites and their geodynamic interpretation: a history. Journal of Geodynamics 32, 165–203.

Goffe, B., Chopin, C., 1986. High-pressure metamorphism in the Western Alps: zoneography of metapelites, chronology and consequences. Schweizerische mineralogische und petrographische Mitteilungen 66, 41–52.

Goffé, B., Goffé-Urbano, G., Saliot, P., 1973. Sur la présence d'une variété magnésienne de la ferrocarpholite en Vanoise (Alpes françaises): sa signification probable dans le métamorphisme alpin. Comptes Rendus de l'Académie des Sciences Paris 277, 1965–1968.

Goffé, B., Schwartz, S., Lardeaux, J.-M., Bousquet, R., 2004. Metamorphic structure of the Western and Ligurian Alps.

Gouzu, C., Itaya, T., Hyodo, H., Matsuda, T., 2006. Excess 40Ar-free phengite in ultrahigh-pressure metamorphic rocks from the Lago di Cignana area, Western Alps. Lithos 92, 418–430.

Gouzu, C., Yagi, K., Thanh, N.X., Itaya, T., Compagnoni, R., 2016. White mica K–Ar geochronology of HP–UHP units in the Lago di Cignana area, western Alps, Italy: tectonic implications for exhumation. Lithos 248, 109–118.

Groppo, C., Beltrando, M., Compagnoni, R., 2009. The P–T path of the ultra□high pressure Lago di Cignana and adjoining high□pressure meta□ophiolitic units: insights into the evolution of the subducting Tethyan slab. Journal of Metamorphic Geology 27, 207–231.

Groppo, C.T., Castelli, D.C.C., Rolfo, F., 2007. HT, Pre-Alpine relics in a spinel-bearing dolomite marble from the UHP Brossasco-Isasca Unit (Dora-Maira Massif, western Alps).

Groppo, C., Castelli, D., 2010. Prograde P-T Evolution of a Lawsonite Eclogite from the Monviso Meta-ophiolite (Western Alps): Dehydration and Redox Reactions during Subduction of Oceanic FeTi-oxide Gabbro. J. Petrol. 51, 2489–2514. https://doi.org/10.1093/petrology/egq065

Groß, P., Handy, M.R., John, T., Pestal, G., Pleuger, J., 2020. Crustal□Scale Sheath Folding at HP Conditions in an Exhumed Alpine Subduction Zone (Tauern Window, Eastern Alps). Tectonics 39, e2019TC005942.

Hacker, B.R., Peacock, S.M., Abers, G.A., Holloway, S.D., 2003. Subduction factory 2. Are intermediate□depth earthquakes in subducting slabs linked to metamorphic dehydration reactions? Journal of Geophysical Research: Solid Earth 108.

Handy, M., Oberhänsli, R., 2004. Explanatory notes to the map: metamorphic structure of the Alps–Age map of metamorphic structure of the Alps–Tectonic interpretation and outstanding problems. Mitt. Österr. Miner. Ges 149, 201–225.

Handy, M.R., Herwegh, M., Kamber, B.S., Tietz, R., Villa, I.M., 1996. Geochronologic, petrologic and kinematic constraints on the evolution of the Err-Platta boundary, part of a fossil continent-ocean suture in the Alps (eastern Switzerland). Schweizerische Mineralogische und Petrographische Mitteilungen 76, 453–474.

Handy, M.R., Schmid, S.M., Bousquet, R., Kissling, E., Bernoulli, D., 2010. Reconciling plate-tectonic reconstructions of Alpine Tethys with the geological–geophysical record of spreading and subduction in the Alps. Earth-Science Reviews 102, 121–158.

Haüy, R.J., 1822. Traite de cristallographie, suivi d'une application des principes de cette science a la determination des especes minerales, et d'une nouvelle methode pour mettre les formes cristallines en projection; par M. l'Abbe Hauy,... Tome premier [-second]: 1. Bachelier et Huzard.

Henry, C., Burkhard, M., Goffe, B., 1996. Evolution of synmetamorphic veins and their wallrocks through a Western Alps transect: no evidence for large-scale fluid flow. Stable isotope, major- and trace-element systematics. Chemical Geology 127, 81–109.

Henry, C., Michard, A., Chopin, C., 1993. Geometry and structural evolution of ultra-high-pressure and high-pressure rocks from the Dora-Maira massif, Western Alps, Italy. Journal of Structural Geology 15, 965–965.

Herwartz, D., Nagel, T.J., Münker, C., Scherer, E.E., Froitzheim, N., 2011. Tracing two orogenic cycles in one eclogite sample by Lu–Hf garnet chronometry. Nature Geoscience 4, 178–183.

Hetényi, G., Molinari, I., Clinton, J., Bokelmann, G., Bondár, I., Crawford, W.C., Dessa, J.-X., Doubre, C., Friederich, W., Fuchs, F., 2018. The AlpArray seismic network: a large-scale European experiment to image the Alpine Orogen. Surveys in geophysics 39, 1009–1033.

Hilairet, N., Reynard, B., Wang, Y., Daniel, I., Merkel, S., Nishiyama, N., Petitgirard, S., 2007. High-Pressure Creep of Serpentine, Interseismic Deformation, and Initiation of Subduction. Science 318, 1910–1913. https://doi.org/10.1126/science.1148494

Hoinkes, G., Koller, F., Rantitsch, G., Dachs, E., Höck, V., Neubauer, F., Schuster, R., 1999. Alpine metamorphism of the Eastern Alps. Schweizerische Mineralogische und Petrographische Mitteilungen 155–181.

Ioannidi, P.I., Angiboust, S., Oncken, O., Agard, P., Glodny, J., Sudo, M., 2020. Deformation along the roof of a fossil subduction interface in the transition zone below seismogenic coupling: The

Austroalpine case and new insights from the Malenco Massif (Central Alps). Geosphere 16, 510–532.
Ishizuka, O., Tani, K., Reagan, M.K., 2014. Izu-Bonin-Mariana forearc crust as a modern ophiolite analogue. Elements 10, 115–120.
Jolivet, L., Faccenna, C., Goffe, B., Burov, E., Agard, P., 2003. Subduction tectonics and exhumation of high-pressure metamorphic rocks in the Mediterranean orogens. Am. J. Sci. 303, 353–409. https://doi.org/10.2475/ajs.303.5.353
Kästle, E.D., Rosenberg, C., Boschi, L., Bellahsen, N., Meier, T., El-Sharkawy, A., 2019. Slab break-offs in the Alpine subduction zone. International Journal of Earth Sciences 1–17.
Kelemen, P.B., Manning, C.E., 2015. Reevaluating carbon fluxes in subduction zones, what goes down, mostly comes up. Proceedings of the National Academy of Sciences 112, E3997–E4006.
Keller, L.M., Hess, M., Fügenschuh, B., Schmid, S.M., 2005. Structural and metamorphic evolution of the Camughera–Moncucco, Antrona and Monte Rosa units southwest of the Simplon line, Western Alps. Eclogae Geologicae Helvetiae 98, 19–49.
Kienast, J.-R., 1983. Le métamorphisme de haute pression et basse température(éclogites et schistes bleus: données nouvelles sur la pétrologie des roches de la croûte océanique subductée et des sédiments associés.
Kienast, J., Velde, B., 1970. Le métamorphisme alpin dans les Alpes franco-italiennes: mise en évidence d'un gradient de température et de pression. CR Acad. Sci. 271, 637–640.
Kienast, J., Pognante, U., 1988. Chloritoid-bearing assemblages in eclogitised metagabbros of the Lanzo peridotite body (western Italian Alps). Lithos 21, 1–11.
Kimura, G., Ludden, J., 1995. Peeling oceanic crust in subduction zones. Geology 23, 217–220. https://doi.org/10.1130/0091-7613(1995)023<0217:POCISZ>2.3.CO;2
Koller, F., 2003. 5th workshop of Alpine geological studies. Field trip guide E5. Low T—high P metamorphism in the Tarntal Mountains (Lower Austroalpine Unit). Geologisch-Paläontologische Mitteilungen Innsbruck 26, 47–59.
Koller, F., Pestal, G., 2003. Die ligurischen Ophiolite der Tarntaler Berge und der Matreier Schuppenzone. Arbeitstagung 65–76.
Kusky, T.M., Windley, B.F., Safonova, I., Wakita, K., Wakabayashi, J., Polat, A., Santosh, M., 2013. Recognition of ocean plate stratigraphy in accretionary orogens through Earth history: A record of 3.8billion years of sea floor spreading, subduction, and accretion. Gondwana Research 24, 501–547. https://doi.org/10.1016/j.gr.2013.01.004
Lafay, R., Deschamps, F., Schwartz, S., Guillot, S., Godard, M., Debret, B., Nicollet, C., 2013. High-pressure serpentinites, a trap-and-release system controlled by metamorphic conditions: Example from the Piedmont zone of the western Alps. Chemical Geology 343, 38–54.
Lagabrielle, Y., 2009. Mantle exhumation and lithospheric spreading: An historical perspective from investigations in the Oceans and in the Alps-Apennines ophiolites. Bollettino della Societa Geologica Italiana 128, 279–293.

Lagabrielle, Y., 1987. Les ophiolites: marqueurs de l'histoire tectonique des domaines océaniques: le cas des Alpes franco-italiennes (Queyras, Piémont).

Lagabrielle, Y., Brovarone, A.V., Ildefonse, B., 2015. Fossil oceanic core complexes recognized in the blueschist metaophiolites of Western Alps and Corsica. Earth-Sci. Rev. 141, 1–26.

Lagabrielle, Y., Cannat, M., 1990. Alpine Jurassic ophiolites resemble the modern central Atlantic basement. Geology 18, 319–322.

Lagabrielle, Y., Fudral, S., Kienast, J.-R., 1990. La couverture océanique des ultrabasites de Lanzo (Alpes occidentales): arguments lithostratigraphiques et pétrologiques. Geodinamica Acta 4, 43–55.

Lagabrielle, Y., Lemoine, M., 1997. Alpine, Corsican and Apennine ophiolites: the slow-spreading ridge model. Comptes Rendus de l'Académie des Sciences-Series IIA-Earth and Planetary Science 325, 909–920.

Lagabrielle, Y., Lemoine, M., Tricart, P., 1985. Paléotectonique océanique et déformations alpines dans le massif ophiolitique du Pelvas d'Abriès (Alpes Occidentales-Queyras-France). Bulletin de la Société Géologique de France 1, 473–480.

Lapen, T.J., Johnson, C.M., Baumgartner, L.P., Dal Piaz, G.V., Skora, S., Beard, B.L., 2007. Coupling of oceanic and continental crust during Eocene eclogite-facies metamorphism: evidence from the Monte Rosa nappe, western Alps. Contributions to Mineralogy and Petrology 153, 139–157.

Lapen, T.J., Johnson, C.M., Baumgartner, L.P., Mahlen, N.J., Beard, B.L., Amato, J.M., 2003. Burial rates during prograde metamorphism of an ultra-high-pressure terrane: an example from Lago di Cignana, western Alps, Italy. Earth and Planetary Science Letters 215, 57–72.

Lardeaux, J.-M., Schwartz, S., Tricart, P., Paul, A., Guillot, S., Béthoux, N., Masson, F., 2006. A crustal□scale cross□section of the south□western Alps combining geophysical and geological imagery. Terra Nova 18, 412–422.

Le Bayon, B., Pitra, P., Ballevre, M., Bohn, M., 2006. Reconstructing P–T paths during continental collision using multi□stage garnet (Gran Paradiso nappe, Western Alps). Journal of Metamorphic Geology 24, 477–496.

Le Mer, O., Lagabrielle, Y., Polino, R., 1986. Une serie sedimentaire detritique liee aux ophiolites piemontaises: analyses lithostratigraphiques, texturales et geochimiques dans le massif de la Crete Mouloun (Haut Queyras, Alpes sud-occidentales, France). Géol. Alpine 62, 63–86.

Lefeuvre, B., Agard, P., Verlaguet, A., Dubacq, B., Plunder, A., 2020. Massive lawsonite formation in carbonate-rich subducted metasediments: implications for mass transfer, decarbonation and fluid-mediated processes (Schistes Lustrés, W. Alps), Lithos (accepted pending minor revisions).

Lemoine, M., Bas, T., Arnaud-Vanneau, A., Arnaud, H., Dumont, T., Gidon, M., Bourbon, M., de Graciansky, P.-C., Rudkiewicz, J.-L., Megard-Galli, J., 1986. The continental margin of the Mesozoic Tethys in the Western Alps. Marine and petroleum geology 3, 179–199.

Lemoine, M., Marthaler, M., Caron, M., Sartori, M., Amaudric du Chaffaut, S., 1984. Découverte de foraminifères planctoniques du Crétacé supérieur dans les schistes lustrés du Queyras (Alpes

occidentales). Conséquences paléogéographiques et tectoniques. Comptes-rendus des séances de l'Académie des sciences. Série 2, Mécanique-physique, chimie, sciences de l'univers, sciences de la terre 299, 727–732.

Lemoine, M., Steen, D., Vuagnat, M., 1970. Sur le probleme stratigraphique des ophiolites piemontaises et de roches sddimentaires associees: observations dans le massif de Chabriire en Haute-Ubaye (Basses-Alpes, France), CR Sot. Sci. Nat. GenGve 5, 44–59.

Lemoine, M., Tricart, P., 1986. Les Schistes lustrés piémontais des Alpes occidentales: approche stratigraphique, structurale et sédimentologique. Eclogae Geologicae Helvetiae 79, 271–294.

Lemoine, M., Tricart, P., Boillot, G., 1987. Ultramafic and gabbroic ocean floor of the Ligurian Tethys (Alps, Corsica, Apennines): In search of a genetic imodel. Geology 15, 622–625.

Leng, W., Gurnis, M., 2015. Subduction initiation at relic arcs. Geophysical Research Letters 42, 7014–7021.

Lippitsch, R., Kissling, E., Ansorge, J., 2003. Upper mantle structure beneath the Alpine orogen from high□resolution teleseismic tomography. Journal of Geophysical Research: Solid Earth 108.

Locatelli, M., Federico, L., Agard, P., Verlaguet, A., 2019a. Geology of the southern Monviso metaophiolite complex (W-Alps, Italy). Journal of Maps 15, 283–297.

Locatelli, M., Verlaguet, A., Agard, P., Federico, L., Angiboust, S., 2018. Intermediate-depth brecciation along the subduction plate interface (Monviso eclogite, W. Alps). Lithos 320, 378–402.

Locatelli, M., Verlaguet, A., Agard, P., Pettke, T., Federico, L., 2019b. Fluid pulses during stepwise brecciation at intermediate subduction depths (Monviso eclogites, W. Alps): first internally then externally sourced. Geochemistry, geophysics, geosystems 20, 5285–5318.

Lombardo, B., 1978. Osservazioni preliminari sulle ofioliti metamorfiche del Monviso (Alpi Occidentali).

Loprieno, A., Bousquet, R., Bucher, S., Ceriani, S., Dalla Torre, F.H., Fügenschuh, B., Schmid, S.M., 2011. The Valais units in Savoy (France): a key area for understanding the palaeogeography and the tectonic evolution of the Western Alps. International Journal of Earth Sciences 100, 963–992.

Luisier, C., Baumgartner, L., Schmalholz, S.M., Siron, G., Vennemann, T., 2019. Metamorphic pressure variation in a coherent Alpine nappe challenges lithostatic pressure paradigm. Nature communications 10, 1–11.

Luoni, P., Rebay, G., Spalla, M.I., Zanoni, D., 2018. UHP Ti-chondrodite in the Zermatt-Saas serpentinite: Constraints on a new tectonic scenario.

Maksymowicz, A., 2015. The geometry of the Chilean continental wedge: Tectonic segmentation of subduction processes off Chile. Tectonophysics 659, 183–196.

Malusà, M.G., Polino, R., Zattin, M., Bigazzi, G., Martin, S., Piana, F., 2005. Miocene to Present differential exhumation in the Western Alps: Insights from fission track thermochronology. Tectonics 24.

Manatschal, G., Müntener, O., 2009. A type sequence across an ancient magma-poor ocean–continent transition: the example of the western Alpine Tethys ophiolites. Tectonophysics 473, 4–19.

Manatschal, G., Sauter, D., Karpoff, A.M., Masini, E., Mohn, G., Lagabrielle, Y., 2011. The Chenaillet Ophiolite in the French/Italian Alps: An ancient analogue for an oceanic core complex? Lithos 124, 169–184.

Manatschal, G., Nievergelt, P., 1997. A continent-ocean transition recorded in the Err and Platta nappes (Eastern Switzerland). Eclogae Geologicae Helvetiae 90, 3–28.

Manzotti, P., Ballèvre, M., Poujol, M., 2016. Detrital zircon geochronology in the Dora□Maira and Zone Houillère: a record of sediment travel paths in the Carboniferous. Terra Nova 28, 279–288.

Manzotti, P., Ballevre, M., Zucali, M., Robyr, M., Engi, M., 2014. The tectonometamorphic evolution of the Sesia–Dent Blanche nappes (internal Western Alps): review and synthesis. Swiss Journal of Geosciences 107, 309–336.

Manzotti, P., Bosse, V., Pitra, P., Robyr, M., Schiavi, F., Ballevre, M., 2018. Exhumation rates in the Gran Paradiso Massif (Western Alps) constrained by in situ U–Th–Pb dating of accessory phases (monazite, allanite and xenotime). Contributions to Mineralogy and Petrology 173, 24.

Manzotti, P., Poujol, M., Ballèvre, M., 2015. Detrital zircon geochronology in blueschist-facies meta-conglomerates from the Western Alps: implications for the late Carboniferous to early Permian palaeogeography. International Journal of Earth Sciences 104, 703–731.

Mark, C., Cogné, N., Chew, D., 2016. Tracking exhumation and drainage divide migration of the Western Alps: A test of the apatite U-Pb thermochronometer as a detrital provenance tool. Bulletin 128, 1439–1460.

Markley, M.J., Teyssier, C., Cosca, M.A., Caby, R., Hunziker, J.C., Sartori, M., 1998. Alpine deformation and 40Ar/39Ar geochronology of synkinematic white mica in the Siviez□ Mischabel Nappe, western Pennine Alps, Switzerland. Tectonics 17, 407–425.

Marthaler, M., Stampfli, G., 1989. Les Schistes lustrés à ophiolites de la nappe du Tsaté: un ancien prisme d'accrétion issu de la marge active apulienne? Schweizerische Mineralogische und Petrographische Mitteilungen 69, 211–216.

Martin, S., Polino, R., 1984. Le metaradiolariti a ferro di Cesana (Valle di Susa-Alpi occidentali). Mem. Soc. Geol. It 29, 107–125.

Maruyama, S., Liou, J., Terabayashi, M., 1996. Blueschists and eclogites of the world and their exhumation. International geology review 38, 485–594.

McCarthy, A., Müntener, O., 2015. Ancient depletion and mantle heterogeneity: Revisiting the Permian-Jurassic paradox of Alpine peridotites. Geology 43, 255–258.

McCarthy, A., Chelle-Michou, C., Müntener, O., Arculus, R., Blundy, J., 2018. Subduction initiation without magmatism: The case of the missing Alpine magmatic arc. Geology 46, 1059–1062.

McCarthy, A., Tugend, J., Mohn, G., Candioti, L., Chelle-Michou, C., Arculus, R., Schmalholz, S.M., Müntener, O., 2020. A case of Ampferer-type subduction and consequences for the Alps and the Pyrenees. American Journal of Science 320, 313–372.

Meffan□Main, S., Cliff, R., Barnicoat, A., Lombardo, B., Compagnoni, R., 2004. A Tertiary age for Alpine high□pressure metamorphism in the Gran Paradiso massif, Western Alps: A Rb–Sr microsampling study. Journal of Metamorphic Geology 22, 267–281.

Menant, A., Angiboust, S., Gerya, T., Lacassin, R., Simoes, M., Grandin, R., 2020. Transient stripping of subducting slabs controls periodic forearc uplift. Nature communications 11, 1–10.

Merle, O., 1982. Mise en place séquentielle de la Nappe du Parpaillon en Embrunais-Ubaye (Flysch à Helminthoïdes, Alpes occidentales).

Merle, O., Brun, J., 1984. The curved translation path of the Parpaillon Nappe (French Alps). Journal of structural Geology 6, 711–719.

Messiga, B., Scambelluri, M., Piccardo, G.B., 1995. Chloritoid-bearing assemblages in mafic systems and eclogite-facies hydration of alpine Mg-Al metagabbros (Erro-Tobbio Unit, Ligurian western Alps). European Journal of mineralogy 1149–1168.

Mevel, C., Caby, R., Kienast, J.-R., 1978. Amphibolite facies conditions in the oceanic crust: Example of amphibolitized flaser-gabbro and amphibolites from the Chenaillet ophiolite massif (Hautes Alpes, France). Earth and Planetary Science Letters 39, 98–108.

Michard, A., 1977. Charriages et metamorphisme haute pression dans les Alpes cottiennes meridionales; a propos des schistes a jadeite de la bande d'Acceglio. Bulletin de la Société Géologique de France 7, 883–892.

Michard, A., Avigad, D., Goffé, B., Chopin, C., 2004. The high-pressure metamorphic front of the south Western Alps (Ubaye-Maira transect, France, Italy). Schweiz. Mineral. Petrogr. Mitt 84, 215–235.

Michard, A., Goffé, B., Chopin, C., Henry, C., 1996. Did the Western Alps develop through an Oman-type stage? The geotectonic setting of high-pressure metamorphism in two contrasting Tethyan transects. Eclogae Geologicae Helvetiae 89, 43–80.

Miller, C., Thöni, M., 1997. Eo-Alpine eclogitisation of Permian MORB-type gabbros in the Koralpe (Eastern Alps, Austria): new geochronological, geochemical and petrological data. Chemical Geology 137, 283–310.

Mohn, G., Manatschal, G., Masini, E., Müntener, O., 2011. Rift-related inheritance in orogens: a case study from the Austroalpine nappes in Central Alps (SE-Switzerland and N-Italy). International Journal of Earth Sciences 100, 937–961.

Mohn, G., Manatschal, G., Beltrando, M., Masini, E., Kusznir, N., 2012. Necking of continental crust in magma□poor rifted margins: Evidence from the fossil Alpine Tethys margins. Tectonics 31.

Monié, P., Philippot, P., 1989. Mise en évidence de l'âge éocène moyen du métamorphisme de haute-pression dans la nappe ophiolitique du Monviso (Alpes occidentales) par la méthode 39Ar-40Ar. Comptes rendus de l'Académie des sciences. Série 2, Mécanique, Physique, Chimie, Sciences de l'univers, Sciences de la Terre 309, 245–251.

Moulas, E., Schmalholz, S.M., Podladchikov, Y., Tajčmanová, L., Kostopoulos, D., Baumgartner, L., 2019. Relation between mean stress, thermodynamic, and lithostatic pressure. Journal of metamorphic geology 37, 1–14.

Mueller, P., Maino, M., Seno, S., 2020. Progressive Deformation Patterns from an Accretionary Prism (Helminthoid Flysch, Ligurian Alps, Italy). Geosciences 10, 26.

Müller, W., Dallmeyer, R.D., Neubauer, F., Thöni, M., 1999. Deformation-induced resetting of Rb/Sr and 40Ar/39Ar mineral systems in a low-grade, polymetamorphic terrane (Eastern Alps, Austria). Journal of the Geological Society 156, 261–278.

Müntener, O., Hermann, J., 1996. The Val Malenco lower crust–upper mantle complex and its field relations (Italian Alps). Schweizerische Mineralogische und Petrographische Mitteilungen 76, 475–500.

Nábělek, J., Hetényi, G., Vergne, J., Sapkota, S., Kafle, B., Jiang, M., Su, H., Chen, J., Huang, B.-S., 2009. Underplating in the Himalaya-Tibet collision zone revealed by the Hi-CLIMB experiment. Science 325, 1371–1374.

Nadeau, S., Philippot, P., Pineau, F., 1993. Fluid inclusion and mineral isotopic compositions (HCO) in eclogitic rocks as tracers of local fluid migration during high-pressure metamorphism. Earth and Planetary Science Letters 114, 431–448.

Nagel, T.J., 2008. Tertiary subduction, collision and exhumation recorded in the Adula nappe, central Alps. Geological Society, London, Special Publications 298, 365–392.

Negro, F., Bousquet, R., Vils, F., Pellet, C.-M., Hänggi-Schaub, J., 2013. Thermal structure and metamorphic evolution of the Piemont-Ligurian metasediments in the northern Western Alps. Swiss Journal of Geosciences 106, 63–78.

Nicolas, A., 1989. Structures of ophiolites and dynamics of oceanic lithosphere. Structures of ophiolites and dynamics of oceanic lithosphere.

Oberhänsli, R., 1978. Chemische Untersuchungen an Glaukophan-führenden basischen Gesteinen aus den Bündnerschiefern Graubündens.

Oberhänsli, R., Bousquet, R., Engi, M., Goffé, B., Gosso, G., Handy, M., Höck, V., Koller, F., Lardeaux, J., Polino, R., 2004. Metamorphic Structure of the Alps. CCGM (Commission of the Geological Maps of the World), Paris.

Oberhansli, R., Goffé, B., 2004. Explonatory notes to the Map: Metamorphic structure of the Alps introduction. Mitteilungen der Österreichischen Mineralogischen Gesellschaft 149, 115–123.

Pelletier, L., Müntener, O., 2006. High-pressure metamorphism of the Lanzo peridotite and its oceanic cover, and some consequences for the Sesia–Lanzo zone (northwestern Italian Alps). Lithos 90, 111–130.

Perrone, G., Cadoppi, P., Tallone, S., Balestro, G., 2011. Post-collisional tectonics in the Northern Cottian Alps (Italian Western Alps). International Journal of Earth Sciences 100, 1349–1373.

Pfeifer, H., Colombi, A., Ganguin, J., 1989. Zermatt-Saas and Antrona zone: A petrographic and geochemical comparison of polyphase metamorphic ophiolites of the West-Central Alps. Schweizerische Mineralogische und Petrographische Mitteilungen 69, 217–236.

Philippot, P., 1990. Opposite vergence of nappes and crustal extension in the French□Italian Western Alps. Tectonics 9, 1143–1164.

Philippot, P., Agrinier, P., Scambelluri, M., 1998. Chlorine cycling during subduction of altered oceanic crust. Earth and Planetary Science Letters 161, 33–44.

Philippot, P., Kienast, J.-R., 1989. Chemical-microstructural changes in eclogite-facies shear zones (Monviso, Western Alps, north Italy) as indicators of strain history and the mechanism and scale of mass transfer. Lithos 23, 179–200.

Picazo, S., Müntener, O., Manatschal, G., Bauville, A., Karner, G., Johnson, C., 2016. Mapping the nature of mantle domains in Western and Central Europe based on clinopyroxene and spinel chemistry: Evidence for mantle modification during an extensional cycle. Lithos 266, 233–263.

Picazo, S.M., Ewing, T.A., Müntener, O., 2019. Paleocene metamorphism along the Pennine–Austroalpine suture constrained by U–Pb dating of titanite and rutile (Malenco, Alps). Swiss Journal of Geosciences 112, 517–542.

Piccardo, G.B., Ranalli, G., Guarnieri, L., 2010. Seismogenic shear zones in the lithospheric mantle: ultramafic pseudotachylytes in the Lanzo Peridotite (Western Alps, NW Italy). Journal of Petrology 51, 81–100.

Piccoli, F., Brovarone, A.V., Ague, J.J., 2018. Field and petrological study of metasomatism and high-pressure carbonation from lawsonite eclogite-facies terrains, Alpine Corsica. Lithos 304, 16–37.

Platt, J., 1986. Dynamics of orogenic wedges and the uplift of high-pressure metamorphic rocks. Geological society of America bulletin 97, 1037–1053.

Platt, J., Behrmann, J., Cunningham, P., Dewey, J., Helman, M., Parish, M., Shepley, M., Wallis, S., Western, P., 1989. Kinematics of the Alpine arc and the motion history of Adria. Nature 337, 158–161.

Plunder, A., Agard, P., Dubacq, B., Chopin, C., Bellanger, M., 2012. How continuous and precise is the record of P-T paths? Insights from combined thermobarometry and thermodynamic modelling into subduction dynamics (Schistes Lustres, W. Alps). J. Metamorph. Geol. 30, 323–346. https://doi.org/10.1111/j.1525-1314.2011.00969.x

Pognante, U., 1991. Petrological constraints on the eclogite□and blueschistfacies metamorphism and P□T□t paths in the western Alps. Journal of Metamorphic Geology 9, 5–17.

Pognante, U., Kienast, J.-R., 1987. Blueschist and eclogite transformations in Fe-Ti gabbros: a case from the Western Alps ophiolites. Journal of Petrology 28, 271–292.

Polino, R., Lemoine, M., 1984. Détritisme mixte d'origine continentale et océanique dans les sédiments jurassico-crétacés supra-ophiolitiques de la Téthys ligure: la série du Lago Nero (Alpes Occidentales franco-italiennes). Comptes-rendus des séances de l'Académie des sciences. Série 2, Mécanique-physique, chimie, sciences de l'univers, sciences de la terre 298, 359–364.

Polino, R., Dal Piaz, G., Gosso, G., 1990. Tectonic erosion at the Adria Margin and accrertionary processes for the Cretaceous orogeny of the Alps.

Polino, R., Borghi, A., Carraro, F., Dela Pierre, F., Fioraso, G., Giardino, M., 2002. Note Illustrative Della Carta Geologica D'italia Alla Scala 1: 50.000–FOGLIO 132-152-153 "BARDONECCHIA".

2227 Ratschbacher, L., Dingeldey, C., Miller, C., Hacker, B.R., McWilliams, M.O., 2004. Formation,
2228 subduction, and exhumation of Penninic oceanic crust in the Eastern Alps: time constraints
2229 from 40Ar/39Ar geochronology. Tectonophysics 394, 155–170.
2230 Rebay, G., Zanoni, D., Langone, A., Luoni, P., Tiepolo, M., Spalla, M.I., 2018. Dating of ultramafic
2231 rocks from the Western Alps ophiolites discloses Late Cretaceous subduction ages in the
2232 Zermatt-Saas Zone. Geological Magazine 155, 298–315.
2233 Reddy, S., Wheeler, J., Cliff, R., 1999. The geometry and timing of orogenic extension: an example
2234 from the Western Italian Alps. Journal of Metamorphic Geology 17, 573–590.
2235 Reddy, S.M., Wheeler, J., Butler, R.W.H., Cliff, R.A., Freeman, S., Inger, S., Pickles, C., Kelley, S.P.,
2236 2003. Kinematic reworking and exhumation within the convergent Alpine Orogen.
2237 Tectonophysics 365, 77–102.
2238 Reinecke, T., 1998. Prograde high-to ultrahigh-pressure metamorphism and exhumation of oceanic
2239 sediments at Lago di Cignana, Zermatt-Saas Zone, western Alps. Lithos 42, 147–189.
2240 Reinecke, T., 1991. Very-high-pressure metamorphism and uplift of coesite-bearing metasediments
2241 from the Zermatt-Saas zone, Western Alps. European Journal of Mineralogy 7–18.
2242 Reynard, B., 2013. Serpentine in active subduction zones. Lithos, Serpentinites from mid-oceanic
2243 ridges to subduction 178, 171–185. https://doi.org/10.1016/j.lithos.2012.10.012
2244 Ricard Y., Richards M., Lithgow-Bertelloni C., Le Stunff Y. 1993. A geodynamic model of mantle
2245 density heterogeneity. Journal of Geophysical Research, 98, 21895-21909.
2246 Ricou, L., Siddans, A., 1986. Collision tectonics in the western Alps. Geological Society, London,
2247 Special Publications 19, 229–244.
2248 Ring, U., 1992. The Alpine geodynamic evolution of Penninic nappes in the eastern Central Alps:
2249 geothermobarometric and kinematic data. Journal of Metamorphic Geology 10, 33–53.
2250 Ring, U., Ratschbacher, L., Frisch, W., Durr, S., Borchert, S., 1991. Late-stage east-directed
2251 deformation in the Platta, Arosa, and lowermost Austroalpine nappes (eastern Swiss Alps).
2252 Neues Jahrbuch für Geologie und Paläontologie-Monatshefte 357–363.
2253 Rosenbaum, G., Lister, G.S., 2005. The Western Alps from the Jurassic to Oligocene: spatio-temporal
2254 constraints and evolutionary reconstructions. Earth-Science Reviews 69, 281–306.
2255 Rosenbaum, G., Lister, G.S., Duboz, C., 2002. Relative motions of Africa, Iberia and Europe during
2256 Alpine orogeny. Tectonophysics 359, 117–129.
2257 Rosenberg, C.L., Schneider, S., Scharf, A., Bertrand, A., Hammerschmidt, K., Rabaute, A., Brun, J.-
2258 P., 2018. Relating collisional kinematics to exhumation processes in the Eastern Alps. Earth-
2259 Science Reviews 176, 311–344.
2260 Royden, L., Faccenna, C., 2018. Subduction orogeny and the Late Cenozoic evolution of the
2261 mediterranean arcs. Annual Review of Earth and Planetary Sciences 46, 261–289.
2262 Rubatto, D., Hermann, J., 2003. Zircon formation during fluid circulation in eclogites (Monviso,
2263 Western Alps): implications for Zr and Hf budget in subduction zones. Geochimica et
2264 Cosmochimica Acta 67, 2173–2187.

Rubatto, D., Angiboust, S., 2015. Oxygen isotope record of oceanic and high-pressure metasomatism: a P–T–time–fluid path for the Monviso eclogites (Italy). Contributions to mineralogy and petrology 170, 44.

Rubatto, D., Gebauer, D., Fanning, M., 1998. Jurassic formation and Eocene subduction of the Zermatt–Saas-Fee ophiolites: implications for the geodynamic evolution of the Central and Western Alps. Contributions to Mineralogy and Petrology 132, 269–287.

Rubatto, D., Gebauer, D., Compagnoni, R., 1999. Dating of eclogite-facies zircons: the age of Alpine metamorphism in the Sesia–Lanzo Zone (Western Alps). Earth and Planetary Science Letters 167, 141–158.

Rubatto, D., Müntener, O., Barnhoorn, A., Gregory, C., 2008. Dissolution-reprecipitation of zircon at low-temperature, high-pressure conditions (Lanzo Massif, Italy). American Mineralogist 93, 1519–1529.

Ruh, J.B., Le Pourhiet, L., Agard, P., Burov, E., Gerya, T., 2015. Tectonic slicing of subducting oceanic crust along plate interfaces: Numerical modeling. Geochemistry, Geophysics, Geosystems 16, 3505–3531.

Saliot, P., Dal Piaz, G., Frey, M., 1980. Métamorphisme de haute pression dans les Alpes franco-italo-suisses. Geologie alpine 56, 203–235.

Sample, J.C., Fisher, D.M., 1986. Duplex accretion and underplating in an ancient accretionary complex, Kodiak Islands, Alaska. Geology 14, 160–163.

Sandmann, S., Nagel, T.J., Herwartz, D., Fonseca, R.O., Kurzawski, R.M., Münker, C., Froitzheim, N., 2014. Lu–Hf garnet systematics of a polymetamorphic basement unit: new evidence for coherent exhumation of the Adula Nappe (Central Alps) from eclogite-facies conditions. Contributions to Mineralogy and Petrology 168, 1075.

Scambelluri, M., Cannaò, E., Gilio, M., 2019. The water and fluid-mobile element cycles during serpentinite subduction. A review. European Journal of Mineralogy 31, 405–428.

Scambelluri, M., Müntener, O., Hermann, J., Piccardo, G.B., Trommsdorff, V., 1995. Subduction of water into the mantle: history of an Alpine peridotite. Geology 23, 459–462.

Scambelluri, M., Pennacchioni, G., Gilio, M., Bestmann, M., Plumper, O., Nestola, F., 2017. Fossil intermediate-depth earthquakes in subducting slabs linked to differential stress release. Nat. Geosci. 10, 960-+. https://doi.org/10.1038/s41561-017-0010-7

Scambelluri, M., Philippot, P., 2001. Deep fluids in subduction zones. Lithos 55, 213–227.

Scambelluri, M., Piccardo, G.B., Philippot, P., Robbiano, A., Negretti, L., 1997. High salinity fluid inclusions formed from recycled seawater in deeply subducted alpine serpentinite. Earth and Planetary Science Letters 148, 485–499.

Schmid, S., Kissling, E., 2000. The arc of the western Alps in the light of geophysical data on deep crustal structure. Tectonics 19, 62–85.

Schmid, S.M., Fügenschuh, B., Kissling, E., Schuster, R., 2004. Tectonic map and overall architecture of the Alpine orogen. Eclogae Geologicae Helvetiae 97, 93–117.

Schmid, S.M., Kissling, E., Diehl, T., van Hinsbergen, D.J., Molli, G., 2017. Ivrea mantle wedge, arc of the Western Alps, and kinematic evolution of the Alps–Apennines orogenic system. Swiss Journal of Geosciences 110, 581–612.

Schmid, S.M., Pfiffner, O.-A., Froitzheim, N., Schönborn, G., Kissling, E., 1996. Geophysical□geological transect and tectonic evolution of the Swiss□Italian Alps. Tectonics 15, 1036–1064.

Schmid, S.M., Scharf, A., Handy, M.R., Rosenberg, C.L., 2013. The Tauern Window (Eastern Alps, Austria): a new tectonic map, with cross-sections and a tectonometamorphic synthesis. Swiss Journal of Geosciences 106, 1–32.

Schmid, S.M., Fügenschuh, B., Kounov, A., Matenco, L., Nievergelt, P., Oberhänsli, R., Pleuger, J., Schefer, S., Schuster, R., Tomljenovic, B., Ustaszewski, K., van Hinsbergen, D.J.J. 2020. Tectonic units of the Alpine collision zone between Eastern Alps and western Turkey. Gondwana Research, 78, 308-374. https://doi.org/10.1016/j.gr.2019.07.005

Schwartz, S., 2000. La zone piémontaise des Alpes Occidentales: un paléocomplexe de subduction. Arguments métamorphiques, géochronologiques et structuraux.

Schwartz, S., Guillot, S., Reynard, B., Lafay, R., Debret, B., Nicollet, C., Lanari, P., Auzende, A.L., 2013. Pressure–temperature estimates of the lizardite/antigorite transition in high pressure serpentinites. Lithos 178, 197–210.

Schwartz, S., Guillot, S., Tricart, P., Bernet, M., Jourdan, S., Dumont, T., Montagnac, G., 2012. Source tracing of detrital serpentinite in the Oligocene molasse deposits from the western Alps (Barrême basin): implications for relief formation in the internal zone. Geological Magazine 149, 841–856.

Schwartz, S., Lardeaux, J.-M., Guillot, S., Tricart, P., 2000. Diversité du métamorphisme éclogitique dans le massif ophiolitique du Monviso (Alpes occidentales, Italie). Geodinamica Acta 13, 169–188.

Schwartz, S., Tricart, P., Lardeaux, J.-M., Guillot, S., Vidal, O., 2009. Late tectonic and metamorphic evolution of the Piedmont accretionary wedge (Queyras Schistes lustrés, western Alps): Evidences for tilting during Alpine collision. Geological Society of America Bulletin 121, 502–518.

Selverstone, J., Sharp, Z., 2013. Chlorine isotope constraints on fluid□rock interactions during subduction and exhumation of the Zermatt□Saas ophiolite. Geochemistry, Geophysics, Geosystems 14, 4370–4391.

Seno, S., Dallagiovanna, G., Vanossi, M., 2005. A kinematic evolutionary model for the Penninic sector of the central Ligurian Alps. International Journal of Earth Sciences 94, 114–129.

Seno, S., Dallagiovanna, G., Vanossi, M., 2003. Palaeogeography and thrust development in the Penninic domain of the Western Alpine chain: examples from the Ligurian Alps. BOLLETTINO-SOCIETA GEOLOGICA ITALIANA 122, 223–232.

Shillington, D.J., Bécel, A., Nedimović, M.R., Kuehn, H., Webb, S.C., Abers, G.A., Keranen, K.M., Li, J., Delescluse, M., Mattei-Salicrup, G.A., 2015. Link between plate fabric, hydration and subduction zone seismicity in Alaska. Nature Geoscience 8, 961–964.

Simon□Labric, T., Rolland, Y., Dumont, T., Heymes, T., Authemayou, C., Corsini, M., Fornari, M., 2009. 40Ar/39Ar dating of Penninic Front tectonic displacement (W Alps) during the Lower Oligocene (31–34 Ma). Terra Nova 21, 127–136.

Skora, S., Mahlen, N., Johnson, C.M., Baumgartner, L.P., Lapen, T., Beard, B.L., Szilvagyi, E., 2015. Evidence for protracted prograde metamorphism followed by rapid exhumation of the Zermatt□Saas Fee ophiolite. Journal of Metamorphic Geology 33, 711–734.

Spalla, M.I., Lardeaux, J.M., vittorio Dal Piaz, G., Gosso, G., Messiga, B., 1996. Tectonic significance of Alpine eclogites. Journal of geodynamics 21, 257–285.

Spandler, C., Pettke, T., Rubatto, D., 2011. Internal and external fluid sources for eclogite-facies veins in the Monviso meta-ophiolite, Western Alps: implications for fluid flow in subduction zones. Journal of Petrology 52, 1207–1236.

Spandler, C., Pirard, C., 2013. Element recycling from subducting slabs to arc crust: A review. Lithos 170, 208–223. https://doi.org/10.1016/j.lithos.2013.02.016

Spray, J.G., 1984. Possible causes and consequences of upper mantle decoupling and ophiolite displacement. Geological Society, London, Special Publications 13, 255–268.

Stampfli, G., Marchant, R., 1997. Geodynamic evolution of the Tethyan margins of the Western Alps. Deep structure of the Swiss Alps-Results from NRP 20 223–239.

Stampfli, G., Mosar, J., Marquer, D., Marchant, R., Baudin, T., Borel, G., 1998. Subduction and obduction processes in the Swiss Alps. Tectonophysics 296, 159–204.

Stampfli, G.M., Borel, G., 2002. A plate tectonic model for the Paleozoic and Mesozoic constrained by dynamic plate boundaries and restored synthetic oceanic isochrons. Earth and Planetary Science Letters 196, 17–33.

Stern, R.J., 2002. Subduction zones. Reviews of geophysics 40, 3–1.

Sternai, P., Sue, C., Husson, L., Serpelloni, E., Becker, T.W., Willett, S.D., Faccenna, C., Di Giulio, A., Spada, G., Jolivet, L., 2019. Present-day uplift of the European Alps: Evaluating mechanisms and models of their relative contributions. Earth-science reviews 190, 589–604.

Stüwe, Schuster, R. 2010. Initiation of subduction in the Alps: Continent or ocean? Geology, 38/2, 175-178

Tamblyn, R., Zack, T., Schmitt, A., Hand, M., Kelsey, D., Morrissey, L., Pabst, S., Savov, I., 2019. Blueschist from the Mariana forearc records long-lived residence of material in the subduction channel. Earth and Planetary Science Letters 519, 171–181.

Tartarotti, P., Guerini, S., Rotondo, F., Festa, A., Balestro, G., Bebout, G.E., Cannaò, E., Epstein, G.S., Scambelluri, M., 2019. Superposed sedimentary and tectonic block-in-matrix fabrics in a subducted serpentinite mélange (High-pressure zermatt saas ophiolite, western alps). Geosciences 9, 358.

Tartarotti, P., Zucali, M., Panseri, M., Lissandrelli, S., Capelli, S., Ouladdiaf, B., 2011. Mantle origin of the Antrona serpentinites (Antrona ophiolite, Pennine Alps) as inferred from microstructural, microchemical, and neutron diffraction quantitative texture analysis. Ofioliti 36, 167–189.

Thöni, M., 1999. A review of geochronological data from the Eastern Alps. Schweizerische Mineralogische und Petrographische Mitteilungen 79, 209–230.

Tilton, G., Schreyer, W., Schertl, H.-P., 1991. Pb– Sr– Nd isotopic behavior of deeply subducted crustal rocks from the Dora Maira Massif, Western Alps, Italy-II: what is the age of the ultrahigh-pressure metamorphism? Contributions to Mineralogy and Petrology 108, 22–33.

Tricart, P., 1984. From passive margin to continental collision; a tectonic scenario for the Western Alps. American Journal of Science 284, 97–120.

Tricart, P., Bourbon, M., Lagabrielle, Y., 1982. Révision de la coupe Péouvou-Roche Noire (zone piémontaise, Alpes franco-italiennes): bréchification synsédimentaire d'un fond océanique ultrabasique. Géol. alp. Grenoble 58, 105–113.

Tricart, P., Lemoine, M., 1991. The Queyras ophiolite West of Monte Viso (Western Alps): indicator of a pecular ocean floor in the Mesozoic Tethys. Journal of Geodynamics 13, 163–181.

Tricart, P., Lemoine, M., 1986. From faulted blocks to megamullions and megaboudins: Tethyan heritage in the structure of the Western Alps. Tectonics 5, 95–118.

Trommsdorff, V., Piccardo, G., Montrasio, A., 1993. From magmatism through metamorphism to sea floor emplacement of subcontinental Adria lithosphere during pre-Alpine rifting (Malenco, Italy). Schweizerische Mineralogische und Petrographische Mitteilungen 73, 191–203.

Trümpy, R., 1960. Paleotectonic evolution of the Central and Western Alps. Geological Society of America Bulletin 71, 843–907.

Trümpy, 2006. Geologie der Iberger Klippen und ihrer Flysch-Unterlage. Eclogae geol. Helv. 99, 79–121. DOI 10.1007/s00015-006-1180-2

Vaggelli, G., Borghi, A., Cossio, R., Fedi, M., Giuntini, L., Lombardo, B., Marino, A., Massi, M., Olmi, F., Petrelli, M., 2006. Micro-PIXE analysis of monazite from the Dora Maira massif, western Italian Alps. Microchimica Acta 155, 305–311.

Van der Klauw, S., Reinecke, T., Stöckhert, B., 1997. Exhumation of ultrahigh-pressure metamorphic oceanic crust from Lago di Cignana, Piemontese zone, western Alps: the structural record in metabasites. Lithos 41, 79–102.

Van Hinsbergen, D.J., Torsvik, T.H., Schmid, S.M., Maţenco, L.C., Maffione, M., Vissers, R.L., Gürer, D., Spakman, W., 2020. Orogenic architecture of the Mediterranean region and kinematic reconstruction of its tectonic evolution since the Triassic. Gondwana Research 81, 79–229.

van Keken, P.E., Hacker, B.R., Syracuse, E.M., Abers, G.A., 2011. Subduction factory: 4. Depth□dependent flux of H2O from subducting slabs worldwide. Journal of Geophysical Research: Solid Earth 116.

Vannucchi, P., Spagnuolo, E., Aretusini, S., Di Toro, G., Ujiie, K., Tsutsumi, A., Nielsen, S., 2017. Past seismic slip-to-the-trench recorded in Central America megathrust. Nat. Geosci. 10, 935–940. https://doi.org/10.1038/s41561-017-0013-4

Vignaroli, G., Faccenna, C., Rossetti, F., 2009. Retrogressive fabric development during exhumation of the Voltri Massif (Ligurian Alps, Italy): arguments for an extensional origin and implications for the Alps–Apennines linkage. International Journal of Earth Sciences 98, 1077–1093.

Vignaroli, G., Rossetti, F., Rubatto, D., Theye, T., Lisker, F., Phillips, D., 2010. Pressure□temperature□deformation□time (P□T□d□t) exhumation history of the Voltri Massif HP complex, Ligurian Alps, Italy. Tectonics 29.

Villa, I.M., Bucher, S., Bousquet, R., Kleinhanns, I.C., Schmid, S.M., 2014. Dating polygenetic metamorphic assemblages along a transect across the Western Alps. Journal of Petrology 55, 803–830.

Vissers, R.L., van Hinsbergen, D.J., Meijer, P.T., Piccardo, G.B., 2013. Kinematics of Jurassic ultra-slow spreading in the Piemonte Ligurian ocean. Earth and Planetary Science Letters 380, 138–150.

Vitale Brovarone, A., Agard, P., 2013. True metamorphic isograds or tectonically sliced metamorphic sequence? New high-spatial resolution petrological data for the New Caledonia case study. Contrib. Mineral. Petrol. 166, 451–469. https://doi.org/10.1007/s00410-013-0885-2

Vitale Brovarone, A., Beyssac, O., Malavieille, J., Molli, G., Beltrando, M., Compagnoni, R., 2013. Stacking and metamorphism of continuous segments of subducted lithosphere in a high-pressure wedge: the example of Alpine Corsica (France). Earth-Science Reviews 116, 35–56.

Vitale Brovarone, A., Picatto, M., Beyssac, O., Lagabrielle, Y., Castelli, D., 2014a. The blueschist-eclogite transition in the Alpine chain: P-T paths and the role of slow-spreading extensional structures in the evolution of HP-LT mountain belts. Tectonophysics 615, 96–121. https://doi.org/10.1016/j.tecto.2014.01.001

Vitale Brovarone, A., Alard, O., Beyssac, O., Martin, L., Picatto, M., 2014b. Lawsonite metasomatism and trace element recycling in subduction zones. Journal of Metamorphic Geology 32, 489–514.

Von Raumer, J., Abrecht, J., Bussy, F., Lombardo, B., Menot, R.-P., Schaltegger, U., 1999. The Paleozoic metamorphic evolution of the Alpine external massifs. Schweizerische Mineralogische und Petrographische Mitteilungen 79, 5–22.

Wada, I., Wang, K., He, J., Hyndman, R.D., 2008. Weakening of the subduction interface and its effects on surface heat flow, slab dehydration, and mantle wedge serpentinization. Journal of Geophysical Research: Solid Earth 113.

Wagreich, M., 2001. A 400□km□long piggyback basin (Upper Aptian–Lower Cenomanian) in the Eastern Alps. Terra Nova 13, 401–406.

Wagreich, M., 1995. Subduction tectonic erosion and Late Cretaceous subsidence along the northern Austroalpine margin (Eastern Alps, Austria). Tectonophysics 242, 63–78.

Wagreich, M., Decker, K., 2001. Sedimentary tectonics and subsidence modelling of the type Upper Cretaceous Gosau basin (Northern Calcareous Alps, Austria). International Journal of Earth Sciences 90, 714–726.

Wakabayashi, J., 2017. Structural context and variation of ocean plate stratigraphy, Franciscan Complex, California: insight into mélange origins and subduction-accretion processes. Progress in Earth and Planetary Science 4, 18. https://doi.org/10.1186/s40645-017-0132-y

Wakabayashi, J., 2015. Anatomy of a subduction complex: architecture of the Franciscan Complex, California, at multiple length and time scales. International Geology Review 57, 669–746. https://doi.org/10.1080/00206814.2014.998728

Wakabayashi, J., Dilek, Y., 2003. Ophiolites in Earth history, Geological Society of London Special Publication 218.

Wannamaker, P.E., Evans, R.L., Bedrosian, P.A., Unsworth, M.J., Maris, V., McGary, R.S., 2014. Segmentation of plate coupling, fate of subduction fluids, and modes of arc magmatism in C ascadia, inferred from magnetotelluric resistivity. Geochemistry, Geophysics, Geosystems 15, 4230–4253.

Weh, M., Froitzheim, N., 2001. Penninic cover nappes in the Prattigau half-window (Eastern Switzerland): Structure and tectonic evolution. Eclogae Geologicae Helvetiae 94, 237–252.

White, D.A., Roeder, D.H., Nelson, T.H., Crowell, J.C., 1970. Subduction. Geological Society of America Bulletin 81, 3431–3432.

Wiederkehr, M., Bousquet, R., Schmid, S.M. & Berger, A. 2008. From subduction to collision: thermal overprint of HP/LT meta-sediments in the north-eastern Lepontine Dome (Swiss Alps) and consequences regarding the tectono-metamorphic evolution of the Alpine orogenic wedge. Swiss Journal of Geosciences 101/Supplement 1, S127–S155. DOI 10.1007/s00015-008-1289-6

Wiederkehr, M., Sudo, M., Bousquet, R., Berger, A., Schmid, S.M., 2009. Alpine orogenic evolution from subduction to collisional thermal overprint: The 40Ar/39Ar age constraints from the Valaisan Ocean, central Alps. Tectonics 28.

Wiederkehr, M., Bousquet, R., Ziemann, M.A., Berger, A. & Schmid, S.M., 2011. 3-D assessment of peak-metamorphic conditions by Raman spectroscopy of carbonaceous material: an example from the margin of the Lepontine dome (Swiss Central Alps). International Journal of Earth Sciences 100,1029–1063. DOI 10.1007/s00531-010-0622-2

Willner, A.P., 2005. Pressure–temperature evolution of a Late Palaeozoic paired metamorphic belt in North–Central Chile (34–35 30′ S). Journal of Petrology 46, 1805–1833.

Winkler, W., Wildi, W., Stuijvenberg, J.V., Caron, C., 1985. Wägital-Flysch et autres flyschs pénniques en Suisse Centrale: Stratigraphie, sédimentologie et comparaisons. Eclogae Geologicae Helvetiae 78, 1–22.

Yamaguchi, A., Ujiie, K., Nakai, S., Kimura, G., 2018. Sources and physicochemical characteristics of fluids along a subduction-zone megathrust: A geochemical approach using syn-tectonic mineral veins in the Mugi mélange, Shimanto accretionary complex. Geochemistry, Geophysics, Geosystems 13. https://doi.org/10.1029/2012GC004137

Yamato, P., Brun, J.P., 2017. Metamorphic record of catastrophic pressure drops in subduction zones. Nat. Geosci. 10, 46–50. https://doi.org/10.1038/NGEO2852

Zanoni, D., Rebay, G., Spalla, M., 2016. Ocean floor and subduction record in the Zermatt□Saas rodingites, Valtournanche, Western Alps. Journal of Metamorphic Geology 34, 941–961.

Zhao, L., Paul, A., Guillot, S., Solarino, S., Malusà, M.G., Zheng, T., Aubert, C., Salimbeni, S., Dumont, T., Schwartz, S., 2015. First seismic evidence for continental subduction beneath the Western Alps. Geology 43, 815–818.

Zhao, L., Malusà, M.G., Yuan, H., Paul, A., Guillot, S., Lu, Y., Stehly, L., Solarino, S., Eva, E., Lu, G., 2020. Evidence for a serpentinized plate interface favouring continental subduction. Nature Communications 11, 1–8.

2500 Zimmermann, R., Hammerschmidt, K., Franz, G., 1994. Eocene high pressure metamorphism in the
2501 Penninic units of the Tauern Window (Eastern Alps): evidence from 40 Ar– 39 Ar dating and
2502 petrological investigations. Contributions to Mineralogy and Petrology 117, 175–186.
2503

Figure captions

Fig. 1

a) General structural map of the Alpine belt (after Handy and Oberhänsli, 2004; Schmid et al., 2004). The two branches of the Alpine 'ocean', the Valais and Liguro-Piemont Penninic domains, are outlined in light and dark blue respectively.

b) Highly schematic cross-section (along A-A', ; after Agard and Lemoine, 2005) illustratings the structural organization of the major paleogeographic domains recognized in the belt, from the Austro-Alpine units on top to the European units below. The sub-division into Western, Central and Eastern Alps corresponds to that adopted in the text. The location of the main geophysical profiles and cross-sections shown in later figures is indicated (B-B' and C-C'; Fig. 7; D-D': Fig. 12). Abbreviations: AM: Argentera-Mercantour; AG: Aar-Gotthard; BO: Belledonne-Oisans; DM: Dora Maira; GP: Gran Paradiso; MB: Mont Blanc; MR: Monte Rosa.

c) Cartoon showing the simplified geodynamic subduction setting of the Alps, with emphasis on subduction interface processes. The respective location of the Valais and Liguro-Piemont oceans can be readily deduced from the structural relationships between the European, Penninic and Austro/Southalpine domains (to be compared with figure 1b).

Fig. 2

a) Close-up view of figure 1a for the Western Alps for comparison with b) and c). Abbreviations as for Fig. 1.

b) Distribution of metamorphic facies (as in Oberhänsli and Goffé, 2004) within the ocean-derived units across the same area.

c) Distribution of lithologies across the oceanic units separating the sedimentary-dominated ('S') domains from those dominated by oceanic crust and serpentinized peridotites (i.e., mafic and ultramafic: 'MUM'). See § 3.1, 3.2.

Note the marked W-E zoning in b) and c). For the sake of convenience, the main sectors of the Western Alps are subd-divided into the Combin, Grivola, Maurienne, Cottian and Queyras (b). The main mafic- and ultramafic-dominated MUM massifs referred to in the text are shown in c).

Fig. 3

a) Representative lithostratigraphic columns for metasedimentary domains of the Western Alps (after Lemoine et al., 1986; Tricart and Lemoine, 1991; Deville et al., 1992; Michard et al., 1996; compilation by Epstein et al., 2019). Inset: detailed section at the base of one of the Queyras units (Tricart et al., 1982).

b) Paleogeography of the Alpine realm at ~120 Ma (Aptian) after Vissers et al. (2013), at its maximum extent (see § 2.3). Uncertainties are on the order of 100-200 km at least.

c) Schematic 3D view of the Alpine domain at ~120 Ma (compare with b) emphasizing the highly stretched nature of the continental margins, the presence of micro-continental blocks (e.g., Briançonnais, Sesia Zone) or extensional allochtons. The location of the main units discussed in the text is modified after Berger and Bousquet (2008), Manatschal and Müntener (2009) and Picazo et al. (2016). The Eoalpine subduction, whose orientation is still debated, is shown to the NE of the Alpine domain considered here (Froitzheim et al., 1996; Kästle et al., 2019). The exact location of subduction initiation within the Alpine domain is unknown, but probably to be looked for to the east, as shown here.

Abbreviations (same as in the following figures, unless specififed; Continental fragments are capitalized): A: Avers; Av: Avic; Bu: Bündnerschiefer; C: Cottian; Ch: Chenaillet; Co: Combin; DM: Dora Maira; E: Engadine; GP: Gran Paradiso; K: Koralpe; M: Maurienne; Ma: Malenco; MR: Monte Rosa; MS: Margna-Sella; Pl: Platta; Pm: Piemonte units; Q: Queyras; R: Rechnitz; Ro: Rocciavre; Sa: Saualpe; SE: Sesia; T: Tauern; Ta: Tasna; Ve: Versoyen; Vi: Monviso; Z: Zermat-Saas.

d) Chronological overview of the main Alpine geodynamic stages. See text for details.

Fig. 4

Typical former oceanic sediments deposited on ophiolitic seafloor (i.e., calcschists, pelagic limestones and shales, radiolarian cherts; locations in the Western Alps).

a) Characteristic calcschist exposure of the Schistes Lustrés (E. of Aiguilles, Queyras).

b)

Direct sedimentary contact between serpentinized and brecciated peridotite criss-crossed by calcite veins ('ophicalcite') and metasediments (Col d'Urine, Pelvas d'Abries; see Lagabrielle et al., 2015). The first horizon is a fine-grained mixture of ultramafic debris and pelagic sediments. The sequence is progressively richer in sedimentary fraction, then changes to carbonate-dominated. These rocks were affected by blueschist facies metamorphism.

c-d) Regular alternations of pelitic- (white arrows) and carbonate-rich horizons (black arrows), overall more carbonate-rich (particularly in d).e) Boudinaged mafic horizon in impure marble (Zermatt-Saas area).

f) Dignostic late Jurassic marble horizon (Crête de la Taillante, north of Col Agnel,Queyras). These tend to be more abundant in the eastern (lower) S units.

g) Carbonates directly overlapping onto a large mafic body (north of Rocca Bianca, Queyras; see also Lagabrielle et al., 2015).

h)) Large km-scale extensional allochton in the Haute Ubaye valley (Western Queyras). The well-stratified dolomitic Triassic limestone from the Peouvou, which dominates the scenery to the right/east of the picture, is wrapped up in organic-rich calcschists (left part of the picture). Dm-scale, very fresh blueschist facies carpholite crystals are found in the scree from landslides reworking the calcschists.

Fig. 5

Characteristic features of the metasedimentary (S) units of the Western Alps (Schistes Lustrés).

a) View across the three main units recognized in the Cottian Alps (near Sestriere), i.e. the upper, middle and lower S units. Compare with the map of Fig. 7d. Note the relatively smooth landscape, which partly results from the erodability of the calcschist-dominated units and the smoother slopes of the more pelitic Lago Nero unit.

b) View across the main units recognized in the Queyras (following Lagabrielle et al., 2015; view from Bric froid), the middle, lower and Monviso units (see Fig. 6a for the extension to the east across MUM units). Note the larger mafic (gabbroic) masses enmbedded in the S units (Pelvas d'Abries, Crête des Lauzes).

c) Alternation of pelitic- and carbonate-rich horizons. The pelitic fraction is littered with black lawsonite crystals.
d) Microphotograph of fresh mm- to cm-scale lawsonite crystals hosting a significant fraction of dispersed organic matter (together with rutile) and showing evidence for growth zoning (Triplex, Fig. 5a; after Lefeuvre et al., 2020).
e) Almost pure, very fresh ferro-magnesian carpholite-bearing veins in pelitic schist (Ubaye valley, Queyras; location in Fig. 4g).
f) Lawsonite blueschist facies metabasalt embedded in the upper S unit, preserving fresh lawsonite and glaucophane (Queyras; courtesy M. Ballèvre).
g) Typical chloritoid-bearing calcschist from the lower S unit (Val Clavalité, southern Aosta valley).
h) Strongly deformed chloritoid-chlorite-bearing mica(calc)schist, with phengite composition attesting to high pressure conditions. Chloritoid is partly retrogressed here.

Fig. 6

Characteristic features of the mafic and ultramafic-dominated (MUM) units of the Western Alps.
a) View onto one of the best-preserved 'slab' fragments in the world (Fig. 8): the 2-2.5 km-thick Lago Superiore unit (Monviso massif, Italy; see Fig. 5b for location). Note the tectonic contact with the overlying blueschist facies Monviso unit, whose lithostratigraphy is completely overturned. In the Lago Superiore unit, the pristine lithological succession of the downgoing lithosphere is preserved to a first approximation with, from bottom to top: ~500m thick serpentinized basal peridotites, eclogitized Mg-rich metagabbros, sills, dykes and a discontinuous layer of Fe-Ti metagabbros hosting garnet, omphacite, abundant rutile and lawsonite pseudomorphs, partly retrogressed metabasalts and a few meters of metamorphosed calcschists at the very top, below the Monviso unit.
b) Eclogite facies metapillows unveiled by glacial retreat (N of Pfülwe pass, Zermatt-Saas): note the abundance of lawsonite pseudomorphs, particularly around the former pillows (see close-up view in Fig. 6e; S. Angiboust for scale)

c-d) Large, several km-thick metaperidotite bodies of the Avic massif (also noticeable from the sparse vegetation; location in Fig. 2). Some hm-scale gabbroic horizons are found here and there, as in c).

e) Metapillows, pillow-breccias and surrounding hyaloclastites metamorphosed under eclogite facies conditions. Note the contrast between the lawsonite-rich rim of the elliptic former pillow, hydrated during seafloor hydrothermal alteration, and the dry garnet-omphacite-bearing core. Lawsonite pseudomorphs are ubiquitous across km-scale exposures between Zermatt and Täsch.

f) Metagabbros boudins, with composition intermediate between magnesian and Fe-Ti rich, in strongly deformed basals (Zermatt-Saas region).

g) Garnet-chloritoid-glaucophane ± omphacite-bearing metabasalt (Val Clavalité, Aosta valley).

h) Garnet-glaucophane-bearing eclogite with large lawsonite pseudomorphs (Zermatt-Saas).

i) Typical garnet-omphacite-rutile-bearing Fe-Ti-rich metagabbro from the Monviso massif (Lago Superiore unit, Fig. 6a).

Fig. 7

Focus on the metasedimentary-dominated (S) units from the Maurienne to Northern Queyras, Western Alps. Abbreviations (all others as in Fig. 3c): Amb: Ambin; Br: Briançonnais; HF: Helminthoid flysch; PF: Penninic front.

a) Schematic crustal-scale section across the Western Alps along profile B-B', approximately at the latitude of Briançon (see location on Fig. 1a; after Agard et al., 2009).

b) Close-up, simplified section across the S units along profile C-C' (location in Fig. 7d). Note the fairly regular increase of P-T conditions from west to east.

c) Structural map of the area from the Maurienne to Northern Queyras, showing the sub-division into three major units (lower, middle and upper S units). In the Queyras-Cottian Alps, three or four units are recognized depending on latitude and authors (see § 3.1; the two upper S units are after Lagabrielle et al., 2015). Temperatures correspond to maximum temperature estimated using the irreversible transformation of organic matter in the rocks (data and calibration from Beyssac et al., 2002; data

from Gabalda et al. 2009; Plunder et al., 2012; Schwartz et al., 2013). Figure modified after Vitale-Brovarone et al. (2014a).

d) Simplified structural map of the area embraced by the landscape view of Fig. 5a, to the east of Sestriere, at the latitude between the Chenaillet and Rocciavre massifs. Mineral isograds outline the eastward increase in temperature. Phengite isopleths, which vary from 3.3 to 3.6 Si per formula unit, outline the eastward increase in pressure. Both are from Agard et al. (2001).

e) Pressure-temperature estimates for the area shown in Fig. 7d (plain ellipses; updated from Agard et al., 2001, 2002). Dotted ellipses refer to studies further north in the Maurienne (PI12: Plunder et al., 2012) or further south in the Monviso area (Locatelli et al., 2018 and references therein; AG20: Angiboust and Glodny, 2020).

f) Boxplots capturing the range of maximum temperatures for the lower, middle and upper units across the area shown in Fig. 7c.

Fig. 8

Strain localization and fluid migration in the MUM fragment of the Monviso massif (Lago Superiore unit).

a) Eclogite breccia formed by angular fragments of eclogitized Fe-Ti-rich metagabbros dispersed in an eclogite-facies matrix/cement (Angiboust et al., 2012a; Locatelli et al., 2018). They reveal the existence of intermediate-depth brittle events, possibly seismic, during the subduction process. These breccia are found along ~15 km in the Lago Superiore unit (see Locatelli et al., 2019a,b for detailed mapping and characterization). c) Relocation of the Lago Superiore unit within its past subduction environment, prior to detachment from the downgoing slab (and that of the Monviso unit; see Fig. 6a; after Locatelli et al., 2018). The km-scale internal shear zones (LSZ, ISZ) operated during eclogite facies metamorphism, prior to tectonic slicing along the basal shear zone now separating the oceanic unit from the continental Dora Maira massif below.

d) Schematic sequence of events leading to the formation of eclogite breccia (after Angiboust et al., 2012a).

e) Inferred restoration prior to subduction highlighting the discontinuous nature of the Alpine oceanic lithosphere (see § 2.2.1). In addition to shear zones formed at ~80 km depth (as testified by the presence of eclogite brecciation), some initial sedimentary

and/or magmatic contacts were reworked or may have guided deformation during subduction.

Fig. 9

a) Characteristic shape of P-T paths for subducted alpine units. For oceanic fragments: Engadine (E; after Bousquet et al., 1998, 2002); Valaisan Petit Saint Bernard (VSB; Bousquet et al., 2002); Cottian Alps (lower, middle and upper units; Agard et al., 2001a; Plunder et al., 2012; see Fig. 4); Monviso (MV; Angiboust et al., 2012a; Locatelli et al., 2018); Zermatt-Saas (Groppo et al., 2009; Angiboust and Agard, 2010). P-T paths for the continental Internal Basement Complexes are shown for comparison (Dora Maira UHP: after Chopin and Shertl, 1999; Groppo et al., 2007; Gran Paradiso: Manzotti et al., 2015).

b) Synthetic pressure-time paths of subducted Alpine fragments. Note the contrast between the early and late subduction period, with no fragments recovered for the first one. Pressure estimates compiled from the literature and available on request (see also Berger and Bousquet, 2008, Agard et al. 2009, 2018; Rebay et al., 2018). Since only rare studies provide closely tied P-T and age, average P-T and time estimates for peak burial had to be averaged independently. Circle size is indicative of the number of available age constraints: there are for example at least fourteen instrumentally well-constrained estimates for the peak burial of Zermatt-Saas area, north of the Aosta valley (Lu-Hf on garnet: Lapen et al., 2003; Herwartz et al., 2008; Skora et al., 2015; Bücher et al., 2020); Sm/Nd on garnet: Bowtell et al., 1994; Amato et al., 1999; Skora et al., 2015; Ar/Ar on phengite: Gouzu et al., 2006; U/Pb on zircon: Rubatto et al., 1998; Rb/Sr: Barnicoat et al., 1995; Skora et al., 2015). Constraints on the exhumation path are comprised in the thicker segment. Fewer studies and ages are available for Monviso (Monié and Philippot, 1989; Duchêne et al., 1997; Cliff et al., 1998; Rubatto and Hermann, 2003; Rubatto and Angiboust, 2015). Hatched gray boxes refer to exhumation constraints for metasediments (Agard et al., 2002). Abbreviations as in figure 3c.

c) Schematic tectonic evolution across the Liguro-Piemont domain of the southern Western Alps (after Agard et al., 2002), from the subduction of oceanic lithosphere onto continental subduction and finally collision. This evolution, along profile B-B' (Fig. 7a), is used as a template to compare and evaluate subducted-related tectonic

contrasts along the alpine orogen (see § 4.2, 4.3 and 6, and Figs. 11-14). Exhumation stages and shear senses (D2,D3) after Agard et al. (2001a) and Plunder et al. (2012). Similar shear senses were reported by Ghignone et al. (2020). Note the tectonometamorphic contrast between the S units and MUM units: the latter show higher P-T values, faster exhumation velocities (Fig. 9a), larger coherent tracts of mafic units, lithostratigraphic features ascribable to OCT in several locations, and burial and exhumation during the final stages of the subduction process, a few Ma at most before the internal crystalline massifs (Fig. 9b). In a broader orogenic perspective, the Alpine belt can be seen as the result of the imbrication of three successive, different scale accretionary/decoupling systems: oceanic (between the S and MUM units), crustal (between continental sediments and deeper subducted crust), and finally lithospheric (e.g., indentation by the Ivrea body during collision, as shown by the last step in the figure).

Fig. 10

Comparison of P-T estimates for all Alpine subducted oceanic fragments, grouped by locality, with diagnostic data worldwide (Agard et al., 2018). For the sake of comparison, P-T estimates shown here are those listed in Agard et al. (2018). Values for the Central and Eastern Alps, not considered then, are those cited in the text. All localities align along or close to the subduction P-T gradient for mature subduction. This observation also allows to rule out significant overpressure in the Alps, since it would engender variable P/T ratios in the rock record (see additional arguments in § 6.1). Maximum pressures largely differ along strike and in particular no deeply buried rocks are recovered east of the Simplon/Lepontine Central Alps (save possibly for the small Lanzada fragment: Figs. 12a,c).

Fig. 11

a) Idealized restoration of the subduction configuration in the Western Alps during the Paleocene, at ~60 Ma, after subduction and partial exhumation of the Sesia micro-continental sliver. The section is a composite one since the Sesia Zone is projected here laterally onto the Helminthoid Flysch-Monviso traverse (section B-B'; Figs. 1a, 7a). This figure is to be compared with figures 3c, 9c and14. Particular attention was

devoted to respecting the scales of the units and their distances from one another. No vertical exaggeration. Tectonic contacts formed during oceanic stages are featured in grey whereas subduction-related ones are shown in black.
b-d) Tectonic evolution towards the end of oceanic subduction, specifically for the southern western Alps (i.e., Sector A; Maurienne to Queyras; § 4.3; Figs. 13,14). Uncertainties concern the age of underplating of the upper S units, or the exact age of peak burial for Dora Maira, most likely between 40 and 35 Ma (§ 3.3). The evolution considers peak burial at 46-45 Ma for Monviso (Fig. 9b; see text) and ~ 38 Ma for Dora Maira. Given convergence velocities on the order of 1 cm/a (§ 2.3), the detachment of the Lago Superiore slice of the Monviso massif (Figs. 6a,8) and part of its exhumation relate to the entrance of the Briançonnais micro-continent into subduction. This is even clearer for sector B i.e. for the broad Zermatt-Saas area, as shown by figure 9b, with the entrance of Gran Paradiso and Monte Rosa.

Fig. 12

a) Geological map of the Central Alps (after Schmid et al., 1996, 2004; Wei and Froitzhzeim, 2001). Same colors as in Fig. 1a. Maximum temperatures outline the collisional overprint across the Valais domain (after Wierderkehr et al., 2011).
b) Simplified section across D-D'.
c) Compilation of P-T paths for the Central Alps (see text for references). Light blue color paths and corresponding stars correspond to localities of the Valais domain shown in Fig. 12a (see Wiederkehr et al., 2011).
d) Paleogeographic restoration of the Central Alps region shortly after the rifting of the Liguro-Piemont domain (after Froitzheim et al., 1996; Mohn et al., 2011) showing key locations of the ocean-continent transitional domain, e.g. the Malenco exhumed sub-continental mantle, Margna-Sella extensional allochtons and Platta oceanic core-complex.
e) Idealized restoration of the subduction configuration in the Central Alps during the Paleocene, at ~60-55 Ma, after subduction and partial exhumation of the Margna-Sella micro-continental sliver. The exact timing of subduction/exhumation of Malenco and the Avers (and Lanzada) units are not known with precision (see text for details) but lie in the range 60-40 Ma. Compare with Fig. 11a.

Fig. 13

a) Distribution of the metamorphic facies of all subducted Alpine oceanic domains. Sectors A-D are defined solely on the basis of marked contrasts in the history of subducted fragments (see § 4.3 for details). Sector boundaries are indicative (and therefore drawn as straight lines) since they were certainly deformed by later collision.

b) Same as a) for sectors A-C featuring the Internal Basement Complexes and the Sesia Zone: an obvious correlation exists (i) between the spatial extent of the mid-Penninic internal Briançonnais IBC and the location of deeply buried - yet recovered - subducted oceanic fragments, and (ii) between the Sesia Zone and sector B (see text).

c) Similar map with Helminthoid flyschs, Préalpes, External crystalline massifs and the entire Briançonnais domain for comparison. Note the match between sector B and the Préalpes or Ivrea body (after Zhao et al., 2015, 2020).Transect C was strongly affected by continental collision in its western part, which may suggest further subdivision of this domain.

Fig. 14

Idealized view of the Alpine subduction zone at ~40 Ma, showing the relative location of all fragments discussed in the text. Compare with figure 3c (same abbreviations).

Further work could help relate these lateral contrasts to inherited structures (Variscan- or rifting-related), differences in incoming material impacting subduction (e.g., sediment input, magmatic production) or differential kinematics. See text for details.

Fig. 15

Conceptual view of the subducted interface as inferred from the Alpine example, i.e. for a slow-spreading, discontinuous oceanic domain with a P/T gradient typical of mature subduction.

a) Inset: key 'ingredients' of the subduction factory, emphasizing mechanical aspects (i.e. long- and short-term coupling) and fluid release. The dashed area corresponds to figure b). More generally this zone is mechanically decoupled in the long-run but transiently coupled/blocked at times, since the plate interface contact steps down into

the slab to strip pieces from it (i.e., the recovered subducted fragments now exposed in the orogen). Adapted from Agard et al. (2018).

b) Close-up view onto the plate interface. The discontinuous crust and part of the mantle are sliced off the slab and become the MUM units, while metasedimentary S units (attesting to a shallower transient stepping-down of the plate contact into the slab) are commonly underplated preferentially at ~30-40 km depth, near the down dip end of the seismogenic zone. Deeper underplating also occurs in the southern Western Alps (middle and upper S units, from the Maurienne to Queyras; Figs. 7c, 11). Note that 'underplating' is loosely used in the literature as synonymous for the detachment of metasedimentary units from the slab and possible plastering below the upper plate, but the mechanics and triggering of this process are probably not different from that detaching MUM units (save for the depth of the décollement). Metasedimentary slices, howewer, seem to return more slowly to the surface (Fig. 9b). Detachment of tectonic slices/fragments probably takes place along former tectonic discontinuities (shown in grey as for figure 11; see Figs. 8c,e) and along newly formed ones (shown as black). The latter case can be demonstrated in Monviso, for example, with shear zones formed at intermediate-depth and bearing evidence for past brittle events (yellow stars; most likely earthquakes), or in Lanzo (past earthquakes marked by pseudotachylites).

A number of studies have dealt with element/fluid transfer across and along the interface/channel, to characterize fluid composition and provide some assessment of fluid migration. It is hoped that the present sketch will prove useful to set back future observations. So far, however, no proven fragment from the mantle wedge has been recovered in the Alps, and none that would have been paired with a deep tectonic slice from the downgoing slab. This is a major limitation for the assessment of effective element/fluid transfer to the mantle wedge and extrapolation to sub-arc depths.

Fig. 1

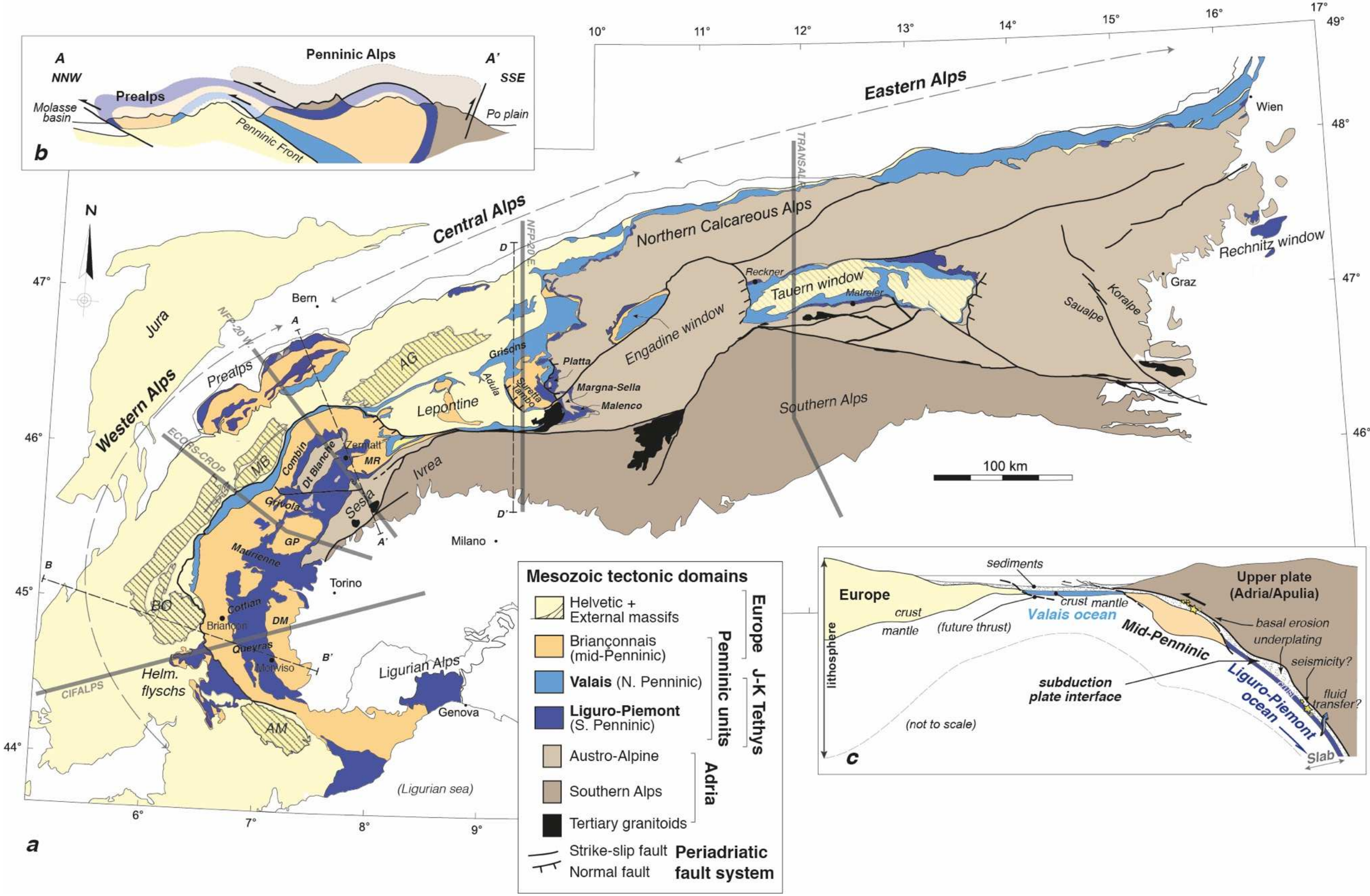

A
NNW
Penninic Alps
A'
SSE
Prealps
Molasse basin
Penninic Front
Po plain
b
Eastern Alps
Central Alps
Western Alps
Wien
Graz
Rechnitz window
Koralpe
Saualpe
Northern Calcareous Alps
TRANSALP
Reckner
Tauern window
Matreier
Engadine window
Southern Alps
Platta
Margna-Sella
Malenco
Grisons
Adula
Suretta
Tambo
Lepontine
NFP-20 E
NFP-20 W
D
D'
AG
Jura
Prealps
Bern
A
A'
ECORS-CROP
MB
Combin
Dt Blanche
Zermatt
MR
Grivola
Sesia
Ivrea
Milano
GP
Maurienne
Torino
BO
Cottian
Briançon
DM
Queyras
Monviso
B
B'
CIFALPS
Helm. flyschs
AM
Ligurian Alps
Genova
(Ligurian sea)
100 km
N
a
Mesozoic tectonic domains
Helvetic + External massifs
Briançonnais (mid-Penninic)
Valais (N. Penninic)
Liguro-Piemont (S. Penninic)
Austro-Alpine
Southern Alps
Tertiary granitoids
Strike-slip fault
Normal fault
Periadriatic fault system
Europe
Penninic units
J-K Tethys
Adria
Europe
crust
mantle
lithosphere
sediments
(future thrust)
crust mantle
Valais ocean
Mid-Penninic
Upper plate (Adria/Apulia)
basal erosion
underplating
seismicity?
fluid transfer?
subduction plate interface
Liguro-Piemont ocean
(not to scale)
Slab
c

Fig. 2

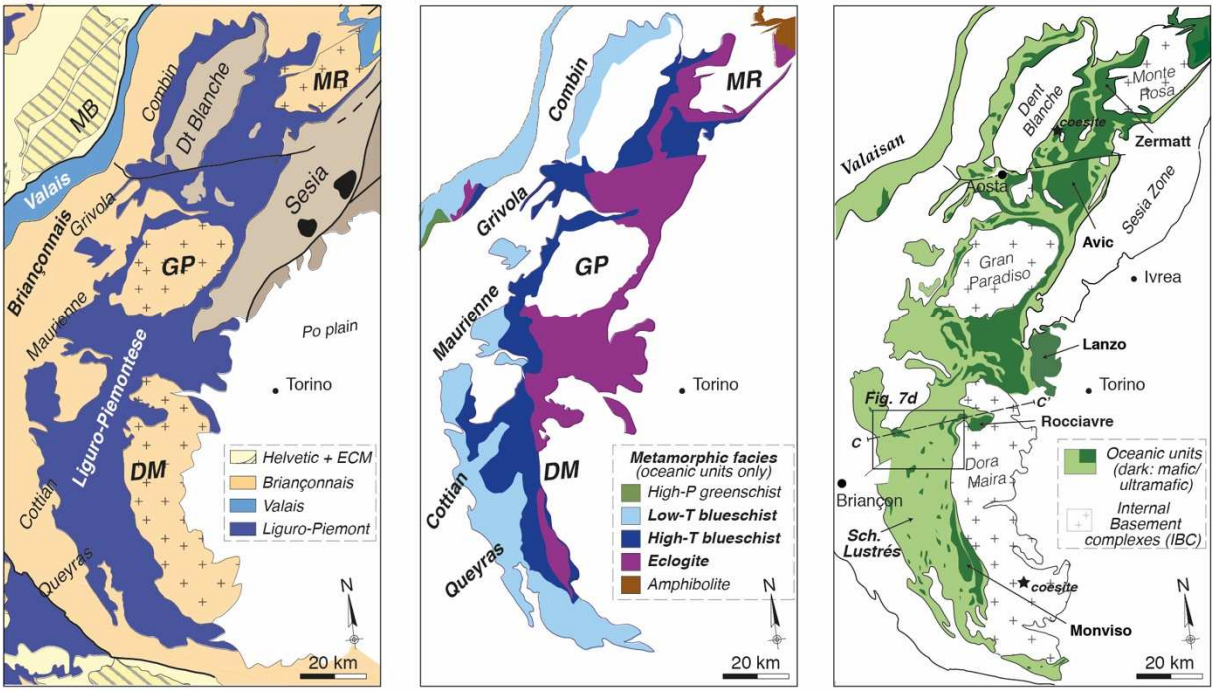
MB
Combin
Dt Blanche
MR
Valais
Briançonnais
Grivola
Sesia
GP
Maurienne
Po plain
Torino
Liguro-Piemontese
DM
Cottian
Queyras
Helvetic + ECM
Briançonnais
Valais
Liguro-Piemont
N
20 km
a
Combin
MR
Grivola
GP
Maurienne
Torino
DM
Cottian
Queyras
Metamorphic facies
(oceanic units only)
High-P greenschist
Low-T blueschist
High-T blueschist
Eclogite
Amphibolite
N
20 km
b
Valaisan
Dent Blanche
Monte Rosa
coesite
Zermatt
Aosta
Sesia Zone
Avic
Gran Paradiso
Ivrea
Lanzo
Torino
Fig. 7d
C
C'
Rocciavre
Dora Maira
Briançon
Sch. Lustrés
Oceanic units
(dark: mafic/
ultramafic)
Internal
Basement
complexes (IBC)
coesite
Monviso
N
20 km
c

2872

Fig. 3

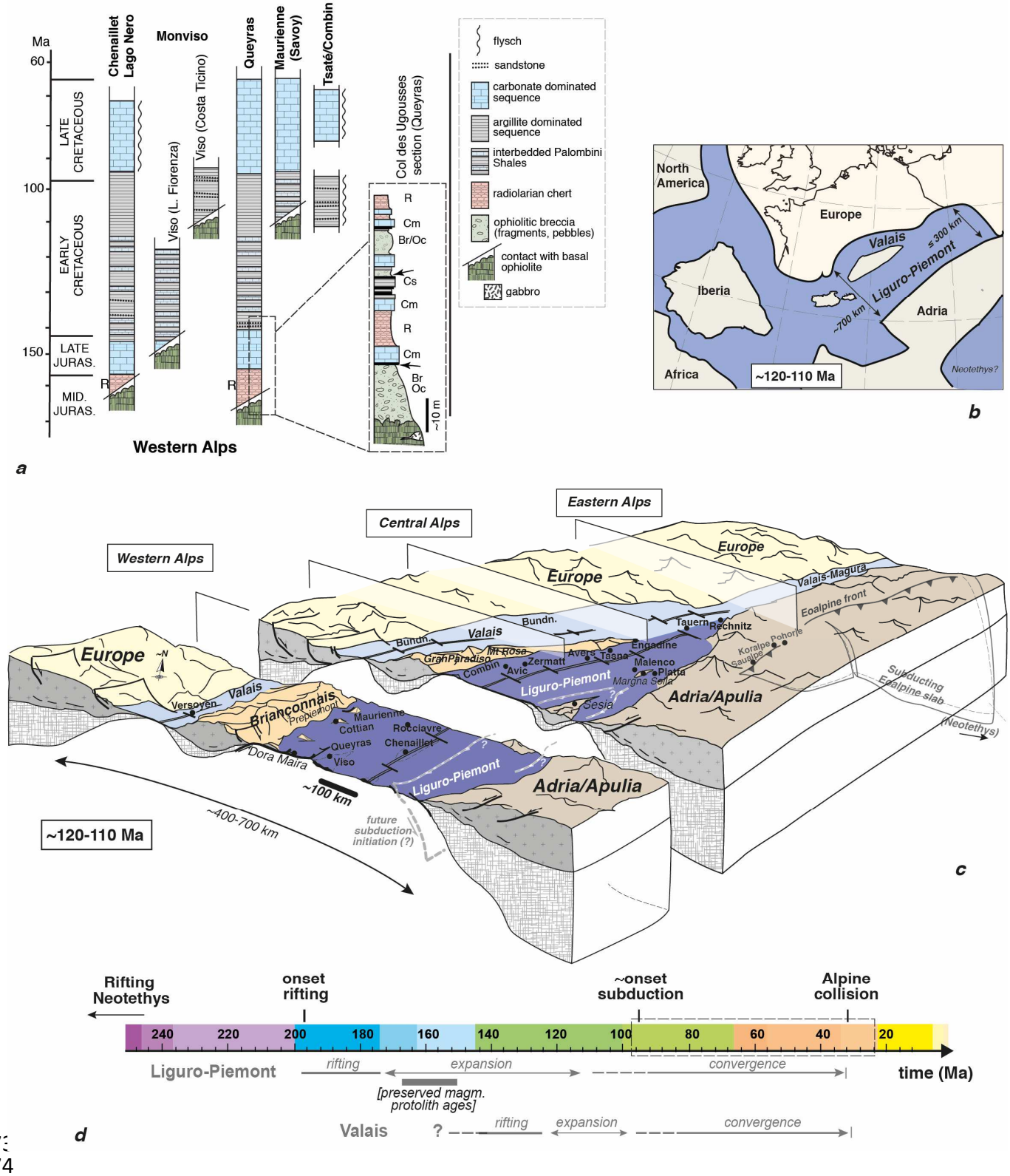

2873
2874

Fig. 4

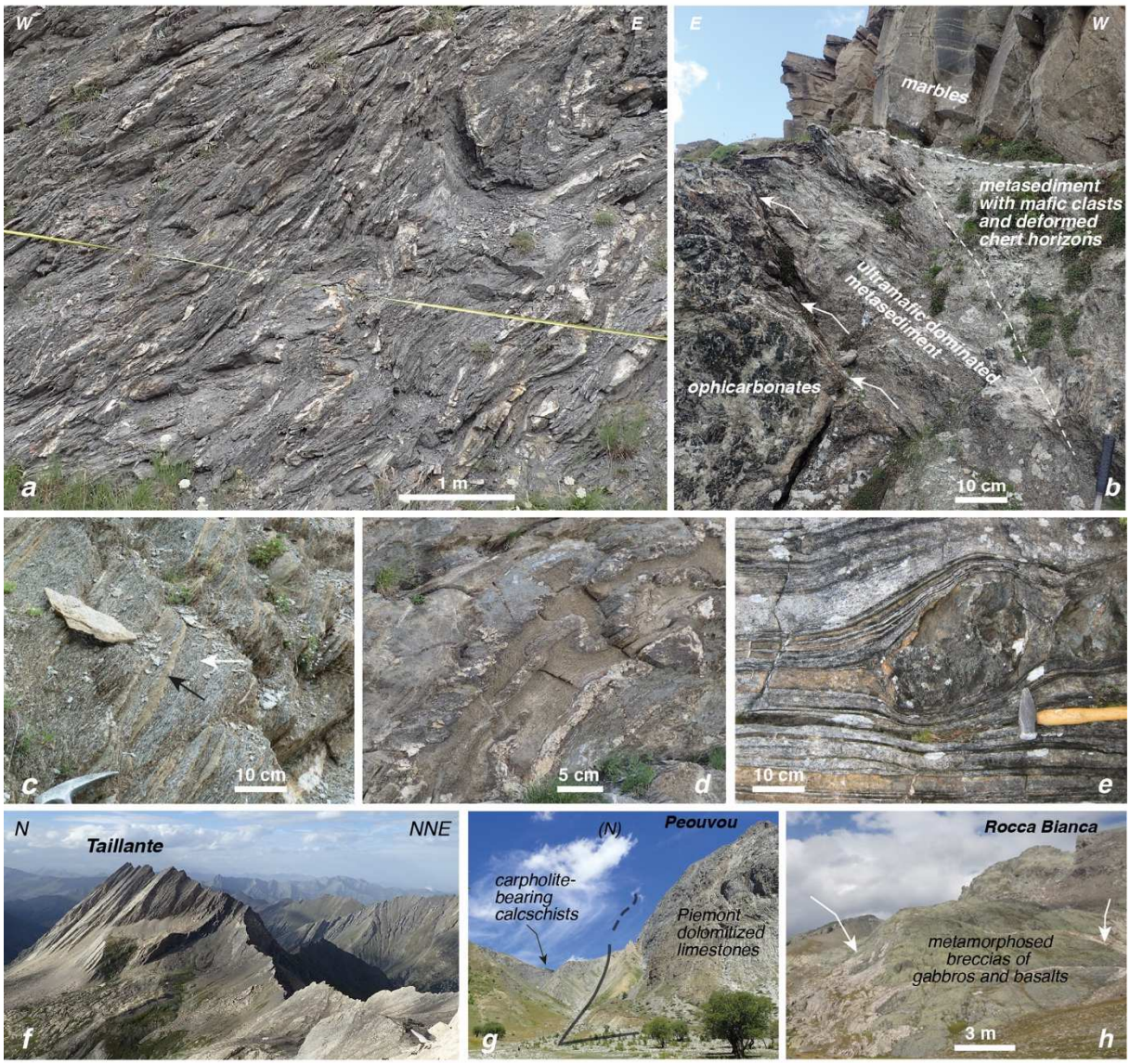
W
E
a
1 m
E
W
marbles
metasediment with mafic clasts and deformed chert horizons
Ultramafic-dominated metasediment
ophicarbonates
10 cm
b
c
10 cm
5 cm
d
10 cm
e
N
Taillante
NNE
f
(N)
Peouvou
carpholite-bearing calcschists
Piemont dolomitized limestones
g
Rocca Bianca
metamorphosed breccias of gabbros and basalts
3 m
h

Fig. 5

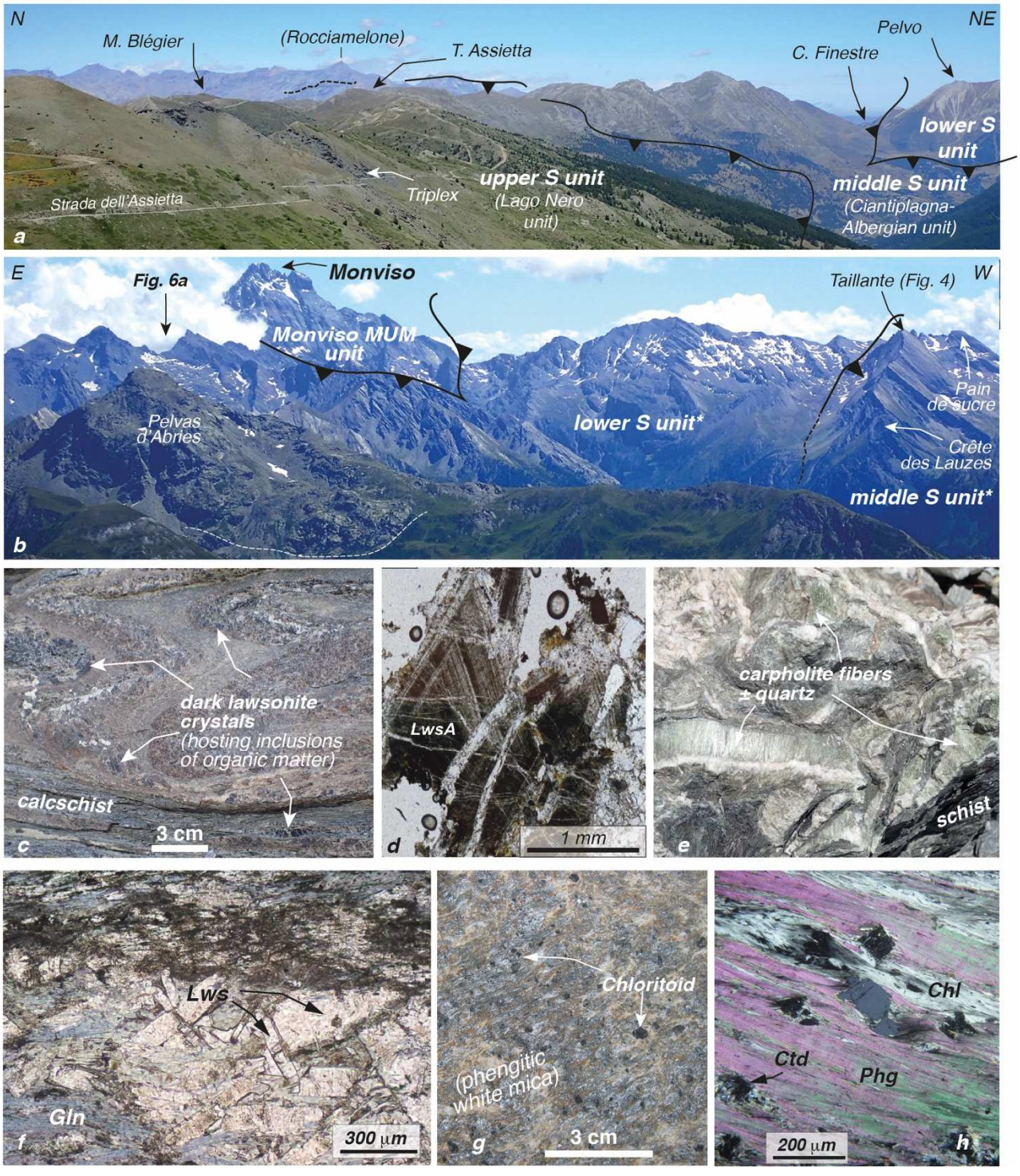
N
M. Blégier
(Rocciamelone)
T. Assietta
Pelvo
NE
C. Finestre
lower S unit
middle S unit
(Ciantiplagna-Albergian unit)
upper S unit
(Lago Nero unit)
Triplex
Strada dell'Assietta
a
E
Fig. 6a
Monviso
Taillante (Fig. 4)
W
Monviso MUM unit
Pain de sucre
Pelvas d'Abries
lower S unit*
Crête des Lauzes
middle S unit*
b
dark lawsonite crystals
(hosting inclusions of organic matter)
calcschist
3 cm
c
LwsA
1 mm
d
carpholite fibers
± quartz
schist
e
Lws
Gln
300 µm
f
Chloritoid
(phengitic white mica)
3 cm
g
Chl
Ctd
Phg
200 µm
h

Fig. 6

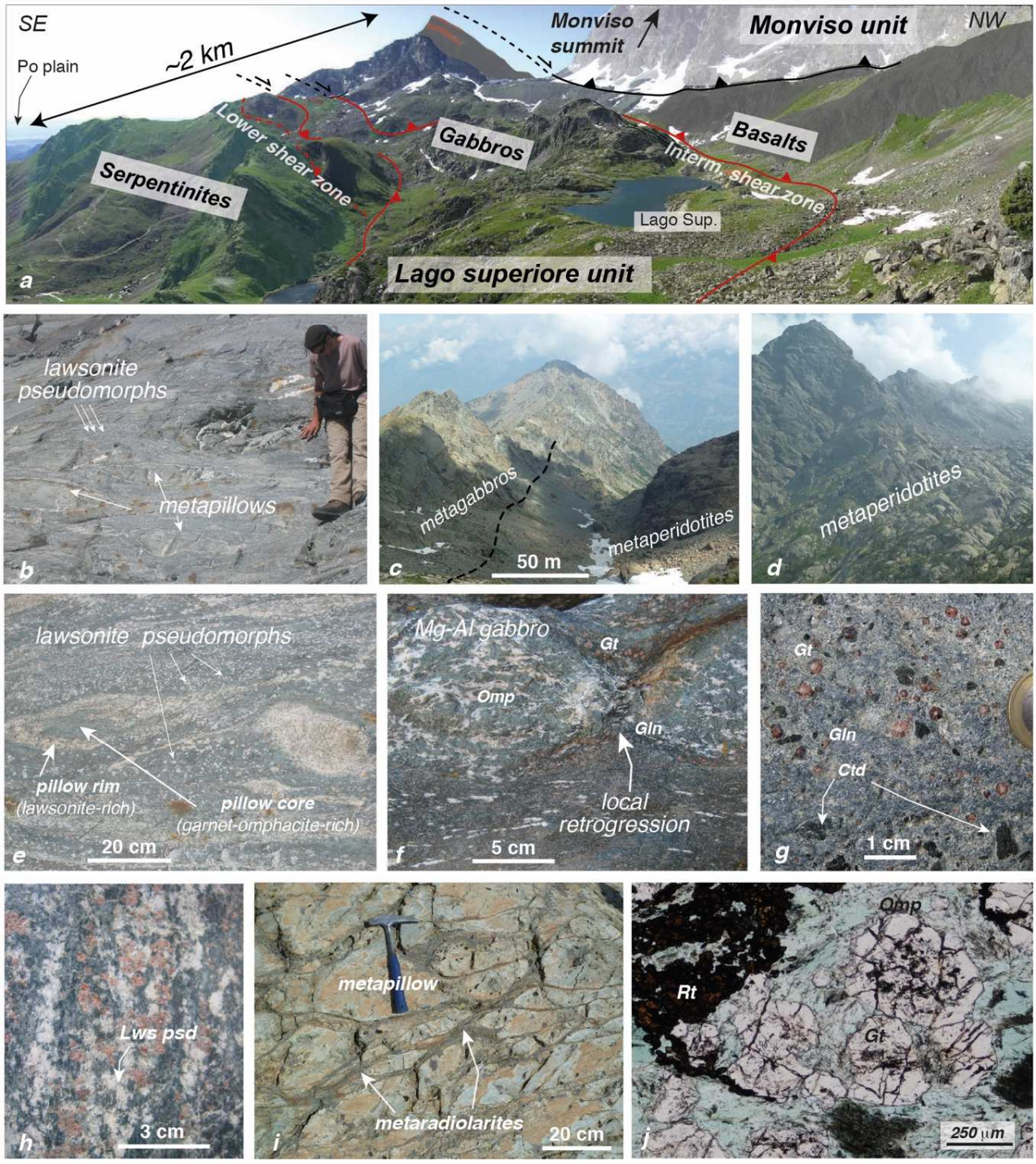
SE
Po plain
~2 km
Monviso summit
Monviso unit
NW
Lower shear zone
Gabbros
Basalts
Interm. shear zone
Serpentinites
Lago Sup.
Lago superiore unit
a
lawsonite pseudomorphs
metapillows
b
metagabbros
metaperidotites
50 m
c
metaperidotites
d
lawsonite pseudomorphs
pillow rim (lawsonite-rich)
pillow core (garnet-omphacite-rich)
20 cm
e
Mg-Al gabbro
Gt
Omp
Gln
local retrogression
5 cm
f
Gt
Gln
Ctd
1 cm
g
Lws psd
3 cm
h
metapillow
metaradiolarites
20 cm
i
Omp
Rt
Gt
250 µm
j

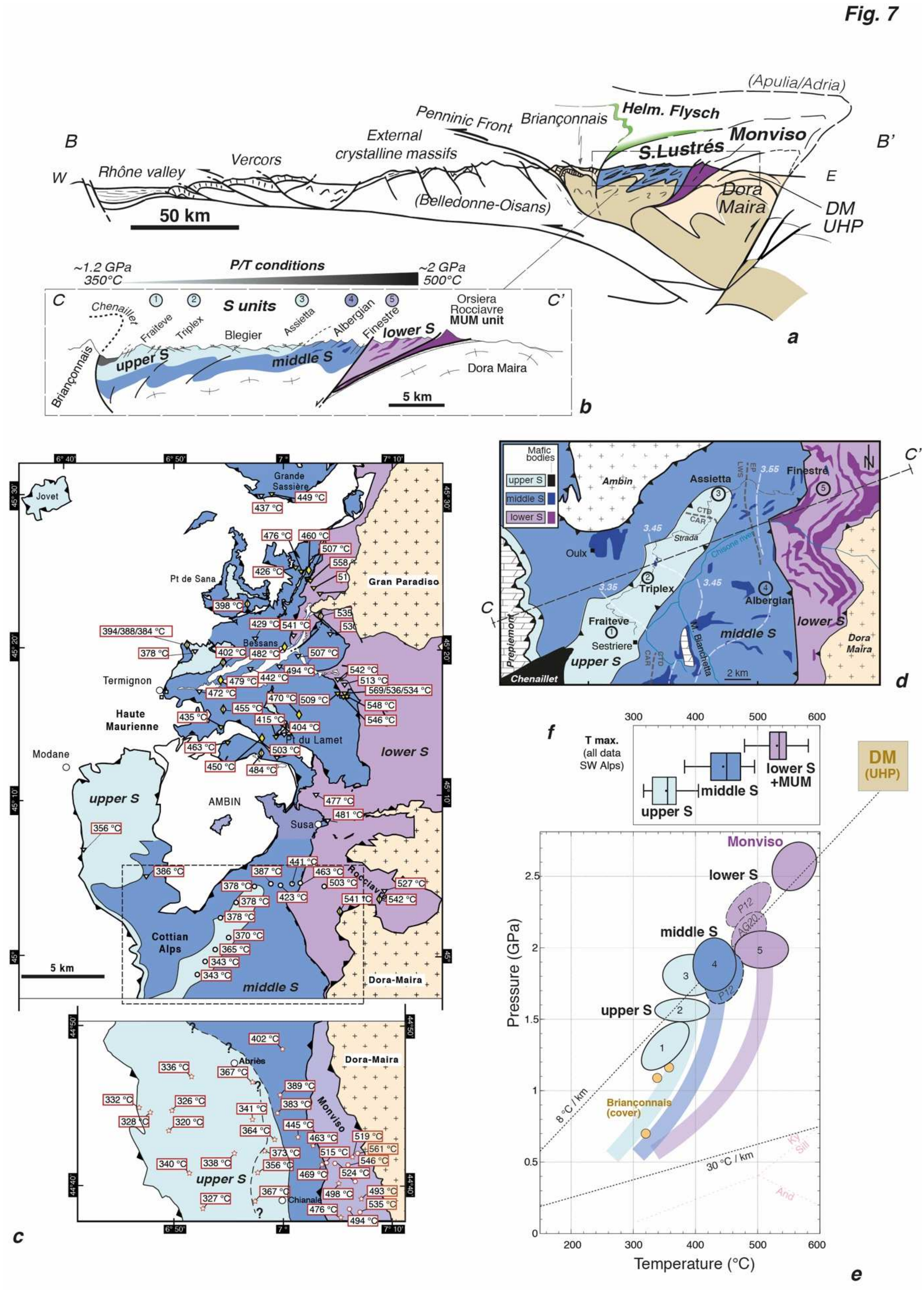
Fig. 7
B
B'
W
E
Rhône valley
Vercors
External crystalline massifs
Penninic Front
Briançonnais
Helm. Flysch
(Apulia/Adria)
Monviso
S.Lustrés
Dora Maira
DM UHP
(Belledonne-Oisans)
50 km
a
P/T conditions
~1.2 GPa 350°C
~2 GPa 500°C
C
C'
S units
Chenaillet
Fraiteve
Triplex
Blegier
Assietta
Albergian
Finestre
Orsiera Rocciavre MUM unit
lower S
upper S
middle S
Briançonnais
Dora Maira
5 km
b
Grande Sassière
Jovet
Pt de Sana
Gran Paradiso
Bessans
Termignon
Haute Maurienne
Modane
Pt du Lamet
lower S
upper S
AMBIN
Susa
Rocciavre
Cottian Alps
middle S
Dora-Maira
5 km
Abriès
Monviso
Chianale
upper S
c
Mafic bodies
upper S
middle S
lower S
Ambin
Assietta
Finestre
Oulx
Triplex
Albergian
Fraiteve
Sestriere
Chenaillet
Preplemont
M. Bianchetta
Chisone river
Dora Maira
2 km
d
T max. (all data SW Alps)
upper S
middle S
lower S +MUM
f
DM (UHP)
Monviso
Pressure (GPa)
Temperature (°C)
Briançonnais (cover)
8 °C / km
30 °C / km
e

2881

Fig. 8

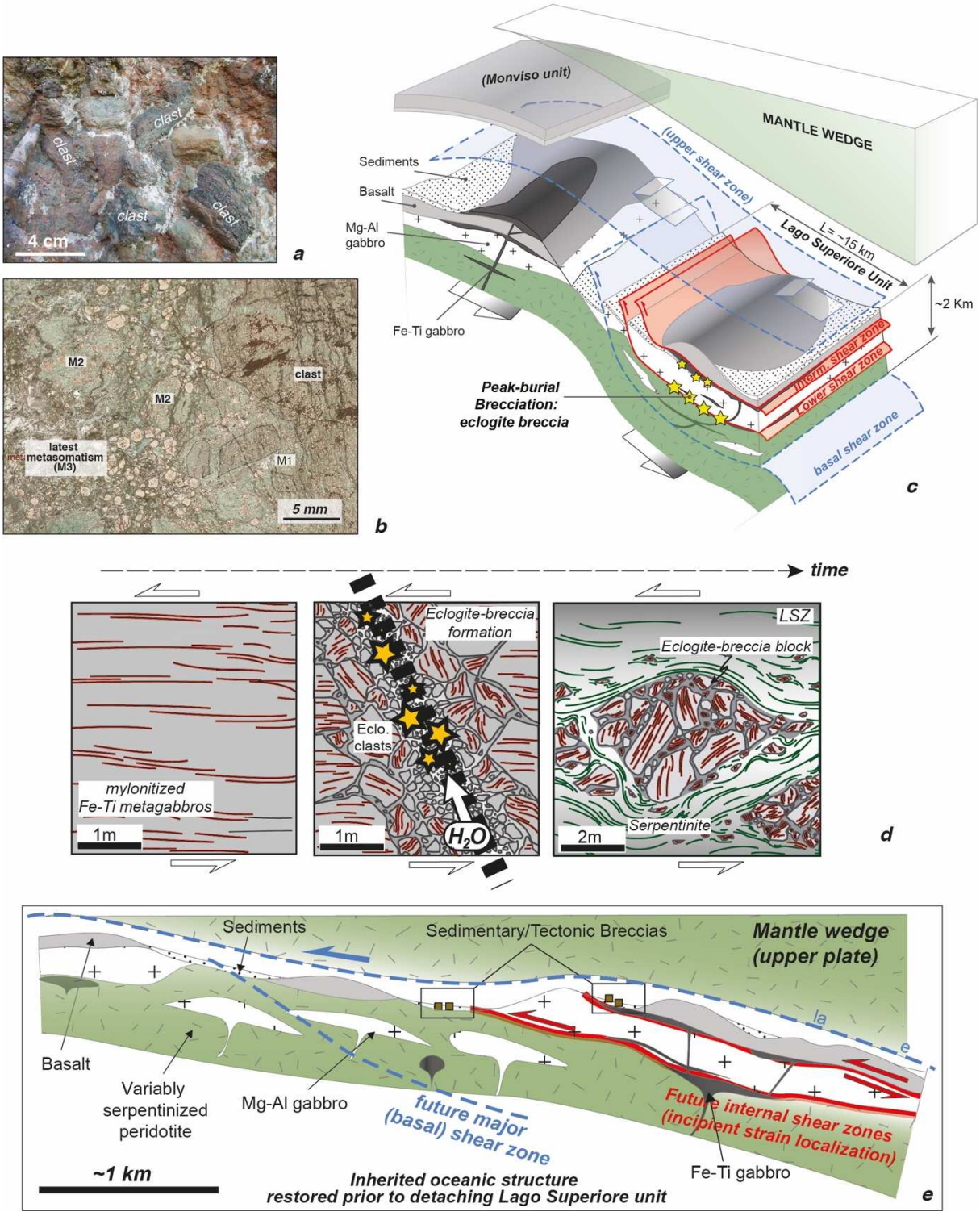
clast
clast
clast
clast
clast
4 cm
a
M2
M2
clast
latest metasomatism (M3)
M1
5 mm
b
(Monviso unit)
MANTLE WEDGE
(upper shear zone)
Sediments
Basalt
Mg-Al gabbro
Fe-Ti gabbro
L = ~15 km
Lago Superiore Unit
~2 Km
Interm. shear zone
Lower Shear zone
basal shear zone
Peak-burial Brecciation: eclogite breccia
c
time
mylonitized Fe-Ti metagabbros
1m
Eclogite-breccia formation
Eclo. clasts
1m
H_2O
LSZ
Eclogite-breccia block
Serpentinite
2m
d
Sediments
Sedimentary/Tectonic Breccias
Mantle wedge (upper plate)
Basalt
Variably serpentinized peridotite
Mg-Al gabbro
future major (basal) shear zone
Future internal shear zones (incipient strain localization)
Fe-Ti gabbro
~1 km
Inherited oceanic structure restored prior to detaching Lago Superiore unit
e

2882

Fig. 9

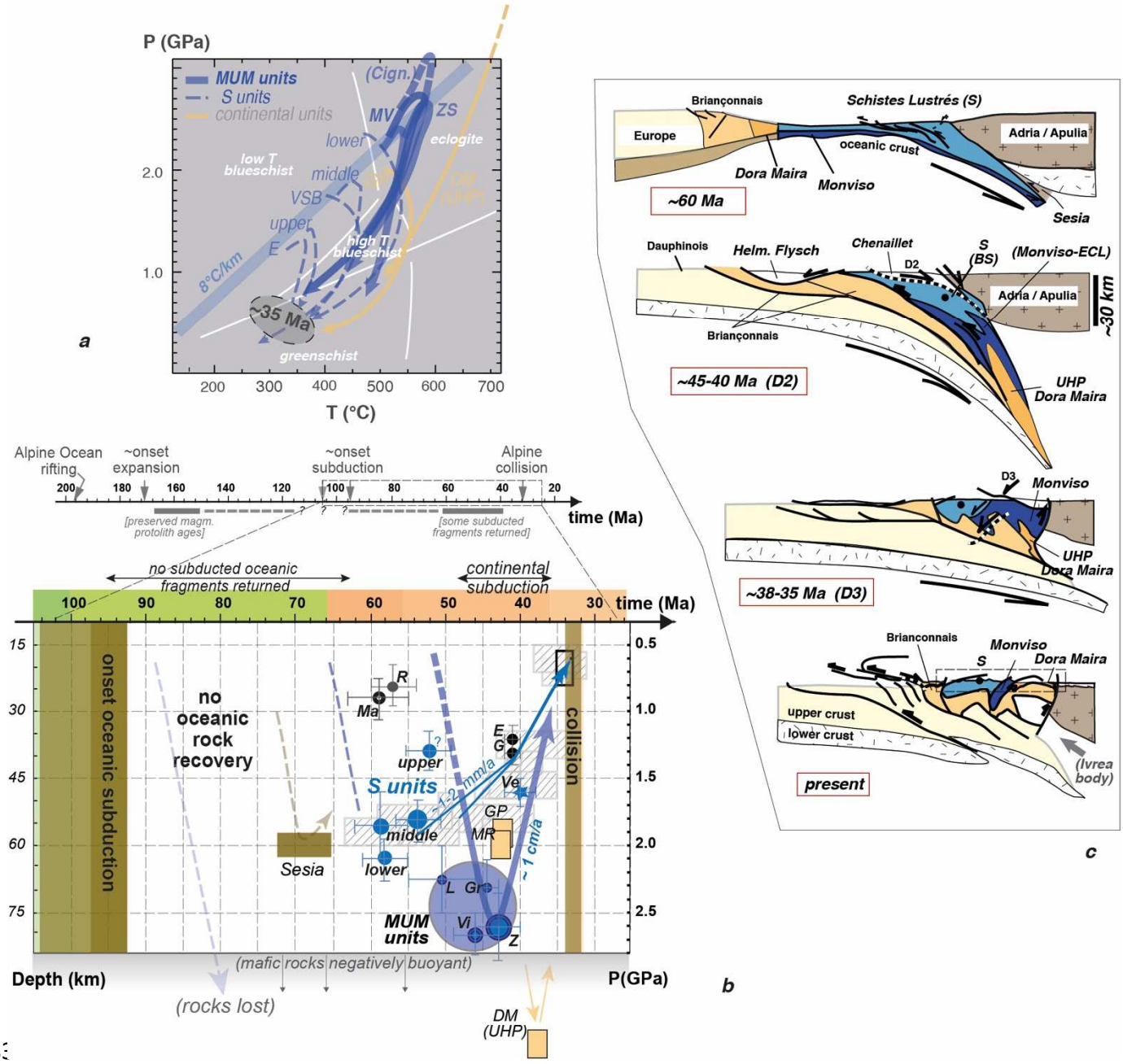

2883
2884

Fig. 10

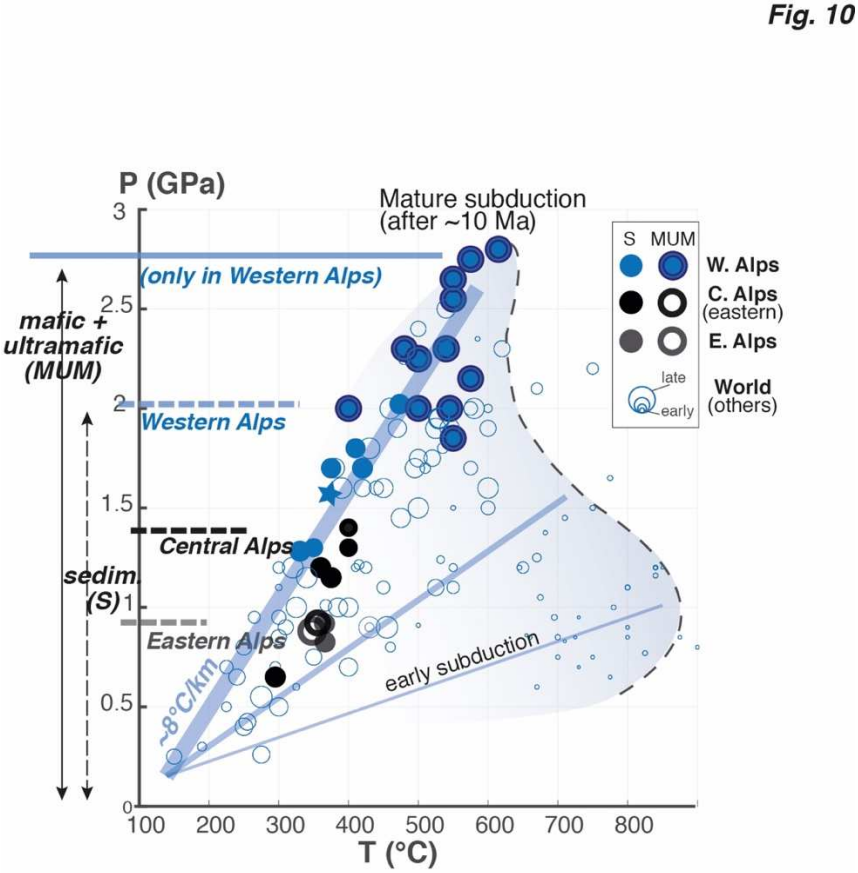
P (GPa)
Mature subduction
(after ~10 Ma)
S MUM
W. Alps
C. Alps
(eastern)
E. Alps
late
early
World
(others)
(only in Western Alps)
mafic +
ultramafic
(MUM)
Western Alps
Central Alps
sedim.
(S)
Eastern Alps
~8°C/km
early subduction
3
2.5
2
1.5
1
0.5
0
100
200
300
400
500
600
700
800
T (°C)

2885

Fig. 11

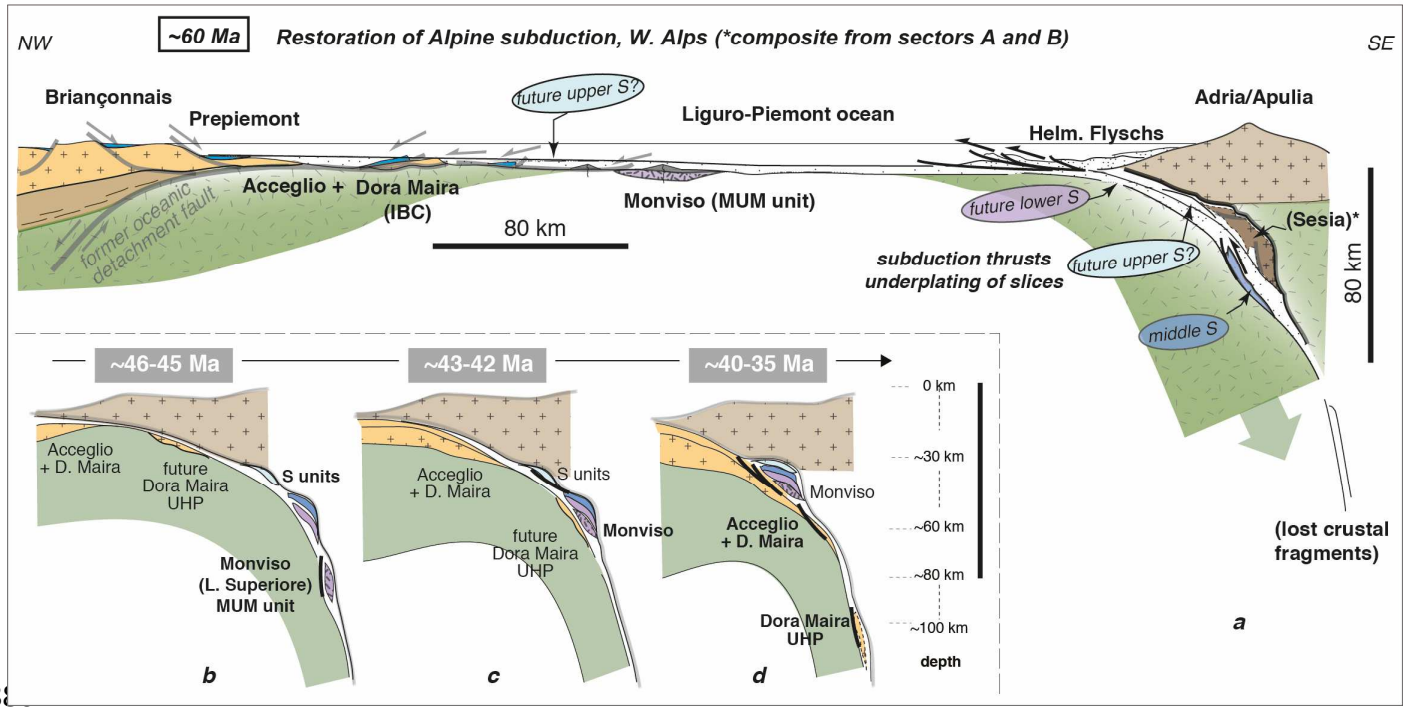
NW
~60 Ma
Restoration of Alpine subduction, W. Alps (*composite from sectors A and B)
SE
Briançonnais
Prepiemont
future upper S?
Liguro-Piemont ocean
Adria/Apulia
Helm. Flyschs
former oceanic detachment fault
Acceglio + Dora Maira (IBC)
80 km
Monviso (MUM unit)
future lower S
(Sesia)*
subduction thrusts underplating of slices
future upper S?
middle S
80 km
~46-45 Ma
~43-42 Ma
~40-35 Ma
0 km
~30 km
~60 km
~80 km
~100 km
depth
Acceglio + D. Maira
future Dora Maira UHP
S units
Monviso (L. Superiore) MUM unit
Monviso
Dora Maira UHP
(lost crustal fragments)
a
b
c
d

Fig. 12

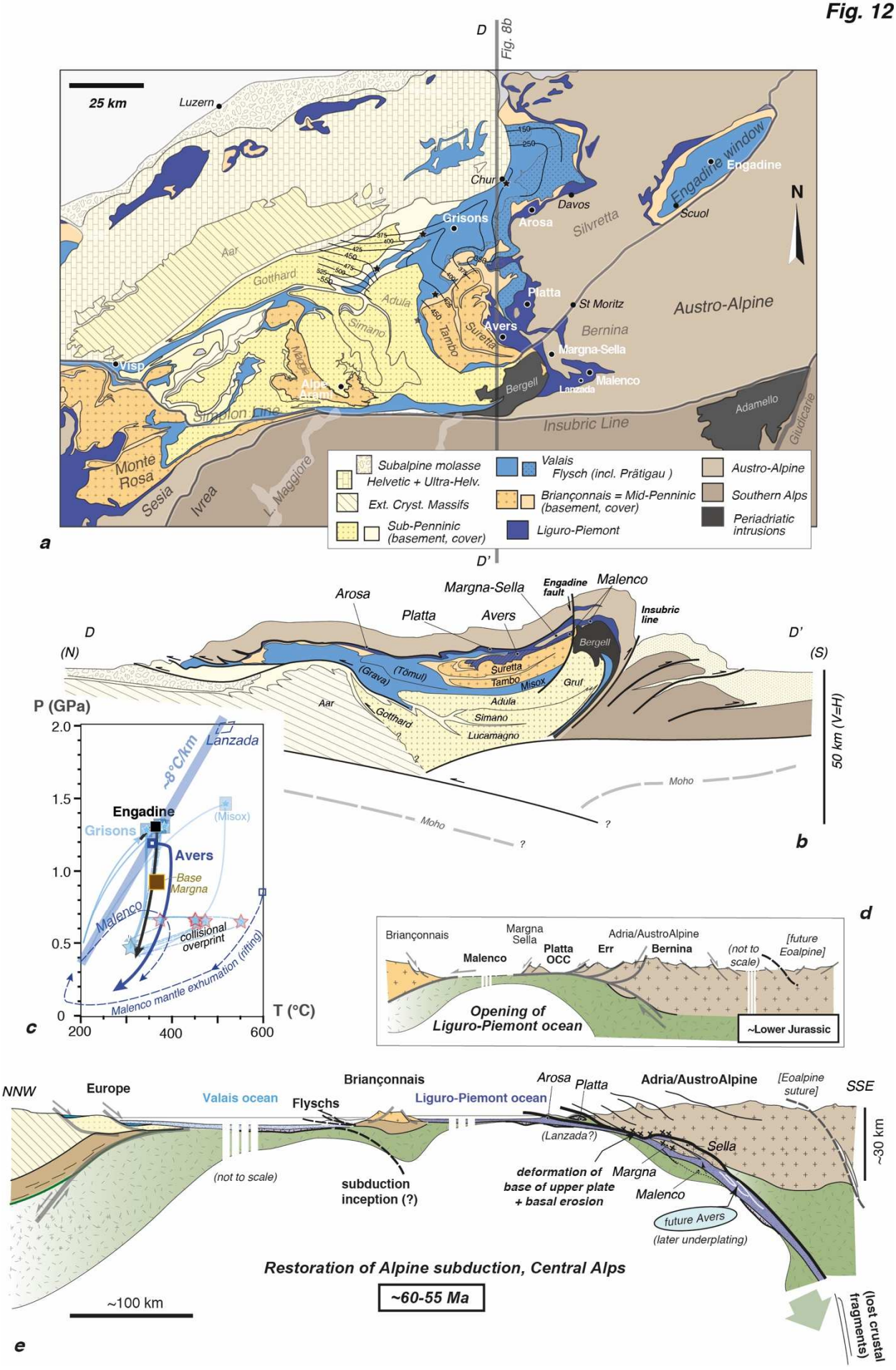
a
25 km
Luzern
Fig. 8b
D
D'
Chur
Davos
Arosa
Grisons
Silvretta
Engadine window
Engadine
Scuol
N
Aar
Gotthard
Adula
Simano
Tambo
Suretta
Platta
St Moritz
Avers
Bernina
Austro-Alpine
Margna-Sella
Malenco
Lanzada
Bergell
Adamello
Giudicarie
Insubric Line
Simplon Line
Visp
Monte Rosa
Sesia
Ivrea
L. Maggiore
Subalpine molasse
Helvetic + Ultra-Helv.
Ext. Cryst. Massifs
Sub-Penninic (basement, cover)
Valais Flysch (incl. Prätigau)
Briançonnais = Mid-Penninic (basement, cover)
Liguro-Piemont
Austro-Alpine
Southern Alps
Periadriatic intrusions
b
Arosa
Margna-Sella
Engadine fault
Malenco
Platta
Avers
Insubric line
(N)
(S)
(Grava)
(Tömul)
Suretta
Tambo
Misox
Gruf
Adula
Aar
Gotthard
Simano
Lucamagno
Moho
50 km (V=H)
c
P (GPa)
2.0
1.5
1.0
0.5
0
~8°C/km
Lanzada
Engadine
Grisons
(Misox)
Avers
Base Margna
Malenco
collisional overprint
Malenco mantle exhumation (rifting)
T (°C)
200
400
600
d
Briançonnais
Margna Sella
Platta OCC
Malenco
Err
Adria/AustroAlpine
Bernina
(not to scale)
[future Eoalpine]
Opening of Liguro-Piemont ocean
~Lower Jurassic
e
NNW
Europe
Valais ocean
Flyschs
Briançonnais
Liguro-Piemont ocean
Arosa
Platta
Adria/AustroAlpine
[Eoalpine suture]
SSE
(Lanzada?)
Sella
Margna
Malenco
~30 km
(not to scale)
subduction inception (?)
deformation of base of upper plate + basal erosion
future Avers
(later underplating)
(lost crustal fragments)
Restoration of Alpine subduction, Central Alps
~60-55 Ma
~100 km

2888

Fig. 13

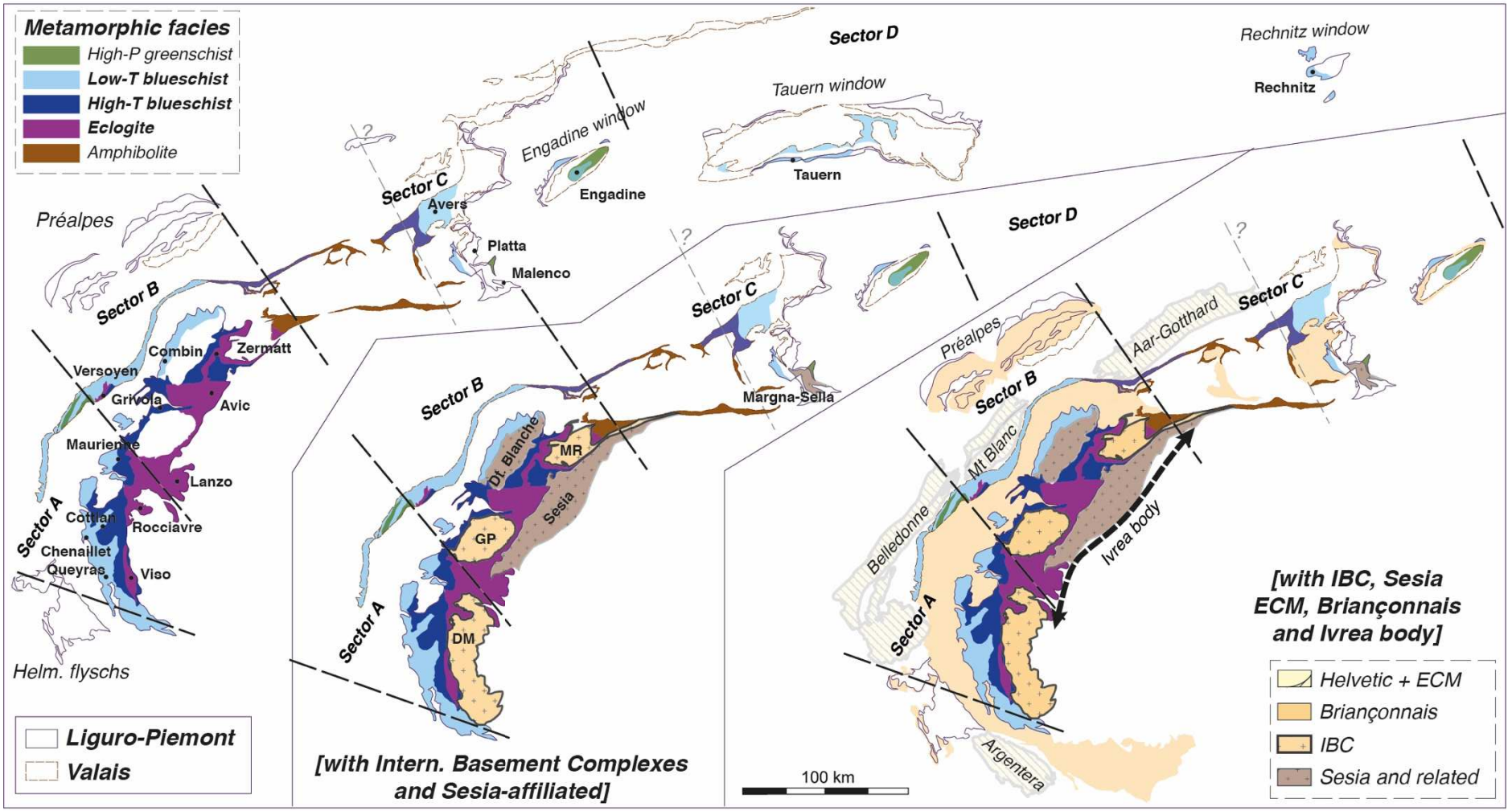
Metamorphic facies
High-P greenschist
Low-T blueschist
High-T blueschist
Eclogite
Amphibolite
Préalpes
Helm. flyschs
Liguro-Piemont
Valais
Sector A
Sector B
Sector C
Sector D
Versoyen
Combin
Zermatt
Grivola
Avic
Mauriennе
Lanzo
Cottian
Rocciavre
Chenaillet
Queyras
Viso
Avers
Platta
Malenco
Engadine window
Engadine
Tauern window
Tauern
Rechnitz window
Rechnitz
Margna-Sella
Dt. Blanche
MR
Sesia
GP
DM
[with Intern. Basement Complexes and Sesia-affiliated]
Aar-Gotthard
Mt Blanc
Belledonne
Ivrea body
Argentera
100 km
[with IBC, Sesia ECM, Briançonnais and Ivrea body]
Helvetic + ECM
Briançonnais
IBC
Sesia and related
a
b
c

Fig. 14

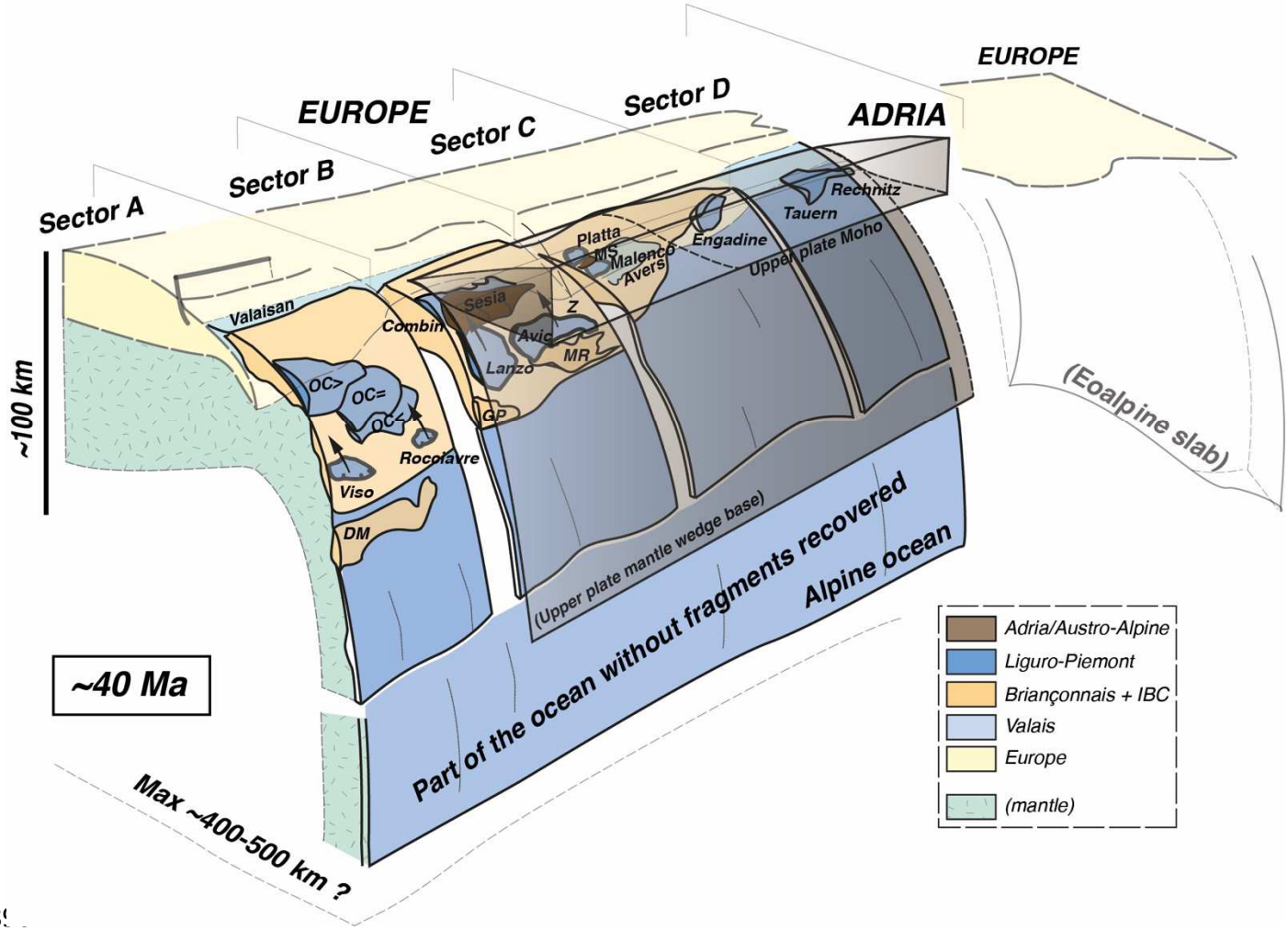
EUROPE
EUROPE
ADRIA
Sector A
Sector B
Sector C
Sector D
~100 km
Valaisan
Combin
Sesia
Z
Platta
MS
Malenco
Avers
Engadine
Tauern
Rechnitz
Upper plate Moho
Avic
MR
Lanzo
QP
OC>
OC=
OC<
Rocciavre
Viso
DM
(Upper plate mantle wedge base)
(Eoalpine slab)
Part of the ocean without fragments recovered
Alpine ocean
~40 Ma
Max ~400-500 km ?
Adria/Austro-Alpine
Liguro-Piemont
Briançonnais + IBC
Valais
Europe
(mantle)

285

Fig. 15

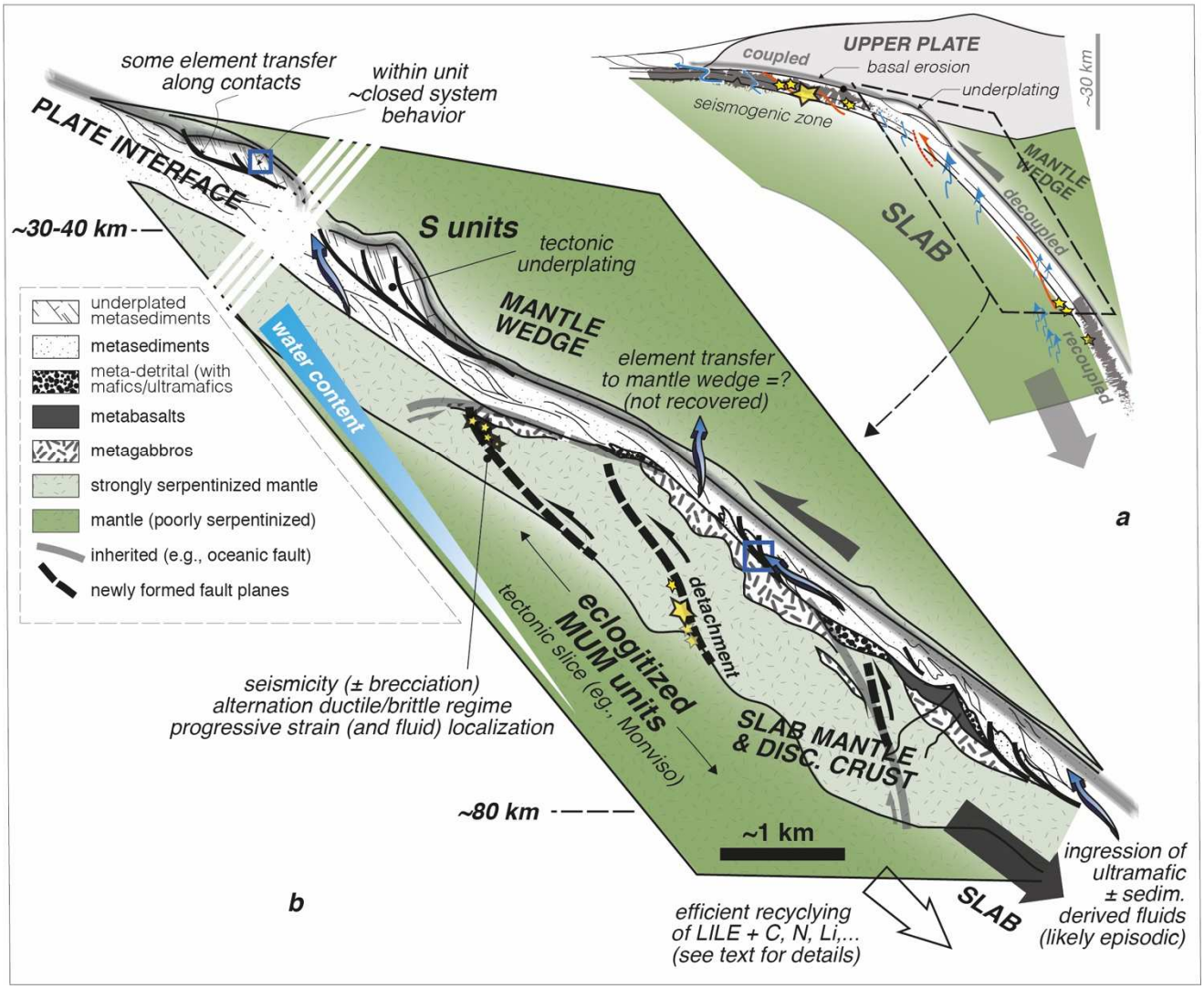
some element transfer
along contacts
within unit
~closed system
behavior
PLATE INTERFACE
~30-40 km
S units
tectonic
underplating
MANTLE
WEDGE
element transfer
to mantle wedge =?
(not recovered)
water content
underplated
metasediments
metasediments
meta-detrital (with
mafics/ultramafics
metabasalts
metagabbros
strongly serpentinized mantle
mantle (poorly serpentinized)
inherited (e.g., oceanic fault)
newly formed fault planes
seismicity (± brecciation)
alternation ductile/brittle regime
progressive strain (and fluid) localization
detachment
eclogitized
MUM units
tectonic slice (eg., Monviso)
SLAB MANTLE
& DISC. CRUST
~80 km
~1 km
b
UPPER PLATE
coupled
basal erosion
underplating
~30 km
seismogenic zone
MANTLE
WEDGE
decoupled
SLAB
recoupled
a
ingression of
ultramafic
± sedim.
derived fluids
(likely episodic)
SLAB
efficient recycling
of LILE + C, N, Li,...
(see text for details)